

Asian Workshop on Polymer Processing
1 - 4 December 2015. University Town (U-Town)
of NUS

User Guide:

Click on the abstract title in the programme to see the abstract content

Click on the bookmarks to go back to the programme

**Asian Workshop on Polymer Processing
1 - 4 December 2015. University Town (U-Town) of NUS
1st December 2015**

Time	Programme
1:30 PM	Transport for AWPP EXCO meeting Centre @ University Town from Park Avenue Rochester Hotel, transport will then proceed to Kent Vale then to University Town.
2:00~5:00 PM	<p>Asian Workshop on Polymer Processing (AWPP) EXCO Meeting</p> <p>Venue: Conference Room 2, Stephen Riady Centre, 2 College Avenue West, University Town, National University of Singapore, Singapore 138607</p> <p><i>Please note that the AWPP EXCO Meeting is strictly for invited guests only.</i></p>
4:30 PM	Transport for AWPP Welcome Reception @ University Town from Park Avenue Rochester Hotel, transport will then proceed to Kent Vale then to University Town.
5:00~7:00 PM	<p>AWPP 2015 – Welcome Reception</p> <p>Venue: University Town, National University of Singapore, 8 College Avenue West, Education Resource Centre (ERC), Level 2, Ngee Ann Kongsi Auditorium, Singapore 138608</p>
7:15 PM	Transport will leave University Town for Kent Vale and then to Park Avenue Rochester Hotel.

**Asian Workshop on Polymer Processing
1 - 4 December 2015. University Town (U-Town) of NUS
2nd December 2015**

Time	Programme	
8:00~8:30 AM	Conference Registration	
8:00 AM	<p style="text-align: center;">Transport to Conference Venue @ University Town, NUS from Park Avenue Rochester Hotel. Transport will then proceed to Kent Vale. Delegates at Kent Vale should be ready for pick up at 08:15 at the main drop-off point at Kent Vale. The drop-off point is across the roundabout in Kent Vale in front of the main entrance.</p> <p style="text-align: center;">Conference Venue: University Town, National University of Singapore, 8 College Avenue West, Education Resource Centre (ERC), Level 2, Ngee Ann Kongsi Auditorium, Singapore 138608</p>	
8:30~8:45 AM	Opening Address by Prof He Chaobin (Chairman, AWPP)	
8:45~9:25 AM	Plenary Lecture <i>Polymeric Membranes for Clean Water and Clean Energy</i> Neal Tai-Shung Chung (NUS, Singapore) Session Chair: He Chaobin	
9:25~10:05 AM	Plenary Lecture <i>Processing Thermoplastic High Performance Composites</i> Florian Doetzer (Composite Cluster Singapore Pte Ltd., Singapore) Session Chair: He Chaobin	
10:05~10:30 AM	Tea break	
	Session-1: Materials from biomass Session Chair: Li Xu	Session-2: Extrusion based processes Session Chair: Pramoda Kumari Pallathadka
10:30~11:00 AM	Keynote Presentation <i>Biodegradable Polymer Composites of Poly(lactic acid) Blends and Natural Fibers</i> S. Pivsa-Art (RMUTT, Thailand)	Keynote Presentation <i>Polyethylene-Thermally Reduced Graphene Nanocomposites: Comparison of Masterbatch and Direct Melt Mixing Approaches on Mechanical, Thermal, Rheological and Morphological Properties</i> V. Mittal (The Petroleum Institute, Abu Dhabi, UAE)
11:00~11:15 AM	Keynote Presentation <i>Recent Development of Direct Fiber Feeding Injection Molding</i> H. Hamada (Kyoto Institute of Technology, Japan)	Invited Talk <i>Effect of Cross-sectional Configuration on Die Swell Behavior and Spin-line Stability in Bicomponent Melt Spinning Process</i> W. Takarada (Tokyo Institute of Technology, Japan)
11:15~11:30 AM		Invited Talk <i>Polymer Melt Differential 3D Printing and Advanced Manufacturing</i> W. Yang (Beijing University of Chemical Technology, China)
11:30~11:45 AM	Invited Talk <i>Nanocomposites based on Biomass Charcoal with Multifunction</i> A. Qin (Guilin University of Technology, China)	Oral Presentation <i>Fiber-breakage Evaluation of Melts passing through Check-ring based on Newly-developed Heating Cylinder with Multi-ports for In-process Sampling</i> M. Sai (University of Tokyo, Japan)
11:45~12:00 PM	Invited Talk <i>Effect of Cellulose Nanofiber on Scratch Resistance of Poly(vinyl alcohol) Composites</i> S. Konagaya (Nagoya University, Japan)	Oral Presentation <i>Study on feedstock of metal injection molding</i> N. Kayamori (Doshisha University, Japan)
12:00~12:15 PM	Oral Presentation <i>Studies of Mechanical Properties of High Density Polyethylene/Vietnamosasa Pusilla Fiber Composite for Decoration Applications</i> S. Suaadaow (RMUTT, Thailand)	Oral Presentation <i>Effect of Titanium Dioxide On the Interface of Poly(lactic acid) between Sheath-core Fibers</i> N. Rongpaisan (RMUTT, Thailand)
12:15~12:30 PM	Oral Presentation <i>Fiber Structure Development in High-speed Melt Spinning of Sheath-core Bicomponent Fibers consisting of Aliphatic Copolyesters of Different Copolymer Composition</i> Q. Qing (Tokyo Institute of Technology, Japan)	
12:30~1:30 PM	Lunch Break	

	Session-3: Polymers for energy and sustainability Session Chair: Warintorn Thitsartarn	Session-4: Modeling and Simulation Session Chair: Jiang Zhenyu
1:30~2:00 PM	Keynote Presentation <i>Electrospinning of Porous Polymer Nanofibers and their Applications as Functional Materials</i> X. Lu (NTU, Singapore)	Keynote Presentation <i>In Silico Processing of Polymers</i> A.Soldera (University of Sherbrooke, Quebec, Canada)
2:00~2:30 PM	Keynote Presentation <i>Nanostructured Additive-enhanced High Performance Superhydrophobic Coating Materials</i> J. Xu (A*STAR IMRE, Singapore)	Keynote Presentation <i>Measurement of Gas-pressure Distributions inside Mold Cavity during Gas-venting Process by Small-diameter Melt Pressure Sensor</i> H. Yokoi (University of Tokyo, Japan)
2:30~2:45 PM	Invited Talk <i>Green Chemistry: Preparation of Environmentally-benign Graft Copolymers via Emulsion System</i> K. Ishimoto (RMUTT, Thailand)	Invited Talk <i>Molecular Simulation of the Effect of Chain Tacticity on Demixing of Polyethylene/Propylene Blends</i> V. Vao-soongnern (Suranaree University of Technology, Thailand)
2:45~3:00 PM	Invited Talk <i>Modification of chemically stable polymeric materials 63. Improvement in the adhesion property of polymeric materials, FRP and CFRPs for car-use</i> H. Kanazawa (Fukushima University, Japan)	Invited Talk <i>Melt-mixing by Pitched-tip Kneading Disks in a Twin-screw extruder</i> T. Kajiwara (Kyushu University, Japan)
3:00~3:15 PM	Oral Presentation <i>Study on Fabricating Carbon Nano Fiber by Cotton Candy Method</i> R. Takematsu (Kyoto Institute of Technology, Japan)	Invited Talk <i>Polymer Processing Simulation Challenges in Describing Highly Elastic Flows</i> K. Tomioka (Nitto Denko Corporation, Japan)
3:15~3:30 PM	Oral Presentation <i>Development of Poly(lactic acid)/Gelatin/Shellac Blend for Green Composite Film from</i> K. Nilgumhang (RMUTT, Thailand)	Invited Talk <i>Evaluation of Distributive Mixing in an Internal Mixer by Partially Filled Flow Analysis</i> K. Higashi (Kobe Steel, Ltd., Japan)
3:30~4:00 PM	Tea Break	
	Session-5: Polymer characterization: Session Chair: Pramoda Kumari Pallathadka	Session-6: Polymer nanotechnology: Session Chair: Prof. Ashok Misra
4:00~4:15 PM	Invited Talk <i>Dynamic Mechanical Properties of Sisal Fiber Cellulose Microcrystal/unsaturated Polyester in-situ Composites</i> C. Wei (Guilin University of Technology, China)	Keynote Presentation <i>Effect of Surface Pre-treatment of Substrate on Wettability of Metal Nano-ink</i> T. Saito (Tokyo Institute of Technology, Japan)
4:15~4:30 PM	Invited Talk <i>Multi-element Analysis of Polymer Using Wavelength Dispersive XRF</i> H.R. Low (Bruker, Singapore)	
4:30~4:45 PM	Invited Talk <i>The Flameretardancy Study of PVA using for Cardboard Bed</i> Y. Mizutani (Kyoto Institute of technology, Japan)	Invited Talk <i>2D Array Nanohole Processing on Ultrathin Polymer Films with Gold Nanoparticles</i> K. Yamada (Kyoto Institute of Technology, Japan)
4:45~5:00 PM	Invited Talk <i>Size, Shapes and Superstructures of Polymeric Materials with a SAXS/WAXS Instrument</i> S. Rodrigues (Xenocs, France)	Oral Presentation <i>Preparation of The Carbon Nano Fiber Using Cotton Candy Method</i> A. Tada (Ohgi Technological Creation Co., Ltd., Japan)
5:00~5:15 PM	Oral Presentation <i>Analysis on Crystallization Behavior of Equi-biaxially Stretched Amorphous Poly(ethylene Terephthalate) Films</i> S. Shibata (Tokyo Institute of Technology, Japan)	Oral Presentation <i>Development of PEEK-Nano-SiC Composites for High Performance Coating and Adhesive Applications</i> A. K. Kadiyala (Indian Institute of Technology Delhi, India)
5:30 PM	Transport will leave University Town for Kent Vale and then to Park Avenue Rochester Hotel.	

Asian Workshop on Polymer Processing
1 - 4 December 2015. University Town (U-Town) of NUS
3rd December 2015

Time	Programme	
8:00 AM	<p>Transport to Conference Venue @ University Town, NUS from Park Avenue Rochester Hotel. Transport will then proceed to Kent Vale.</p> <p>Delegates at Kent Vale should be ready for pick up at 08:15 at the main drop-off point at Kent Vale. The drop-off point is across the roundabout in Kent Vale in front of the main entrance.</p> <p>Conference Venue: University Town, National University of Singapore, 8 College Avenue West, Education Resource Centre (ERC), Level 2, Ngee Ann Kongsi Auditorium, Singapore 138608</p>	
8:45~9:25 AM	<p style="text-align: center;">Plenary Lecture <i>Foamability of Multi-Phase Polymeric Materials</i> A. K. Ghosh (IIT Delhi, India) Session Chair: Leong Yew Wei</p>	
9:25~10:05 AM	<p style="text-align: center;">Plenary Lecture <i>Material Development for Automotive Application</i> T. Kitayama (Sumitomo Chemical Co. Ltd., Japan) Session Chair: Leong Yew Wei</p>	
10:05~10:30 AM	Tea break	
	<p>Session-7: Nanocomposite Session Chair: Takushi Saito</p>	<p>Session-8: Biodegradable materials Session Chair: Sommai Pivsa-Art</p>
10:30~11:00 AM	<p>Keynote Presentation <i>Functional Polynorbornenes: Ultra-high Tg Thermosetting Fibers and Composites</i> J.C. Claverie (UQAM, Canada)</p>	<p>Keynote Presentation <i>Redox-responsive poly(amido amine)s from trifunctional amines for bioapplications</i> Y. Liu (A*STAR IMRE, Singapore)</p>
11:00~11:30 AM	<p>Keynote Presentation <i>Towards high-performance polypropylene/expanded graphite/carbon nanotubes ternary composites with significantly enhanced thermal and electrical conductivity via constructing double percolated filler network</i> Q. Fu (Sichuan University, China)</p>	<p>Keynote Presentation <i>Enhancing Dispersion of Nanoparticles in Molten Polymers</i> N. Phonthammachai (SCG Chemicals Co., Ltd., Thailand)</p>
11:30~ 12:00 PM	<p>Keynote Presentation <i>Synergistic Dispersion of Carbon Nanomaterials in Polymer Nanocomposites</i> T. Liu (Fudan University, China)</p>	<p>Keynote Presentation <i>Processing Conditions and Properties of Nonwoven Kenaf Reinforced Acrylic Based Polyester Composites</i> Z. A. M. Ishak (Universiti Sains Malaysia, Malaysia)</p>
12:00~12:15 PM	<p>Invited Talk <i>Dynamic Mechanical Analysis and Heat Seal Property of Biodegradable Polymer Blends and Composite Films</i> S. Thumsorn (RMUTT, Thailand)</p>	<p>Invited Talk <i>Controlled Urea and Ammonium Sulfate Released from Poly(lactic acid) for Slow Released Fertilizer Application</i> S. Niamlang (RMUTT, Thailand)</p>
12:15~12:30 PM	<p>Invited Talk <i>Graphene Nanoplatelet/Poly(butylene adipate-co-terephthalate) Hybrids: Physical Properties</i> R. Gupta (RMIT University, Australia)</p>	<p>Invited Talk <i>Influence of Reactive Agents on Flow Property and Mechanical Properties of Biodegradable Polyesters</i> S. Suttirungwong (Silpakorn University, Thailand)</p>
12:30~12:45 PM	<p>Invited Talk <i>Development of starch based bio-film and life cycle assessment</i> X. Zhang (A*STAR SIMTech, Singapore)</p>	<p>Oral Presentation <i>Biodegradable and Renewable Poly(lactide)-lignin Composites: Synthesis, Interface and Toughening Mechanism</i> Y. Sun (NUS, Singapore)</p>
12:45~1:45 PM	Lunch Break	
	<p>Session-9: Molding based processes Session Chair: Toshitaka Kanai</p>	<p>Session-10: Polymer blends Session Chair: Mohit Sharma</p>
1:45~2:15 PM	<p>Keynote Presentation <i>Fabrication of Micro-needle Array using Biocompatible Polymers by Precision Molding</i> H. Ito (Yamagata University, Japan)</p>	<p>Keynote Presentation <i>Semi-interpenetrating Network of Polyoxymethylene with Oligo-benzoxazine via Reactive Blending</i> S. Chirachanchai (Chulalongkorn University, Thailand)</p>
2:15~2:45 PM	<p>Keynote Presentation <i>Skin Structure and Scratch Behavior of Injection Molded Polypropylene</i> M. Kotaki (Kaneka Americas Holding, Inc. USA)</p>	<p>Keynote Presentation <i>The Relationship Between Morphology and Impact Toughness of Poly(L-lactic acid)/Poly(ethylene oxide) Blends</i> C. Chan (The Hong Kong University of Science and Technology, China)</p>
2:45~3:00 PM	<p>Invited Talk <i>Physical Degradation Theory and Physical Regeneration Method for Recycling of Waste Plastics</i> S. Yao (Fukuoka University, Japan)</p>	<p>Invited Talk <i>Adhesion Behavior of "Warm-off" Type Acrylic PSAS</i> H. Murakami (Nagasaki University, Japan)</p>
3:00~3:15 PM	<p>Invited Talk <i>Melt Transcription Molding Process with Higher Precision and Productivity for Thin Thermoplastic Products with Micro- and Nano-structured Surface</i> K. Furuki (The Japan Steel Works, Ltd., Japan)</p>	<p>Oral Presentation <i>Preparation of Poly(lactic acid) Nanofiber by Nanofiber by Cotton Candy Method</i> R. Wongpajan (Kyoto Institute of Technology, Japan)</p>
3:15~3:30 PM	<p>Oral Presentation <i>High Expansion Open-cell Poly(lactide) (PLA) Foam from Blends with Fibrillar Polytetrafluoroethylene (PTFE)</i> S. Ishihara (Kyoto University, Japan)</p>	<p>Oral Presentation <i>Control of Glass Transition Temperature In Immiscible Rubber Blend</i> N. Kuhakongkiat (Japan Advanced Institute of Science and Technology, Japan)</p>
3:30~3:45 PM	<p>Oral Presentation <i>Measurement of Demolding Resistance In Incline Direction to Texturing Cavity Surface using 3-Component Force Transducer</i> K. Daiki (University of Tokyo, Japan)</p>	<p>Oral Presentation <i>PP/LLDPE Hybrid in Axial Powder Flow Apparatus</i> E. Junsri (RMUTT, Thailand)</p>
3:45~5:30 PM	<p>Poster Session and Tea Break</p> <p>Venue: University Town, National University of Singapore, 8 College Avenue West, Education Resource Centre (ERC), Level 2, Ngee Ann Kongsi Auditorium, Singapore 138608</p> <p>Results of Top 3 posters will be announced at 17:15.</p>	
5:45 PM	Transportation from University Town to Conference Banquet Venue	
6:00~8:30 PM	Conference Banquet	
	Venue: Kent Ridge Guild House, Level 2, Cluny & Dalvey Rooms, 9 Kent Ridge, Drive, Singapore 119241	
8:45 PM	Transport will leave Kent Ridge Guild House for Kent Vale and then to Park Avenue Rochester Hotel.	

**Asian Workshop on Polymer Processing
1 - 4 December 2015. University Town (U-Town) of NUS
4th December 2015**

Time	Programme	
8:45 AM	<p style="text-align: center;">Transport to Conference Venue @ University Town, NUS from Park Avenue Rochester Hotel. Transport will then proceed to Kent Vale.</p> <p style="text-align: center;">Delegates at Kent Vale should be ready for pick up at 09:00 at the main drop-off point at Kent Vale. The drop-off point is across the roundabout in Kent Vale in front of the main entrance.</p>	
	Session-13: Functional Polymers Session Chair: Anup Gosh	Session-14: High Performance Polymers Session Chair: Warintorn Thitsartarn
9:30~10:00 AM	Keynote Presentation <i>Effect of Pre-annealing on 3-D Orientation Development Behavior During Simultaneous and Sequential Biaxial Stretching of Poly(ethylene naphthalate) Films</i> T. Kikutani (Tokyo Institute of Technology, Japan)	Keynote Presentation <i>Spinnability and Theoretical Analysis of the Spunbond Process for Polypropylene</i> T. Kanai (KT Polymer, Japan)
10:00~ 10:15 AM	Invited Talk <i>Solid Electrolyte Function of Side-chain Crystalline Block Co-polymer</i> S. Yao (Fukuoka University, Japan)	Invited Talk <i>Percolation model for reinforcement efficiency of carbon nanotubes in thermoplastic composites</i> Z. Jiang (South China University of Technology, China)
10:15~10:30 AM	Invited Talk <i>Durability and Properties of Jute Fiber Treatment in Green Filled Rubber</i> W. Ariyawiriyanan (RMUTT, Thailand)	Invited Talk <i>Evaluation of grass fiber reinforced engineering plastics for water heater</i> H. Nishimura (Kyoto Institute of Technology, Japan)
10:30~10:45 AM	Oral Presentation <i>The Flameretardancy Study of Corrugated Cardboard using for Cardboard Bed</i> Y. Mochizuki (Kyoto Institute of Technology, Japan)	Oral Presentation <i>Analysis of Dispersive Behavior and Mixing State of Filler Mixed into SBR and BR</i> S. Kaneko (Doshisha University, Japan)
10:45~11:00 AM	Oral Presentation <i>Poly(lactic acid)/Polypropylene Blends for Cosmetic Case Products</i> J. Kordsa-Art (RMUTT, Thailand)	Oral Presentation <i>Measurement of Three-Dimensional Temperature Distributions Inside Cavity Filling Melts using Integrated Thermocouple Sensor</i> S. Ishida (The University of Tokyo, Japan)
11:00~12:00 PM	Lunch Break	
12:00:00 PM	Transport will leave University Town for Kent Vale and then to Park Avenue Rochester Hotel. (For Delegates not attending Fusion World Tour)	
1:00~3:00 PM	Fusion World Tour Venue: 1 Fusionopolis Way, #13-10, Connexis North, Singapore 138632 Information for Group 1 (13:00 – 14:00) Transportation will be provided at 12:15 from University Town to Fusionopolis. After the tour, transportation will be provided from Fusionopolis to Park Avenue Rochester Hotel, then to Kent Vale. Information for Group 2 (14:00 – 15:00) Transportation will be provided at 13:15 from University Town to Fusionopolis. After the tour, transportation will be provided from Fusionopolis to Park Avenue Rochester Hotel, then to Kent Vale.	

Asian Workshop on Polymer Processing
1 - 4 December 2015. University Town (U-Town) of NUS

S/N	Poster Information
P01	Swarna, " <i>Influence of Suspending Medium on Rheological Behavior of Shear Thickening Fluids</i> ", Indian Institute of Technology Delhi, India
P02	T. Konno, " <i>Structure and Engineering Properties of PMMA Nano-alloy obtained by High Speed Shearing Process</i> ", Yamagata University, Japan
P03	Y. Yamada, " <i>Evaluation of Higher-order Structure and Thermal Properties of High Thermal Conductivity PC Composites obtained by Structural Phase Separation Method</i> ", Yamagata University, Japan
P04	H. Suenaga, " <i>Evaluation of Structure-physical Properties of Reactive Molded Polyamide 6 and its FRTP</i> ", Yamagata University, Japan
P05	T. Sako, " <i>Surface Localization of Poly(methyl methacrylate) in a Blend with Polycarbonate</i> ", Japan Advanced Institute of Science and Technology, Japan
P06	R. Watanabe, " <i>Self-healing behavior of Styrene-butadiene-styrene Triblock Copolymer</i> ", Japan Advanced Institute of Science and Technology, Japan
P07	K. Yoshida, " <i>Interphase Transfer of Plasticizer between Immiscible Rubbers</i> ", Japan Advanced Institute of Science and Technology, Japan
P08	S. Sato, " <i>Anomalous Molecular Orientation of Extruded Sheet for Polypropylen/polybutene-1 Blends</i> ", Japan Advanced Institute of Science and Technology, Japan
P09	S. Iwasaki, " <i>Development of Evaluation Method Capable of Judging the Appropriate Product Lifetime of the Rubber Material Used In Residential-use Cogeneration Systems</i> ", Osaks Gas Co. Ltd., Japan
P10	R. Hasuo, " <i>Synthesis and Characterization of a Side-chain Crystalline Silicone PSA</i> ", Nagasaki University, Japan
P11	S. Tabuchi, " <i>Warm-off" Type Acrylic PSA containing a Side-chain Crystalline Graft Copolymer</i> ", Nagasaki University, Japan
P12	M.S. Huang, " <i>Effect of Clamping Force Set Value on Injection Molding Qualities</i> ", National Kaohsiung First University of Science and Technology, Taiwan
P13	H. Kanazawa, " <i>Modification of Chemically Stable Polymeric Materials 64. Improvement In the Hydrophilic and Adhesion Properties of Polymeric Materials and FRPs</i> ", Fukushima University, Japan
P14	M. Sugimoto, " <i>Improved Elongational Viscosity of Polycarbonate Melts</i> ", Yamagata University, Japan
P15	S.K. Hong, " <i>Numerical Simulation of Injection/compression Molding for Multiscale Structure</i> ", Korea Institute of Industrial Technology (KITECH), Republic of Korea
P16	N. Oda, " <i>Long Time Structure Constitution of Amorphous Polymer</i> ", Fukuoka University Graduate School, Japan
P17	K. Hirakawa, " <i>Creation of Polar Solvent Type TR Fluid and its Function</i> ", Fukuoka University Graduate School, Japan
P18	Y. Hasebe, " <i>TR Fluid Function for Differences in the Chemical Structure of the Side Chain Crystallizable Block Copolymer</i> ", Fukuoka University Graduate School, Japan
P20	S. Jamornsurriya, " <i>Atomistic Simulation of Gas Diffusion in Glassy Poly(Vinyl Pyrrolidone) Matrix</i> ", Suranaree University of Technology, Thailand
P21	C. Y. Chang, " <i>A Highly Efficient REEL to REEL Hot Embossing Process for Fabrication of Polymer Microlens Array</i> ", National Kaohsiung University of Applied Sciences, Taiwan
P22	H.W. Bai, " <i>Towards High-performance Poly(L-lactide) Melt Spun Fibers by Tailoring Crystallization with the Aid of Nucleating Agent</i> ", Sichuan University, China
P23	G. Wang, " <i>Novel Biomedical Materials Based on Carbon Dots</i> ", A*STAR IMRE, Singapore
P24	W. Ren, " <i>Synthesis and Antimicrobial Activities of Quaternized PEI-g-chitosan Polycations</i> ", A*STAR IMRE, Singapore
P25	Z. M. Png, " <i>Valorization of Palm Resource for Grease Lubricant</i> ", A*STAR IMRE, Singapore
P26	J. He, " <i>Controlled Growth of MOF-based Hybrid Nanomaterials</i> ", A*STAR IMRE, Singapore
P27	C. C. Yap, " <i>Hydrothermal Synthesis of Carbon Spheres from Glucose</i> ", A*STAR IMRE, Singapore
P28	X. Zhang, " <i>Effect of Modified Starch and Nanoclay on Biodegradability and Mechanical Propertied of Polylactic Acid Ternary Blends</i> ", A*STAR IMRE, Singapore
P29	H. Yan, " <i>Structural Engineering of Polyurethane for Multiple Functional Coatings</i> ", A*STAR IMRE, Singapore

POLYMERIC MEMBRANES FOR CLEAN WATER AND CLEAN ENERGY

Oral presentation

(Neal) Tai-Shung Chung^{1,2}

¹*Department of Chemical and Biomolecular Engineering,
National University of Singapore, Singapore 117585, Singapore*

²*Water Desalination & Reuse Center, King Abdullah University of Science and Technology,
23955-6900 Saudi Arabia*

Corresponding author email address: chencts@nus.edu.sg

Abstract - Clean water, clean energy, global warming and affordable healthcare are four major concerns globally resulting from clean water shortages, high fluctuations of oil prices, climate changes and high costs of healthcare. Clean water and public health are also highly related, while energy is essential for sustainable prosperity.

Among many potential solutions, advances in membrane technology are one of the most direct, effective and feasible approaches to solve these sophisticated issues. Membrane technology is a fully integrated science and engineering which consists of materials science and engineering, chemistry and chemical engineering, separation and purification phenomena, environmental science and sustainability, statistical mechanics-based molecular simulation, process and product design.

In this presentation, we will introduce our efforts on materials design and polymeric membrane development for clean water production and osmotic power generation, then highlight our recent development on functional membranes for biofuel separation, natural purification and separation.

The osmotic power generation via the mixing of water streams with different salinities across a semi-permeable pressure retarded osmosis (PRO) membrane is one of our foci. If the osmotic power generator is integrated with the reverse osmosis (RO) plant using its retentate as the draw solution, not only are we able to mitigate the disposal issues of RO retentate, but also lower the overall energy consumption for RO plants. As a result, seawater desalination will be much cost-effective and this integration will entirely revolutionize the future desalination industry and energy production.

Keywords: membrane technology, clean water, clean energy, osmotic energy, biofuel, gas separation

PROCESSING THERMOPLASTIC HIGH PERFORMANCE COMPOSITES

Keynote presentation

Florian Doetzer¹

¹ *Composite Cluster Singapore, Singapore*

Corresponding author email address: doetzer@compositecluster.com

Abstract

High performance composites, originally developed in Aerospace & Defense applications, have traditionally used thermoset matrix materials. However, with the needs for automation, short production cycles and low processing cost, the interest in thermoplastic matrix systems has risen sharply.

While companies like ourselves are developing new processing and manufacturing methods for thermoplastic composites, there is also a growing need for modification of raw materials (Matrix-polymers and Reinforcement fibers) according to specific product needs. The successful application of new processing and design solutions requires a close collaboration between materials experts and design & manufacturing engineers.

Important points will be highlighted during the presentation and range from material compliance in challenging environmental conditions to compatibility of new material combinations. Additionally, inherent advantages of thermoplastic composites, such as fast processing times or adhesive-free bonding, will be put into perspective with the development of new processing and design solutions.

Keywords: Composites, CFRP, Thermoplastic, AFP

Foamability of Multi-Phase Polymeric Materials

Prof. Anup K.Ghosh

*Centre of Polymer Science and Engineering
Indian Institute of Technology Delhi, New Delhi*

Blending with other polymers and/ or fillers is a well-established and widely used method of enhancing and modifying the properties of a polymer. Immiscible polymer blends by and large outnumber miscible ones. Thus, there is a huge spectrum of multi-phase polymeric materials comprising of immiscible blends and filled polymers. Foaming of polymeric materials results in significant weight reduction and also leads to new properties. Thus, the foaming of multi-phase polymeric materials is of immense academic and commercial interest. It has been well established that the morphology of multi-phase materials determines not only their own properties, but also the morphology and other properties of their foams. In case of polymer blends, a smaller size of the dispersed domains results in superior properties of the blends and better foam morphology. In case of filled polymers, the quality of dispersion (exfoliation/ intercalation in case of nanocomposites) again governs the extent of property enhancement and also the quality of foams. The morphology of multiphase polymeric materials is by and large governed by their rheological properties. The rheological properties of any polymeric system can be tuned by proper selection of process parameters. In fact, rheology can be used as a tool to predict and control morphology, which in turn controls foamability. The key to successful foaming of a multi-phase polymeric materials thus lies in gaining a complete understanding of the rheological properties of the polymer (s) involved and in proper selection of process parameters, so as to achieve the desired morphology of both the multi-phase system as well as its foam.

MATERIAL DEVELOPMENT FOR AUTOMOTIVE APPLICATION

(Oral Presentation)

Takeo Kitayama

*Corporate Planning and Coordination Office, Sumitomo Chemical Co., Ltd.
27-1, Shinkawa 2-chome, Chuo-ku, Tokyo 104-8260, Japan
Email: kitayamat1@sc.sumitomo-chem.co.jp*

Abstract

To meet the demand for growing Asian market, Sumitomo Chemical has expanded the petrochemical complex to Singapore as the very first one in other parts of Asia than Japan in 1984. Furthermore the large-scaled petrochemical complex has been constructed at Saudi Arabia in 2009. Now new technology for polymer modification realized the characteristic improvement of thermoplastic materials such as S-SBR and PP compounds which can contribute to the automotive industry.

Keywords: S-SBR, PP compounds, Singapore, Saudi Arabia

1. Introduction

In recent years, with increasing environment concern for energy saving, various thermoplastic materials have been used in such fields as automobiles, electronics and medicals. However the thermoplastics for general use cannot satisfy all requirements in the market. The appearance of the thermoplastics with higher performance have been expected. Many studies were carried out on polymer and composite development in order to comply with the demands for performance enhancement.

In the automotive application, engineering plastics and metals have been extensively replaced by polypropylene (PP) based materials in automotive parts such as bumper facias, instruments panels and door trims in order to achieve weight reductions and cost savings.

The growth of PP compounds for automotive applications has thus far been supported by the improved performance of PP resins – which serve as the base of PP compounds – and advancements in compound technology. With respect to the former, catalysts and the polymerization process have been continually, energetically improved in order to control the primary and higher-order structures of polymers. Regarding the latter, improvements in the performance and dispersibility of elastomers, as well as the control of particle size, dispersion and interface of inorganic fillers, have been attempted up to the present time.

The other plastic materials, which can contribute automotive industries, are considered to be rubbers which can apply for tires.

The market for solution styrene-butadiene rubber (S-SBR) which is mainly used for the treads of the energy-saving tires for automobiles has continued to expand rapidly while the fuel efficiency requirements for automobiles have been tightened worldwide. It is estimated that the annual S-SBR demand for 2011 will be between 400 and 350 thousands tons.

Energy-saving performance is achieved through a variety of improvements and innovations from the fundamental structure of the tire to various types of materials, but among these the role played by the tread, which is the part coming into contact with the surface of the ground, is particularly important. This means providing polymer materials that give energy-saving performance and road surface grip, which is related to safety, in the trade-off between these two properties, and this is an area where the most is expected of the manufacturers of polymers for tires.

Sumitomo chemical has diversified and accumulated a variety of technologies to create new value in the 100-year history. In 1958, petrochemical production in Japan was started for the first time and later on, after experience of “oil-crisis”, it was expanded in Singapore to pursue competitive feedstock and growing Asian market in 1984. This project was the very first petrochemical complex in Asian region except Japan.

Afterwards, in 2009, a world-scale integrated oil refining and petrochemical complex was built up in Saudi Arabia. The technological innovations such as polymer and composite

development are believed to be the basis of the global expansion.

In this report, recent accomplishments of plastic and rubber developments through Asian market situation and our production expansion are presented.

2. Market trend of plastic materials

Plastic materials have been extensively used for diverse range of applications due to outstanding mechanical properties, excellent moldability and low cost production. One of the industries that used large quantity of plastic materials is the automobile and the number of automotive production is projected to increase in future in Asia, and China in particular (Fig.1).

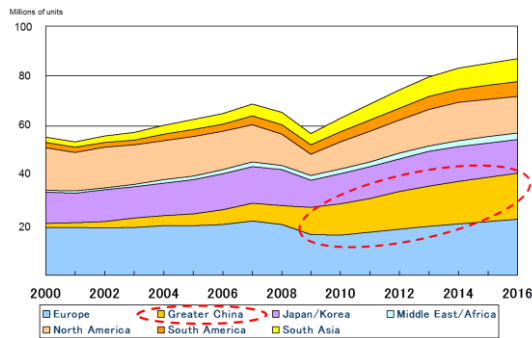


Figure 1. Projected global automobile production

PP, which is one of the general plastic materials, accounts for more than half of all plastic materials used in automobiles and the weight of PP in one middle class automobile has reached more than 65kg in our calculation. PP compounds are used variety of parts in automobile and several grades of PP compounds, with their diverse performance characteristics, have been developed by compounding with various other materials in order to satisfy the performance requirements. Besides the PP compounds growth, PP production is expected to see significant growth by about 3% in the world and the higher growth ratio in Asia.

Considered in terms of environment concern, transportation sector makes up to 20% of carbon dioxide emissions in Japan and approximately 90% of that is from automobiles.

With this background, the Ministry of Land, Infrastructure, Transport and Tourism established the FY 2015 fuel economy standards based on the Act on the Rational Use of Energy. According to these standards, in FY 2015,

improvements on an average of 23.5% over actual performance in FY 2004 are required for the fuel economy of passenger cars.

3. Business footprint

3-1. Singapore project

In 1984, we have located petrochemical complex in Singapore because of various advantages the country offers, including its geographical proximity to the vigorously growing Asian market, and availability of a stable supply source for the raw materials. The cracker's current capacity of Singapore complex is about one million tons per year with two lines. The downstream productions are also run, which are PP, polyethylene (PE) and polymethyl methacrylate (PMMA). Besides, there are other products (EO, EG, PO, SM) operated by our partners. Each of those downstream products is highly valued by customers with its quality and stable supply and the business performances are going well.

A new solution styrene-butadiene rubber (S-SBR) manufacturing plant constructed in Singapore.

In 2014, the S-SBR is manufactured by our proprietary production process technology and advanced polymer modification technology that is a key to achieving higher product performance and has won high praise from customers in the tire manufacturing industries both in Japan and overseas for being a highly fuel-efficient tire material with outstanding abrasion resistance.

3-2. Rabigh project

In 2005, we established PetroRabigh, a joint venture with Saudi Aramco, to develop large scaled complex in Rabigh, Saudi Arabia. The operation began in 2009, and Phase 2 expansion will get completed next year (2016). Main product slate in Phase 1 project contains PE, PP and propylene oxide (PO). PP compounding production was carried out in "Rabigh Plus Tech Park" located next to PetroRabigh.

In phase 2, the expansion includes building a new aromatics complex at the project site, using additional ethane and naphtha as feedstock. The project's main products will be ethylene propylene rubber (EPR), thermoplastic polyolefin (TPO), PMMA, low density polyethylene/ethylene vinyl acetate (LDPE /

EVA), para-xylene/benzene, cumene and phenol/acetone.

4. New solution SBR

To maintain strength in tires, the raw rubber starting material must first of all be vulcanized, and it must be compounded with a filler (reinforcing filler) to improve strength. The designs for compounding in passenger car tire treads have been greatly transfigured in the last 20 years or so. Silica is used frequently instead of the carbon black that has been known for a long time as a filler. From the standpoint of fuel efficiency performance and wet grip performance, using silica as a filler, in other words, silica compounding, is an indispensable technology for high-performance fuel efficient tires that started in Europe and has spread to the rest of the world.

Since the surface of silica is coated with hydrophilic silanol groups, its affinity for hydrocarbon polymers is typically lower than carbon black, and there are difficulties in that good dispersion is difficult and without modification the reinforcing properties are inferior.

By introducing polar functional groups and increasing the polarization of the polymer itself, we can expect to have a good direct effect on the affinity for the hydrophilic silica. With silica compounding, we cannot expect physical binding as is seen between carbon and rubber components; therefore, the introduction of polar functional groups to the polymer chain is even more important.

4-1. Alkoxysilyl group modified SBR

If one alkoxy group of the tri-alkoxysilane compound reacts with the living polymer SBR, SBR(1) with two alkoxy groups and functional group F introduced to the chain terminal is obtained (Fig.2). If two alkoxy groups of the tri-alkoxysilane compound react with the living polymer SBR, two SBR chains are bonded, and a coupled polymer (2) with one remaining alkoxy group and functional group F introduced at the bonding site is produced. In addition, if three alkoxy groups of the tri-alkoxysilane compound react identically with the living polymer SBR, only functional group F is introduced, and a three branch star polymer (3) having no alkoxy groups is produced. It becomes important to increase the proportion of

production of SBR (1) with many alkoxysilyl groups introduced to express fuel efficiency performance in silica compounding systems.

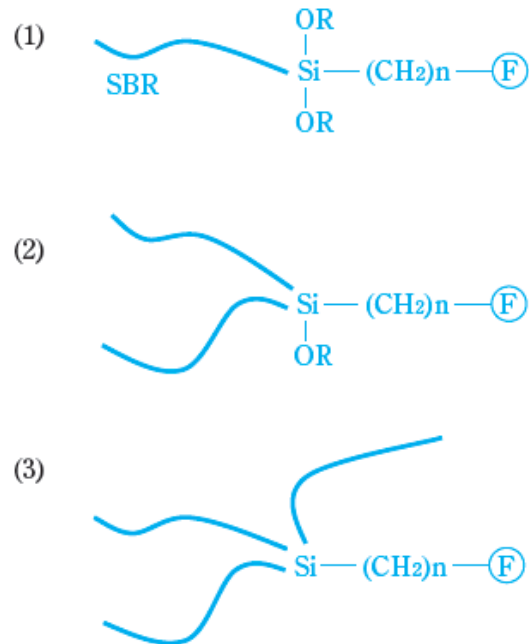


Figure2. Resulting SBR structures (1)-(3)

4-2. Next generation multifunctional SBR

We have not only introduced multiple functional groups at the chain terminals but also along the chain at multiple sites.

We synthesized polymers with the same type of functional group introduced in different numbers and sites. Specifically, we synthesized ones with the functional groups introduced on both ends of the polymer chain and ones with the functional groups introduced in the middle and at the end of the chain of the polymer for polymers where two functional groups were introduced, and for polymers where three functional groups were introduced, we synthesized ones where the functional groups were introduced at substantially even intervals along the chain. The structures and performance evaluation results for the polymers obtained are summarized in Table 1. A value measured using a Lubke resilience tester at 60°C according to JIS K-6255 was used for the resilience, which is one index of fuel efficiency performance. The larger the value for resilience is the more superior fuel efficiency performance is indicated.

Table 1. Evaluation results of multi-functional polymers.

	Mw	ML 1+4 100°C	Resilience
	35.7	56	57
	34.8	51	64
	37.7	63	62
	29.5	53	65

While there was always a functional group introduced on one end of the polymer in both of the polymers where two groups were introduced, the polymers with three groups introduced all introduced the functional groups along the chain. In the case of the functional groups used this time, the resilience value gave better results in all cases than for the polymers with one modified terminal. The more the number of functional groups is increased, the higher the resilience is, and in comparing two types of polymers with two functional groups introduced, the polymers with functional groups introduced at both terminals gave better results than the polymers with functional groups in the middle and chain terminal. It is predicted that these results will vary greatly according to the type of functional group introduced, and it is possible that performance not possible up to now will be expressed through molecular design that makes use of the characteristics of functional groups.

BIODEGRADABLE POLYMER COMPOSITES OF POLY(LACTIC ACID) BLENDS AND NATURAL FIBERS

Oral presentation

S. Pivsa-Art^{1*}, W. Pivsa-Art^{1,2}, H. Yamane² and H. Ohara²

¹ *Department of Chemical and Materials Engineering, Faculty of Engineering, Rajamangala University of Technology Thanyaburi, Thailand*

² *Department of Biobased Materials Science, Kyoto Institute of Technology, Kyoto, Japan*
Corresponding author email address: sommai.p@en.rmutt.ac.th

Abstract - Polymer composites are essential materials due to their advantages on light weight, high mechanical properties and good processability. Polymers for the composites are petroleum-based plastics and are durable to degradation which resulted in environmental problems from their wastes. Therefore, biodegradable polymers and natural fibers are attractive materials for environmental friendly composites. Poly(lactic acid) is a biodegradable polymer having potential to replace the conventional plastic. The PLA/biodegradable polymer blends and natural fibers were fabricated and their properties were evaluated for processing applications. Poly(3-hydroxybutyrate-*co*-valerate) (PHBV) poly(butylensuccinate-*co*-adipate) (PBSA) were selected to blend with PLA. PLA/PHBV blends reinforced with bamboo fibers (BF) were prepared using a twin screw extruder. The content of BF in composites was 5, 10 and 20 phr. Their mechanical properties were slightly decreased due to phase separation of the polymers and the reinforced fibers. For another composites fabrication method, the PLA/PBSA blend reinforced with jute fiber using Micro-braiding technique was developed. It was found that polymer blends of PLA/PBSA of 90:10 and 85:15 by weight could be fabricated to fibers suitable to prepare braided yarns. The unidirectional oriented braid yarns with core jute fibers were compressed at 180 °C to give the biocomposites. The ratio of polymers and fibers was 73:27 by weight. The melting temperatures of PLA in the fibers from polymer blends and in the compressed samples were found to be similar in the range of 149-153°C. The results indicated that the different fabrication process has no effect to the thermal property of the blends. The tensile strength of PLA/PBSA/Jute composites increased up to 65% compared with the polymer blends. The braided yarn of PLA/PBSA ratio 85:15 by weight reinforced with jute as a core was prepared to analyze the biodegradability. The braided yarn shows slightly decreasing of their mechanical property but their biodegradability is excellent. The ratio of PLA/PBSA was 85/15. Compression molding of the braided yarn gave composites but their mechanical properties were decreased. Biodegradability measurement of the braided yarns of PLA/PBSA/Jute shows potential for agricultural application of the composites.

Keywords: Polymer composites, Biodegradable polymers, Poly(lactic acid), Natural fibers.

RECENT DEVELOPMENT OF DIRECT FIBER FEEDING INJECTION MOLDING

Oral presentation

Hiroyuki HAMADA¹

¹ Department of Advanced Fibro-Science, Kyoto Institute of Technology, Japan
Corresponding author email address: hhamada@kit.ac.jp

Abstract -GF/Recycled-PET

1. Introduction

In this study aims to produce the fiber reinforced thermoplastics in order to receive the superior properties. This technique called the direct fiber feeding injection molding is known as DFFIM, which can reduces compounding processes that leads to the fiber breakage during also. The glass fiber reinforce RPET composite (GF/RPET) were studied the effect of processing windows and effect of glass fiber loading content on mechanical properties.

2. Experimental

The high quality commercial recycled PET pellets (RPET), which were recycled from pet plastic bottle, were supplied by Negoro Sangyo Co., Ltd. with IV of 0.65 dl/g and molecular weight of 12,600 g/mol. The EX-1844 grade of glass fiber roving with the number of bundle is 2000 and 4000 from Nippon Electric Glass Co., Ltd., Japan with the sizing agent for PET were used as reinforcing fiber. The dumbbell specimens were made by 30 tons injection machine (TOYO MACHINERY & METAL CO.,LTD TI-30F6, Japan). The matrix feeding screw speed (MFS) were varied from 20, 40 and 60 rpm and screw speed of injection unit was fixed at 180 rpm. The injection temperature was set at 200-270°C with 60°C cooling temperature and 20 second cooling time.

3. Effect of fiber content on mechanical properties

Fig. 2 (a) and (b) show tensile properties and flexural properties of GF/RPET composite, respectively. They indicate that the decreasing of MFS, which led to be higher fiber loading content in GF/RPET composites, has an effect with improving of the mechanical properties. All of tensile modulus, tensile strength, flexural modulus and flexural strength values directly significantly increase with increasing fiber loading content of GF/RPET composite.

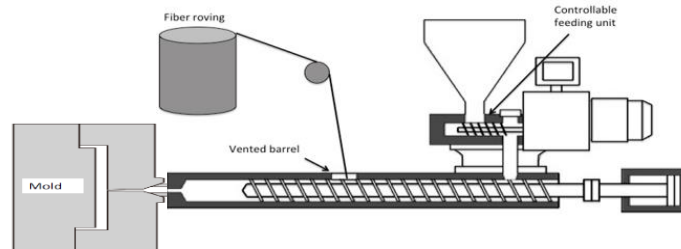


Fig.1 Concept of DFFIM(Direct Fiber Feeding Injection Molding)

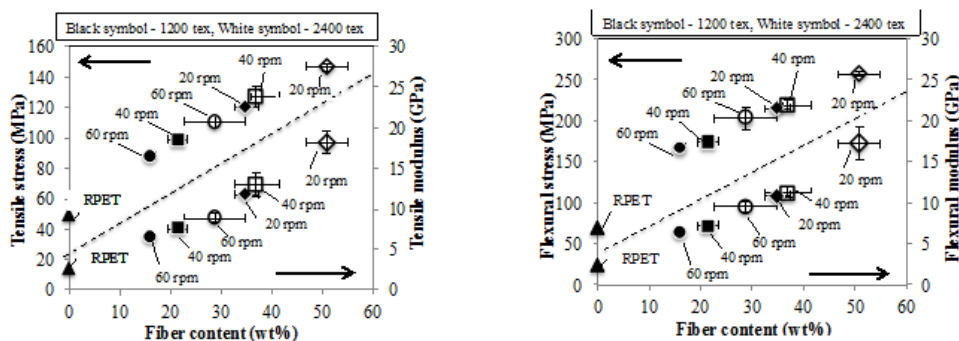


Fig. 2 (a) Tensile properties and (b) Flexural properties

Keywords: DFFIM, Injection Molding, Glass Fiber, Composite materials

POLYETHYLENE-THERMALLY REDUCED GRAPHENE NANOCOMPOSITES: COMPARISON OF MASTERBATCH AND DIRECT MELT MIXING APPROACHES ON MECHANICAL, THERMAL, RHEOLOGICAL AND MORPHOLOGICAL PROPERTIES

Oral presentation

V. Mittal^{1*}, and A.U. Chaudhry²

¹Department of Chemical Engineering, The Petroleum Institute, Abu Dhabi, UAE

²Department of Materials Engineering, Colorado School of Mines, USA

Corresponding author email address: vmittal@pi.ac.ae

Abstract - Two routes of nanocomposite generation viz. masterbatch method and direct melt mixing were compared in the current study in relation with the properties of the polyethylene-thermally reduced graphene nanocomposites compatibilized with functional polymers. Filler dispersion was observed to improve in the masterbatch method due to preferential interactions of compatibilizer with the filler, before melt mixing with the matrix polymer. This also translated into improved mechanical properties as more than 2 times increment in tensile modulus was observed in the composite HDPE/G/5 EAA/MB (41%, masterbatch method) as compared to HDPE/G/5 EAA/MM (20%, melt mixing method). In addition, different compatibilizers also influenced the properties to different extent owing to their physical interactions with the filler, however, composites generated with masterbatch were always superior in extent of property enhancements. Increasing the compatibilizer content to 10% also caused varying degree of matrix plasticization. The storage modulus as well as the complex viscosity of the HDPE/G/5 EAA/MB composite was the highest as compared to HDPE/G/5 EMAZ/MB and HDPE/G/5 EVA-MA/MB composites. HDPE/G/5 EAA/MB and HDPE/G/5 EMAZ/MB composites did not show any decrease in degree of crystallinity as compared to pure polymer, whereas the corresponding composites generated with melt mixing exhibited slight decrease in the crystallinity. The composites were observed to have enhanced thermal stability as compared to HDPE. 5% EAA based composites exhibited even higher thermal stability than HDPE/G composites due to improved filler dispersion. Composites generated with masterbatch approach had also higher degree of phase mixing than the corresponding melt mixed composites. In addition, optimization of chemical binding of the filler with the compatibilizer during the masterbatch approach would also be discussed for polyethylene-chlorinated polyethylene nanocomposites with graphene.

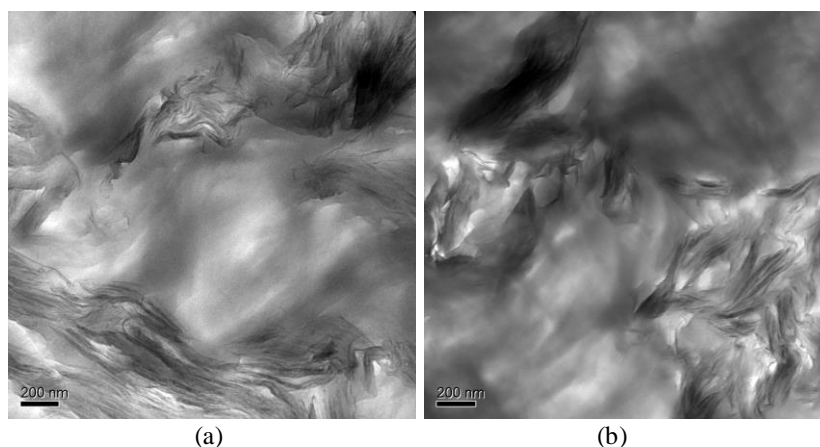


Figure 1. Comparison of morphology of nanocomposites generated by (a) direct melt mixing and (b) masterbatch approach.

(EAA: ethylene acrylic acid copolymer, EVA-MA: ethylene vinyl acetate-graft-maleic anhydride, EMAZ: ethylene methacrylic acid copolymer with zinc ion, MB: masterbatch approach, MM: melt mixing approach)

Keywords: thermally reduced graphene, nanocomposites, morphology, modulus, compatibilizer, thermal stability.

EFFECT OF SURFACE PRE-TREATMENT OF SUBSTARATE ON WETTABILITY OF METAL NANO-INK

Oral presentation

T. Saito^{1*}, Y. Yokoyama¹, T. Kawaguchi¹ and I. Satoh¹

¹ Department of Mechanical and Control Engineering, Tokyo Institute of Technology, Japan

Corresponding author email address: tsaito@mep.titech.ac.jp

Abstract - Metal nano-particle has great potential to change optical, thermal, and electric properties. One attractive application in recent years is the printable electronic circuits as metal nano-ink. To ensure the reliability of the printed circuits, improvement of the adhesion strength between metal nano-ink and substrate is important. In this study, thin Au coat was introduced to the substrate surface, and their effects on the spreading of silver nano-ink was experimentally investigated. In the experiment, the contact angle variation of the silver nano-ink was measured on glass plate and polyimide film which surface treatment condition was individually changed. The stain size of a single droplet was also measured so as to discuss the control of the circuit width. The results showed that the contact angle of the ink was complexly changed with the Au coat thickness. Therefore, precise design of surface treatment is important to correctly control the spreading process for metal nano-ink.

Keywords: Nano-ink, Surface treatment, Surface wetting

1. Introduction

Metal nano-ink has great possibility to the fabrication technique of printable electronics such as electric circuits and devices, and inkjet printing or screen printing is often used for this purpose. However, the authors believe that metal nano-ink still has more possibility for broader application. As the fundamental knowledge, the wetting control of nano-ink and the improvement of adhesion strength to the substrate are important. In this study, thin Au coat was sputtered to the substrate surface so as to control the wetting condition of silver nano-ink, and its effect on the adhesion strength of the ink was experimentally investigated.

2. Experimental Procedure

Nano-silver ink (A-1, Mitsubishi Materials Electronic Chemicals Co., Ltd.) was used in this study. Cover glass plate (S7213, Matsunami Glass Ind., Ltd.) and polyimide film of 12.5 μm thickness (Kapton 50H, DuPont-Today Co., Ltd.) were used as the substrates. The substrate surface was coated with Au thin layer as the pre-treatment by using physical vapor deposition (SC-701AT, Sanyu Electron Co., Ltd.). Coated thickness was controlled by the sputtering time and it was evaluated as 33, 100, 200, 300, and 400 \AA .

To investigate the influence of pre-treatment for substrate, contact angle was measured by the contact angle meter (DMs-400, Kyowa Interface Science Co., Ltd.) For each measurement, 1 μL of nano-silver ink was precisely measured and moved to the substrate surface with the specially designed needle. Instantaneous contact angle was measured at 1 second after the needle release. After 24 hours dry at the room temperature, adhesion strength change with and without pre-treatment was evaluated by the texture analyzer (TA_XT 2i, Stable Micro Systems Ltd.), and the stain diameter of the ink was measured. Measurement conditions for the adhesion test was as follows; Probe diameter 5 mm, 2 seconds pushing at 49.05 N, Pull up rate of the probe 2mm/s.

3. Results and Discussion

As shown in Fig. 1 (a), the contact angle on the metal surface was larger than that of glass and polymer surface. However, the adhesion strength was improved in case of the metal surface (Fig. 1 (b)). From these results, it was indicated that the wettability of the nano-ink consisting of dispersed nano-particles and solvent was unrelated to the adhesion strength. Effect on the adhesion strength by Au coat for the substrates was investigated, and its impact was not large enough. To improve the reliability of the micro-scale wiring, the small spreading size and strong adhesion of the nano-ink are desirable. Therefore, the obtained data points through the measurement were plotted as the adhesion strength vs stain size of the nano-ink. The result showed that good adhesion strength of 11.6 MPa was obtained on the glass substrate with Au coat of 200 \AA , and its stain size was 3.0 mm.

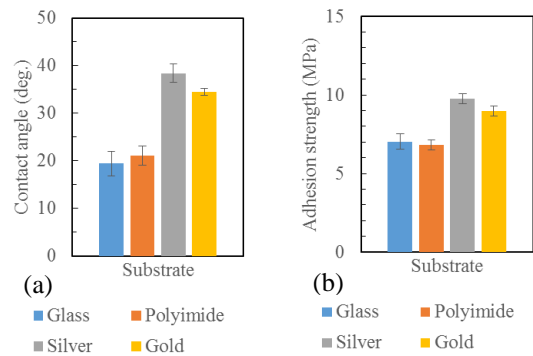


Fig. 1 Variation of the contact angle and adhesion strength

ELECTROSPINNING OF POROUS POLYMER NANOFIBERS AND THEIR APPLICATIONS AS FUNCTIONAL MATERIALS

Oral presentation (keynote speech)

Xuehong Lu*, Junhua Kong, Yuliang Dong, Huiqing Wu

School of Materials Science and Engineering, Nanyang Technological University, Singapore

Abstract Electrospinning has been well established as an effective route for producing polymer nanofibers. In comparison with various methods used to generate polymer nanofibers, electrospinning is one of the easiest techniques to obtain long nanofibers with uniform diameter. Furthermore, it allows facile manipulation of nanofiber morphology, such as creating surface pores or interpenetrating pores in the nanofibers. Such porous polymer nanofibers have attracted increased attention in recent years owing to their potential for a wide variety of applications. In this keynote talk, our recent work on electrospun porous polymer nanofibers will be introduced, with the focuses on morphology control, nanofiber collection method, fabrication of porous polymer nanocomposite nanofibers and applications of electrospun porous polymer and nanocomposite nanofibers as functional materials for various applications.

Firstly, the potential of surface-modified electrospun porous polymer nanofibers for enhancing moisture wicking of textiles (Fig. 1) and improving functions of water treatment membranes will be discussed. Then, a liquid collection method for modifying electrospun porous polymer nanofibers will be introduced. This method allowed us to use porous polystyrene nanofibers as templates to create porous carbon nanofibers with novel morphologies for energy storage applications (Fig. 2). Finally our recent work on electrospun porous nanocomposite nanofibers will also be introduced. The effects of incorporation of different types of inorganic nanoparticles on the porous morphology of the nanofibers as well as the underlying mechanism will be illustrated.

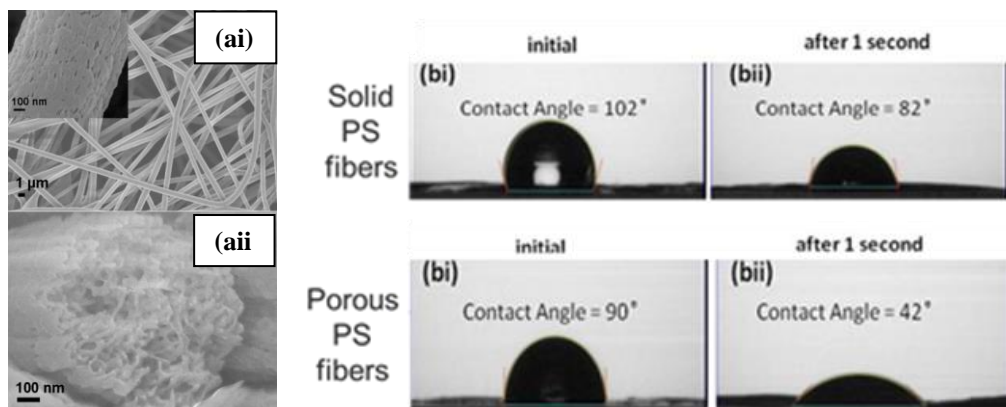


Fig. 1 (ai) FESEM images of electrospun porous polystyrene (PS) nanofibers coated with polydopamine (PDA) and (a ii) the cross-sectional view of a coated PS porous nanofiber. (b) Change of water contact angle of the coated solid and porous PS nanofibrous mats with time.

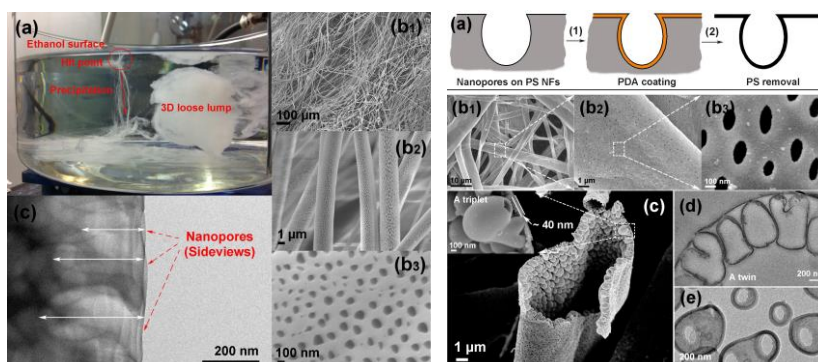


Fig. 2 (Left) (a) Collection of electrospun PS porous nanofibers using ethanol. (b₁-b₃) Morphology of the as-prepared PS nanofibers. (Right) (a) A scheme showing that the surface pores could be used as templates to create PDA nanocups. (b₁-b₃) FESEM images of the fibers after removing PS. (c-e) Morphology of the carbonized PDA nanocups.

Keywords: electrospinning, nanofibers, functional materials

NANOSTRUCTURED ADDITIVE-ENHANCED HIGH PERFORMANCE SUPERHYDROPHOBIC COATING MATERIALS

Oral presentation

Y. Hong and J. W. Xu*

*Institute of Materials Research and Engineering, Agency for Science, Technology and Research (A*STAR), Singapore
Corresponding author email address: jw-xu@imre.a-star.edu.sg*

Abstract - Superhydrophobic coatings are able to deliver many functions such as water-repellent, anti-sticking, contamination prevention, reducing fluid drag and self-cleaning. Therefore they have been paid much attention because of its wide potential applications in many areas, including energy conversion, waterproof textiles, smart structural coating materials, and microfluidics. Numerous artificial superhydrophobic surfaces have been developed by using a low surface energy material in combination with a particular surface roughness. Morphologies of superhydrophobic surface can be facilely controlled by various nanostructures, such as nanoparticles, nanowires, nanotubes. On the other hand, fluorine-containing materials and even perfluoropolymers were widely used for superhydrophobic coating due to low friction coefficient and reduced adhesion to surfaces. This talk will summarize recent advance of superhydrophobic materials in my group and a variety of potential industry applications will be addressed.

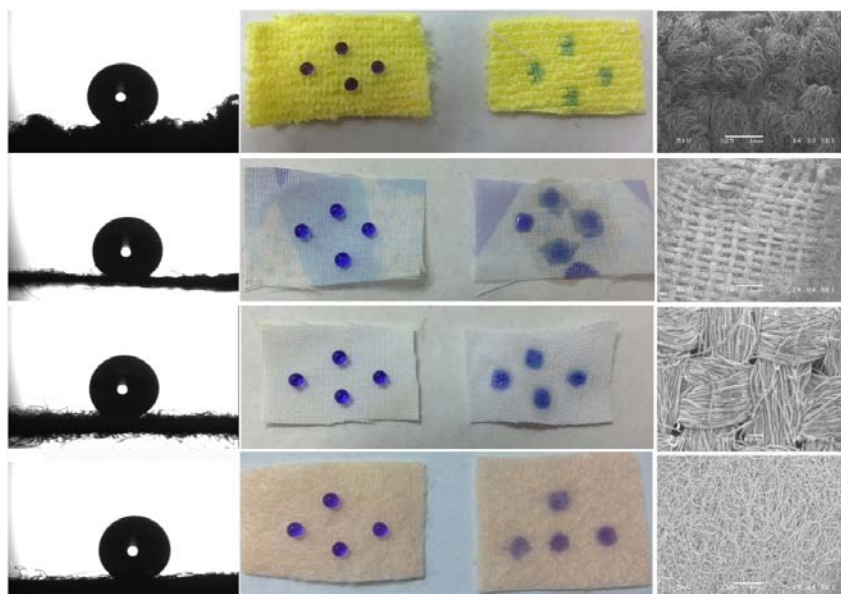


Figure 1. The wetting behavior of water droplets on various commercial textiles

Keywords: Superhydrophobic coating; Polyhedral oligomeric silsesquioxane; Nanostructured additives.

References:

- (1) Tuteja, A.; Choi, W.; Ma, M.; Mabry, J. M.; Mazzella, S. A.; Rutledge, G. C.; McKinley, G. H.; Cohen, R. E. *Science* **2007**, *318*, 1618-1622.
- (2) Ganesh, V. A.; Nair, A.S.; Raut, H.K.; Tan, T.T.Y.; He, C.; Ramakrishna, S.; Xu, J. *J. Mater. Chem.*, **2012**, *22*, 18479-18485.
- (3) Xu, J.; Li, X.; Cho, C. M.; Toh, C. L.; Shen, L.; Mya, K. Y.; Lu, X.; He, C. *J. Mater. Chem.*, **2009**, *19*, 4740-4745.

IN SILICO PROCESSING OF POLYMERS

Oral presentation

A. Soldera*

*Department of Chemistry, Quebec Center for Functional Materials, Université de Sherbrooke, Canada
Email address: Armand.Soldera@USherbrooke.ca*

Abstract –

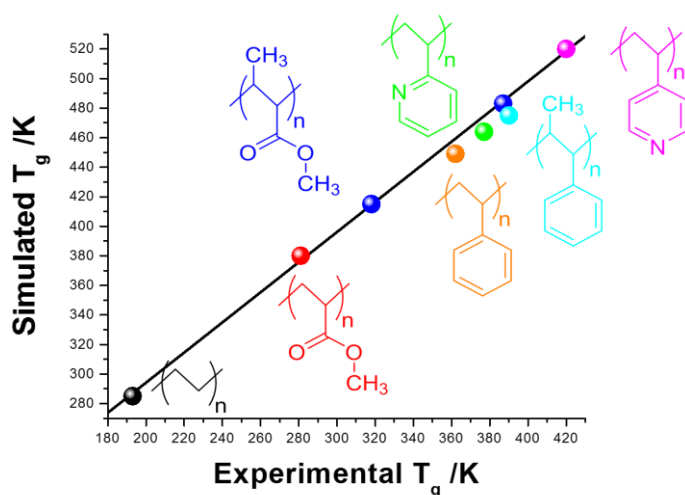
This presentation is an overview of the simulation tools available to assist engineers and experimentalists in the design and the processing of materials. There is definitely a gap between the traditional engineering approach and the atomistic simulation methodology. While one works with complex systems constituted of polymers whose very structure is known only from industries commercializing them, the other studies ideal systems. The polymers are therein mainly pure homopolymers with low number of defects. The question that will be thus addressed in this presentation is: Is simulation able to tackle problems encountered by polymer engineers during the synthesis, processing and scale-up of various compounds? One method allowing to answer this question is to reveal the domain where the TOP-DOWN and BOTTOM-UP approaches actually intersect.

In fact, the link between the micro- and the macro-structures is far from being straightforward. To describe real systems, a series of models with a specific set of rules and restrictions following chemical, physical and thermodynamical guiding principles is required. These models must be chosen accurately to efficiently describe the system of interest. More specifically, each scale needs a certain level of approximation to address the specific problem. To ascertain accuracy of the representation, validation with experiments is a crucial step. To illustrate this intimate link between experiments and simulation in addressing engineering problems, several examples stemming from collaborations between our lab and engineers from various industries are discussed.

The first part is dedicated to the preparation of the simulated system. Reaching the mechanical equilibrium, as it is experimentally the case, is shown to be the crucial step. To extract efficient conclusions from simulations, a validation step is nevertheless mandatory. As it is shown in the figure below, a linear relationship is demonstrated between simulated and experimental glass transition temperatures for a series of vinylic polymers. Further and more complex simulations can then be fostered. In particular, predicting the effect of pressure on the melting temperature could be of great interest in the processing of novel polymeric compounds. Finally, examples related to an increase in performance of polyelectrolyte membranes for fuel cells are investigated, with an emphasis on the possible increase in proton conductivity through the effect of polydispersity and the shearing of membranes.

Keywords: molecular dynamics, glass transition, melting temperature, PEMFC

Figure: Simulated and experimental glass transition temperatures for a series of vinylic polymers.



MEASUREMENT OF GAS-PRESSURE DISTRIBUTIONS INSIDE MOLD CAVITY DURING GAS-VENTING PROCESS BY SMALL-DIAMETER MELT PRESSURE SENSOR

Oral presentation

H. Yokoi^{1*} and T. Shimizu¹

¹ Institute of Industrial Science, The University of Tokyo, Japan
Corresponding author email address: hiyokoi@iis.u-tokyo.ac.jp

Abstract - Based on the newly-developed measuring mold in which the measurement point can be shifted by moving the cavity block with the thin sensor installed, gas-pressure distributions were successfully measured to evaluate the gas-venting performance for different gas-vent configurations. The results are summarized in the following. (1) Gas-vent effects decreased exponentially according to the decrease in the cross-sectional area of the gas-vent flow channels. (2) Under the same cross-sectional area of the gas-vent flow channel, the shallower the gas-vent channel, the less the gas-vent effects become. (3) Moreover, even in the same total cross-sectional area, multi-grooves vent units have poorer gas-vent effects than single-groove ones.

Keywords: Gas-vent, Gas pressure distributions, Injection molding

1. Introduction

In the designing of the gas-venting system for injection molds, it is very important to efficiently discharge air or gas out of the mold cavity in a short time during the melt filling process. However, little technical data is available on how much the setup positions and the detailed profiles of gas-vent systems influence the gas-venting performance because there are no practical evaluation methods. Under such circumstances, we have developed a method of measuring gas-pressure distribution inside a mold cavity during the melt filling stage using a thin-diameter pressure sensor which can be moved along the cavity width direction¹. By applying this measuring mold, we attempted to measure the pressure distributions just before the gas-vent zone under different configurations of gas-vent system in order to evaluate each gas-venting performance.

2. Fundamental Structure of Measuring Mold of Gas-pressure Distributions and Experimental Methods

In this experiment, we measured the gas pressure distributions inside a tiny region in front of the gas-vent zone parallel to the cavity end wall. Since the diameter of conventional gas-pressure sensors is usually too large to measure the pressure at any minute spot, a piezoelectric sensor with a thin pressure head for measuring melt pressures was utilized instead of the conventional one. For the purpose of measuring the whole area from the cavity center to cavity sides, the sensor-installed block-

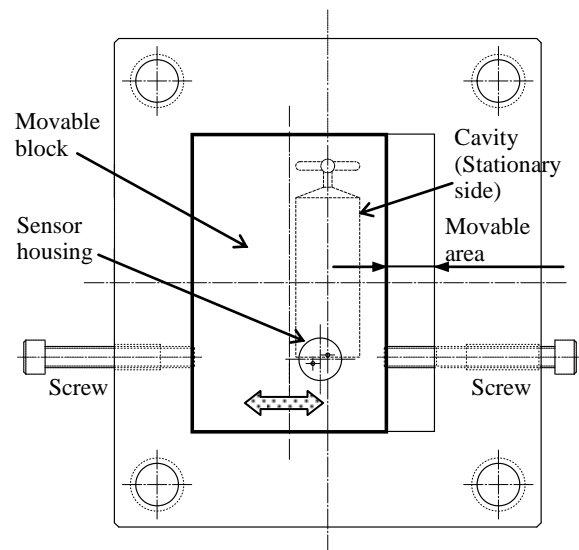


Fig.1 Mold structure for measuring gas pressure distributions (Movable side)

insert can be driven along the cavity width inside a stationary-side mold base (Fig.1). The rectangular cavity size is 75mm in length, 30mm in width, and 2mm in thickness, the parting-face structure of which is shown in Figs. 2 and 3. At the end of the cavity, a gas-vent block is fixed as shown in Fig.4. Based on this mold structure, we can easily evaluate gas-venting performance by measuring the pressure distribution for each block by changing the gas-vent block with different configurations of gas-vent systems. Table 1 shows the dimensions of each gas-venting system from V0 to V10. In the experiments, all the gas/air was released not through the parting

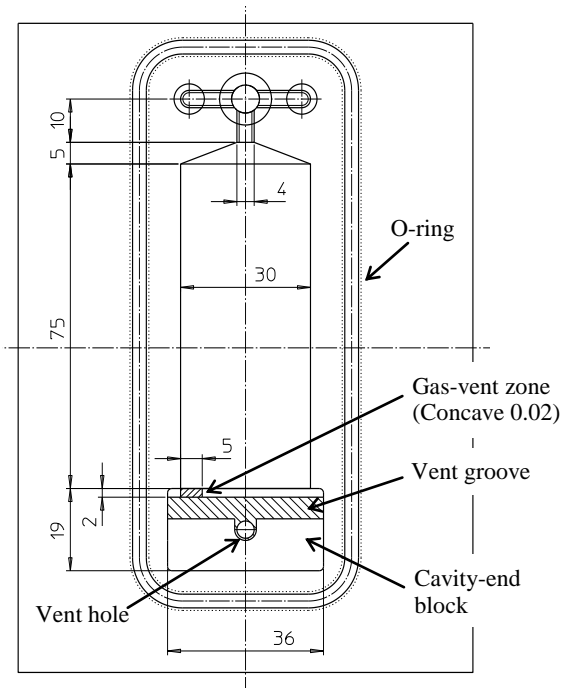


Fig.2 Dimension of cavity block for stationary side (Unit: mm)

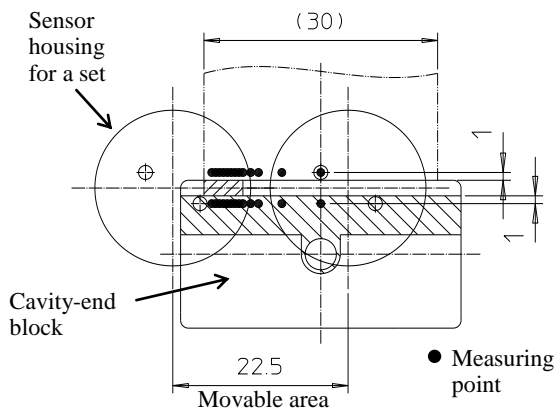


Fig.3 Cavity-end block and pressure measuring points (Unit: mm)

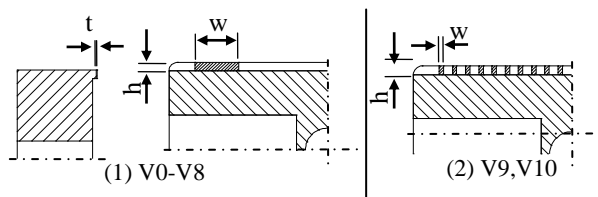


Fig.4 Dimension of cavity-end block

Table 1 Dimension of gas-vent zone for the evaluation experiment

Shape	w [mm]	h [mm]	t [mm]	A* ¹ [mm ²]
V0	0	—	0	0
V1	5	1	0.015	0.15
V2	10	1	0.015	0.30
V3	15	1	0.015	0.45
V4	5	1	0.03	0.30
V5	5	2	0.015	0.15
V6	2.5	1	0.015	0.075
V7	5	1	0.0075	0.075
V8	5	3	0.015	0.15
V9	0.5	1	0.015	0.15
V10	0.5	1	0.0075	0.075

*1 ; A=w×t×20

faces but through venting holes due to the complete sealing mechanism of the parting faces in between movable and stationary molds, as well as in between all the block-inserts.

As for the thin-diameter melt pressure sensor, the 6006B (Priamus System Technologies AG) of 1.8mm in diameter was used. Along the line ($y = 1\text{mm}$) away from the cavity end ($y = 0\text{mm}$), gas pressures are measured by shifting the sensor's location every 2mm from the cavity side ($x = 1\text{mm}$) to the center ($x = 15\text{mm}$). The resin used is ABS220 (Asahi Kasei Chemicals Corp.), and the molding conditions are as follows; Resin temperature = 220°C, Mold temperature = 40°C, Injection rate (IR) = 16.8 cm³/s, 50.6 cm³/s.

3. Results and Discussions

Figure 5 exemplifies the gas pressure curves measured with V0 and V1 in IR = 50.6cm³/s and $x = 1\text{mm}$, where the injection start time is 0s. In the case of V0 (No gas-vent condition), the gas pressure rapidly increased as the melt approached to the end of cavity, then hesitated for a moment just before the melt reached the sensor head, and suddenly rose as if it draw a vertical line, which corresponds to the melt's compression stage. The reason why the rising tendency of gas pressure curves once hesitated may be because the melt front velocity instantaneously decreased due to the high gas pressure generated through the gas compression process by the flowing melts. Compared to V0, the gas pressure in V1 dropped significantly, and there were no hesitation tendency and vertical rising behaviors of the pressure curve, which were observed in V0 just before the melt reached the sensor head. Because of

the gas-venting effect from the cavity end in V1, the gas was not compressed rapidly, resulting in the phenomenon of less rise in pressure.

In order to more precisely analyze the correlation between the gas-vent configurations and the pressure distributions along the cavity width direction, we compared the widthwise pressure profiles drawn with peak values extracted at each position for various gas-vent configurations. The examples of the measurement result are described in Fig.6. The gas pressure gradually drops toward the cavity side, from the cavity center up to around $x = 5-7\text{mm}$, then it starts to rise, even though there is no obvious correlation with the setup location of gas-vent zone. Such a behavior of the gas pressure change curve is thought to be caused by a specific cavity filling pattern called “ear flow”, where the flow front advances more near both cavity sides to form a dent filling pattern. As a result, the flow front advanced more at two locations away from both cavity sides by 5 to 7mm, to contact the cavity end wall at the two locations at the very beginning. The gas pressure dropped due to the easy release process of the compressed gas toward both sides of the above-mentioned contact zone. Subsequently the extruded gas was compressed resulting in the rise of the gas pressure around the cavity side ($x = 0\text{mm}$) and center ($x = 15\text{mm}$) areas.

For the purpose of quantitatively evaluating the venting effect for each gas-vent configuration, we attempted to relatively compare the average data of all the gas-pressure peak values within a measuring range right before the end wall of the cavity end. Here, it can be assumed that the higher the gas-pressure, the higher is the gas-compression ratio, i.e., the lower the gas-venting effect becomes. The relationship between the average gas-pressure and total cross-sectional area “ S ” of the gas-vent flow channel at low injection rates ($\text{IR} = 16.8\text{cm}^3/\text{s}$) is demonstrated in Fig.7. When the land width “ h ” of the gas-vent channel is 1mm, the smaller area “ S ” was found to damage the gas-venting effect exponentially. Moreover, the multi-grooves gas-vent proved to have rather low venting performance compared to the single-groove gas-vent, which consisted of the same gas-vent depth “ t ” and area “ S ” as those in the above multi-grooves vent. In the same area “ S ” but at a different depth “ t ”, the venting effect of the multi-grooves unit drastically differs from that of the single-groove unit as the area “ S ” decreases, especially in gas-vent channel narrower than 0.2mm^2 . In addition, the shallower the depth “ t ” of the gas-vent channel, the lower was the gas-venting effect.

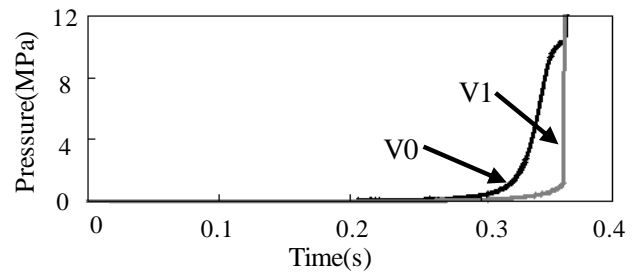
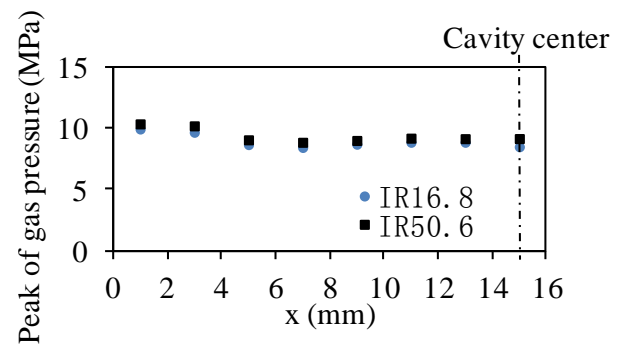
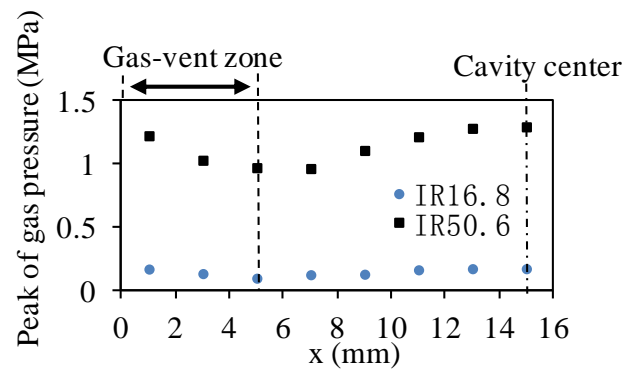


Fig.5 Change curves of gas pressure measured by cavity pressure sensor ($\text{IR} = 50.6\text{cm}^3/\text{s}$, $x = 1\text{mm}$)



(1) Shape V0



(2) Shape V1

Fig.6 Distribution of the peak values of gas pressure along the cavity width direction just before the cavity-end

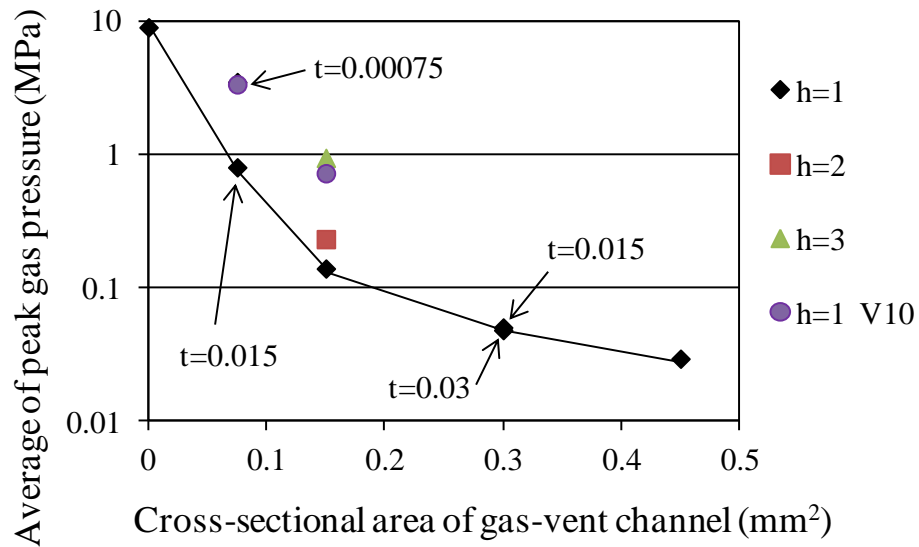


Fig.7 Relationship between the average of gas peak pressure and the cross-sectional area of gas-vent channel

4. Conclusions

We succeeded in measuring not only the time-sequential pressure change curves at minute spots but also the widthwise distributions of gas-pressure peak values along the end zone of the cavity as a final melt filling area by using a thin-diameter pressure sensor, which is usually applied for measuring melt pressures. Based on the measuring mold in which the measurement point can be shifted by moving the cavity block with the thin sensor installed, gas-pressure distributions were measured to evaluate the gas-venting performance for different gas-vent configurations.

The results are summarized in the following.

- (1) Gas-vent effects decreased exponentially according to the decrease in the cross-sectional area of the gas-vent flow channels.
- (2) Under the same cross-sectional area of the gas-vent flow channel, the shallower the gas-vent channel, the less the gas-vent effects become.
- (3) Moreover, even in the same total cross-sectional area, multi-grooves vent units have poorer gas-vent effects than single-groove ones.

Reference

- 1) H.Yokoi, H.Yokoyama: JSPF Tech. Papers, pp.51-52 (2013) *in Japanese*

TOWARDS HIGH-PERFORMANCE POLYPROPYLENE/EXPANDED GRAPHITE/CARBON NANOTUBES TERNARY COMPOSITES WITH SIGNIFICANTLY ENHANCED THERMAL AND ELECTRICAL CONDUCTIVITY VIA CONSTRUCTING DOUBLE PERCOLATED FILLER NETWORK

Oral presentation

K. Wu¹, Y. Xue¹, W.X. Yang¹, S.G. Chai², F. Chen¹ and Q. Fu^{1*}

¹*College of Polymer Science and Engineering, State Key Laboratory of Polymer Materials Engineering, Sichuan University, Chengdu 610065, China*

²*Guangdong Shengyi Technology Limited Corporation, Dongguan, 523039, China*

Corresponding author email address: qiangfu@scu.edu.cn

Abstract - Carbon based fillers, such as carbon nanotubes (CNTs) and expanded graphite (EG), are often used to improve the thermal and electrical conductivity of polymer matrix. Unfortunately, although a typical percolation phenomenon of electrical conductivity is usually observed as the filler content reaches to the threshold, thermal conductivity usually presents a trend of a linear increase with filler content. In this work, we will report the importance of the formation of double percolated filler network in polypropylene (PP) matrix with dense CNTs network located within loosened EG network in tailoring electrical and thermal properties of polymer composites. Besides achieving a much high electromagnetic interference shielding effectiveness of 58.5 dB, a sharp increase of both thermal and electrical conductivity is observed for the first time. Morphological observation via TEM, SEM and rheology confirm the formation of tiny-sized CNTs network within EG network as the CNTs content is above 2 wt %. And effective medium theory model reveals that formation of double percolated filler network, in which three types of connections exist between EG and EG, EG and CNTs as well as CNTs and CNTs, could effectively reduce the interface thermal resistance of CNTs. Our work provides a new strategy for the preparation of polymer composites with excellent thermal and electrical conductivity via constructing double percolated filler network.

Keywords: double percolated filler network, thermal conductivity, electrical conductivity

SYNERGISTIC DISPERSION OF CARBON NANOMATERIALS IN POLYMER NANOCOMPOSITES

Oral presentation

T.X. Liu*

State Key Laboratory of Molecular Engineering of Polymers, Department of Macromolecular Science,
Fudan University, China

Corresponding author email address: txliu@fudan.edu.cn

Abstract - Homogeneous dispersion or full exfoliation of nanoparticles in polymer matrices is one of the most important factors to achieve high-performance and multifunctional polymer nanocomposites. In the past years, our research group is making efforts to realize homogeneous and stable dispersion and high orientation of carbon nanomaterials (e.g., graphene, carbon nanotubes) in aqueous and organic media as well as polymer matrices by using physical “hybridization” approach via effective combination (via hydrogen bonding, π - π stacking, electrostatic interaction, etc) among different kinds of nanoscale building blocks (e.g., carbon nanomaterials, clay) (Figure 1). The hybrid nanofillers thus prepared are prone to be homogeneously and stably dispersed in different media or polymer matrices, which are beneficial for fabricating high-performance polymer nanocomposites. In this presentation, some recent work progress on achieving co-exfoliation or synergistic dispersion and stabilization of carbon nanomaterials in aqueous and organic media and polymer matrices are discussed.

Keywords: Carbon nanomaterials; Hybridization; Synergistic dispersion; Polymer nanocomposites.

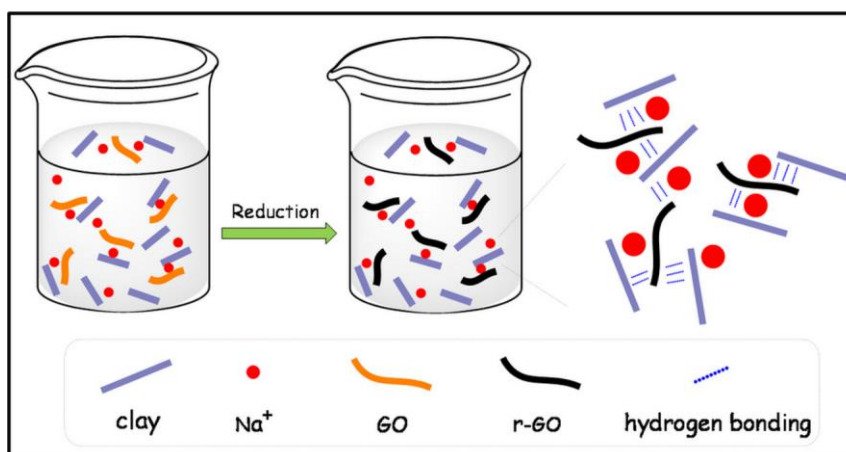


Figure 1. Proposed mechanism for the assisted-dispersion of reduced graphene oxide (r-GO) with nanoclay (sodium montmorillonite) as an effective dispersant.

Acknowledgements: The financial support from the National Natural Science Foundation of China (51125011, 51433001) is appreciated.

References

1. C. Zhang, L. L. Ren, X. Y. Wang, T. X. Liu, *J. Phys. Chem. C* **2010**, *114*, 11435-11440.
2. C. Zhang, W. W. Tjiu, W. Fan, Z. Yang, S. Huang, T. X. Liu, *J. Mater. Chem.* **2011**, *21*, 18011.
3. C. Zhang, S. Huang, W. W. Tjiu, W. Fan, T. X. Liu, *J. Mater. Chem.* **2012**, *22*, 2427.
4. Z. Yang, M. K. Liu, C. Zhang, W. W. Tjiu, T. X. Liu, H. Peng, *Angew. Chem. Int. Ed.* **2013**, *52*, 3996.

Redox-responsive poly(amido amine)s from trifunctional amines for bioapplications

Oral presentation

Ye Liu

*Institute of Materials Research and Engineering, A*STAR (Agency for Science, Technology and Research), 3Research Link, Singapore 117602. Email: ye-liu@imre.a-star.edu.sg*

Abstract - Through exploring the large difference in thiol concentration between intra- and extracellular space, thiol-responsive disulfide containing polymers, which will be stable in intracellular spaces but be degraded in extracellular spaces, are promising for many bioapplications such as targeted drugs/genes delivery and bioimaging[1, 2]. On the basis of our previous fundamental understanding of the reactivity sequence of three types of amines in trifunctional amino compounds in Michael addition polymerization[3-5], we develop thiol-responsive linear and hyperbranched poly(amino ester)s via Michael addition polymerization of trifunctional amines and disulfide-containing bisacrylamides. These linear and hyperbranched thiol-responsive poly(amido amine)s from trifunctional amines are explored for drugs delivery,[6, 7] gene delivery,[8] bioimaging,[9] and MRI[10].

References:

1. Bauhuber, S., Hozsa, C., Breunig, M., & Gopferich, A. *Advanced Materials*, 2009, 21, 3286-3306.
2. Meng, F.H., Hennink, W. E., Zhong, Z.. *Biomaterials*, 2009, 30, 2180-2198.
3. Liu, Y. Wu, D. C., Ma, Y. X. Tang G. P., Wang S., He, C. B., Chung, T. S., Goh, S. T. *Chemical Communications*, 2003, 2630-2631.
4. Wu, D. C., Liu, Y., He, C. B., Chung, T. S., Goh, S. T. *Macromolecules*, 2004, 37, 6763-6770.
5. Wu, D. C. Liu Y., Chen, L., He, C. B., Chung, T. S., Goh, S. T.. *Macromolecules* 2005, 38, 5519-5525.
6. Wu, D. C., Loh, X. J., Wu, Y. L., Lay, C. L., Liu, Y. *Journal of the American Chemical Society*, 2010, 132, 15140-15143.
7. Cheng W. R., Wang G., Pan X. Y., Zhang Y., Tang B. Z., Liu Y. *Macromolecular Bioscience*, 2014, 14, on-line.
8. Ping Y., Wu, D. C. Kumar N. J., Cheng W. R., Lay C. L., Liu Y., *Biomacromolecules*, 2013, 14, 2083-2094.
9. Cheng W. R., Kumar N. J., Zhang Y., Liu Y. *Macromolecular Bioscience*, 2014, 14, 347.
10. Cheng W. R., Rajendran R., Gu L. Q., Ren W., Zhang Y., Chuang K. H., Liu Y. *J. Mater. Chem. B.*, accepte

Keywords: Michael addition polymerization; trifunctional amines; redox-responsive; drug delivery; gene delivery.

Enhancing Dispersion of Nanoparticles in Molten Polymers

Nopphawan Phonthammachai

Composite Research, R&D Center, SCG Chemicals Co., Ltd.

Nanoparticle dispersion in polymer matrix is one of the key challenges controlling the properties of composite structure, especially in molten polymer systems. Many efforts have been paid to improve the dispersion through particle modifications using surfactant, organic molecules and liquid media. The aggregation of particles was minimized but still cannot reach fully exfoliated or mono-dispersed level, while the organic residue left inside composite structure causing the poor properties and scale-up development is also a concern. Therefore, the combination between chemical treatment and processing technique was proposed. The in situ grafting of targeted surface modified molecules those were not affecting the thermal stability and overall properties, but improving the particle dispersion in molten polymeric system, was applied. Together with unique processing technique, the dispersion of nanoparticles was dramatically enhanced.

PROCESSING CONDITIONS AND PROPERTIES OF NONWOVEN KENAF REINFORCED ACRYLIC BASED POLYESTER COMPOSITES

Oral presentation

M.S. Salim¹, M.F. Ahmad Rasyid² and Z.A Mohd. Ishak*

¹*School of Materials and Mineral Resources Engineering,
Universiti Sains Malaysia, Engineering Campus, 14300, Nibong Tebal, Pulau Pinang*

²*Cluster for Polymer Composites
Science and Engineering Research Centre, Universiti Sains Malaysia,
Engineering Campus, 14300 Nibong Tebal, Pulau Pinang*

Corresponding author email address: zarifin@usm.my

The awareness of green and more sustainable products and technologies has gained much interest in the recent years. Realizing the importance of using eco-friendly material, a new cross-linkable acrylic-copolymer resin has been introduced as an alternative for the production of greener composites due to the non-corrosive, no volatile-organic compounds (VOCs) and no emission of carcinogenic gases during cross-linking. Within this current work, the dependence of the mechanical properties of nonwoven kenaf fibre (KF) reinforced acrylic based polyester composites on the processing variables (temperature, time and pressure) of the compression moulding has been studied. Prior to moulding, nonwoven KF with areal density of 1300 g/m² was impregnated by acrylic based resin using impregnation line. Through optimization of the processing conditions, a light weight composite of consisting of 45w_t% fiber weight fraction with flexural strength and modulus of 49.50 MPa and 4.32 GPa respectively, has been produced. The curing behaviour of acrylic resin was investigated by differential scanning calorimetry (DSC). As expected, the time required for curing was found to decrease with the increases of temperature. Figure 1 shows the effect of pressing time and pressure on the flexural strength and modulus of the composite fabricated at 200°C .

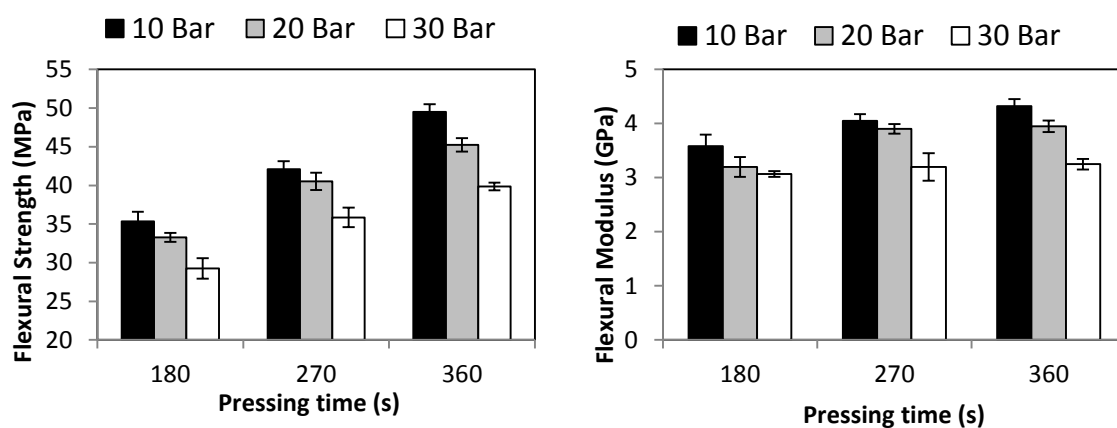


Figure 1: Flexural properties of composites at different processing conditions

It is known that the mechanical behaviour of fibre-reinforced composites is dependent on a complex interplay of the properties of the constituent phases of resin, fibre, and the interfacial region (wettability). Surface treatment was applied to natural fibre in order increase the wettability towards resin aiming at enhancing the mechanical properties of the developed

composites. A prominent treatment of mercerization by NaOH was conducted to the KF to investigate the surface modification and the changes in surface energy. The AFM topographies of treated KF are shown in Fig 2 (a-b) and Table 1 exhibits the outcomes of fibre characterization and effect of fibre treatment on the flexural properties of composites.

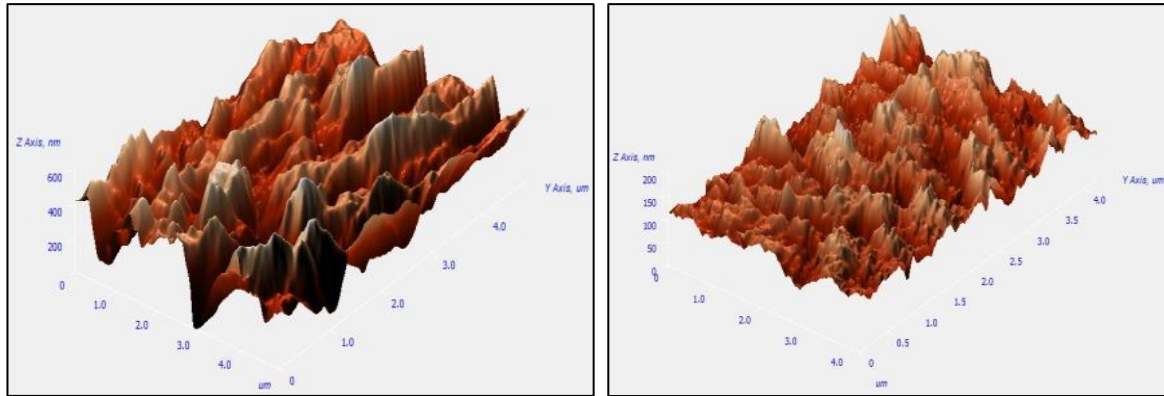


Figure 2: Surface topography of KF a) untreated, b) alkali treated

The increasing value of area peak density of alkali treated KF indicates the increasing amount of peaks per unit area on KF surface due to the removal of lignin and hemicellulose. This occurrence provides better interfacial adhesion between fibre and matrix by enhancing the specific contact area, promoting friction between them; thus higher mechanical properties of the resulting composites can be expected. The improvement in interfacial adhesion may quantitatively shown by surface energy evaluation. Higher value of surface energy for alkali treated KF suggest that better wettability towards acrylic resin could be achieved. This explains for the superior properties of the alkali treated composite as compared to the untreated counterpart.

Table 1: Effect of alkali treatment on the properties of KF and its composites

KF treatment	Density (g/cm ³)	Area peak density (μm ⁻¹)	Surface Energy (mN/m)	Composites	
				Flexural Strength (MPa)	Flexural Modulus (GPa)
Untreated	1.25	10.60	58.66	49.5	4.32
Alkali	1.39	37.10	97.05	59.9	5.01

The optimal flexural properties was obtained using pressing temperature, pressing time and pressing pressure of 200°C, 360s and 10 Bar, respectively. It was observed that alkali treatment plays a significant role in intensifying the wettability of KF and an effective method to further enhance the properties of the composites. The developed of nonwoven KF reinforced acrylic based polyester composite has the potential to be integrated for automotive applications due to their high specific stiffness and strength values.

FABRICATION OF MICRO-NEEDLE ARRAY USING BIOCOMPATIBLE POLYMERS BY PRECISION MOLDING

KN presentation

Hiroshi Ito

*Graduate School of Science and Engineering, Yamagata University,
4-3-16 Jonan, Yonezawa, Yamagata 992-8510, Japan
Corresponding author email address: ihiroshi@yz.yamagata-u.ac.jp*

Abstract –

We have studied the surface structure formation by precision processing technology. The micro-needle array was produced from a biocompatible material that was a relatively minimal effect on the human skin by needle remaining. Microneedle array features were fabricated by micro-injection molding and casting using biocompatible polymers such as polycarbonate (PC), polypropylene (PP), polylactic acid (PLA) and polyvinyl alcohol (PVA). PC and PP based microneedle array features with high aspect ratio for needle height was fabricated by several injection molding techniques. Injection compression molding and injection molding with super critical carbon dioxide fluid with or without vacuum process inside the cavity of mold were performed. Effects of process parameters on processability and surface replication of the molded parts were evaluated. The height replication ratio for micro-needle was improved by using injection compression molding. Moreover, the effect of vacuum process inside cavity of mold under filling process was small. However the height replication ratio for micro-needle showed the highest values using the injection molding with super critical carbon dioxide fluid with vacuum inside the cavity of mold process. In addition, the thermal nanoimprint with surface modification of polyvinyl alcohol was coated with hyaluronic acid solution biocompatible material was applied. The replication ratio of fabricated micro-needle array was also measured by 3D laser microscope. The molded article surface morphology was observed by scanning electron microscope. The presence of hyaluronic acid on the surface of the micro needle array was measured by the fourier transform infrared spectrophotometer. The micro-needle array surface indentation was measured by using a nano indenter. This study was found that, the hyaluronic acid can be able to coat on micro needle array surface with the thickness of the hyaluronic acid lower than 10 μm . The micro-needle array with the maximum in the replication rate of 94% of the micro-needle array can be fabricated and its elastic modulus was about 0.63 GPa.

Keywords: Precise molding, Micro-needle array, Biocompatible polymers, casting, thermal imprint

SKIN STRUCTURE AND SCRATCH BEHAVIOR OF INJECTION MOLDED POLYPROPYLENE

Masaya Kotaki

Kaneka US Material Research Center, Kaneka Americas Holding, Inc.,
800 Raymond Stotzer Pkwy, College Station, TX 77843, USA

*email: masaya.kotaki@kaneka.com

Abstract

Surface appearance is an important characteristic of products in many different applications. Damages created on the surface significantly reduce the quality of the products in many cases. Therefore the understanding of the surface fracture mechanisms and the means to improve the resistance to the surface damages are required to improve the quality of products. The objective of this study was to understand the relationship between structure near the surface and surface fracture behavior under scratch loading of polypropylene (PP).

A progressive load scratch test according to ISO 19252 was performed in this study to investigate surface fracture behavior of injection molded PP. Effects of injection speed, molecular weight of PP and slipping agent on scratch behavior are investigated. Highly oriented skin structure was obtained at ultra-high injection speed of 1000 mm/s. Skin structure was also significantly influenced by molecular weight and slipping agent in terms of molecular orientation, crystalline orientation and types of crystalline structure. The skin structure was characterized by Raman spectroscopy and wide-angle X-ray diffraction (WAXD). The results showed that the degree of molecular/crystalline orientations and β -phase content in the skin layer significantly improved scratch properties of PP (Fig.1).

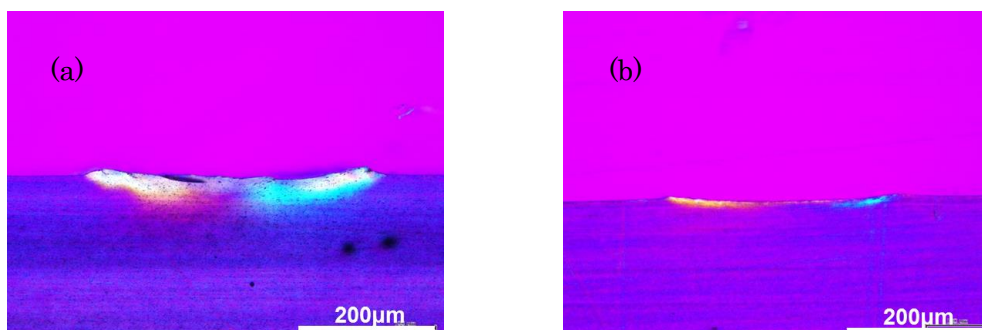


Fig. 1 Polarized optical micrographs of transverse subsurface of scratch damages; (a) low molecular weight and (b) high molecular weight injection molded PP.

SEMI-INTERPENETRATING NETWORK OF POLYOXYMETHYLENE WITH OLIGO-BENZOXAZINE VIA REACTIVE BLENDING

N. Mantaranon¹, V. Jiratrakan³, and S. Chirachanchai^{1,2,*}

¹ *The Petroleum and Petrochemical College, Chulalongkorn University, Bangkok, Thailand*

² *Center for Petroleum, Petrochemical, and Advanced Materials, Chulalongkorn University, Bangkok, Thailand*

³ *Thai Polyacetal Co.,LTD, Padaeng Industrial Estate,1Padaeng Rd., Map-Ta-Phut, Rayong 21150, Thailand*

*Corresponding author email address: csuwabun@chula.ac.th

Abstract – Polyoxymethylene (POM) is an engineering thermoplastic using in daily life products such as gears, springs, chains, screws, nuts, fan wheels, pump parts, valve bodies, etc. However, POM is sensitive to acid hydrolysis and oxidation including thermal degradation. In term of chemical structure, the degradation of POM results in formaldehyde, which not only leads to the instability but also the generation of toxic vapor. To overcome this limitation, in the past, various approaches such as copolymerization with trioxyethylene¹, blending with other thermoplastics² or formaldehyde absorbing agents³ were reported. The fact that benzoxazine is a phenolic resin obtained from phenol, amine, and formaldehyde via Mannich reaction and polybenzoxazine can be obtained by further curing via ring opening polymerization, this leads us to an idea to stabilize POM by allowing benzoxazine formed in POM. Here, by simply adding bis-phenol A and methylamine and carrying out the reactive melt-blending with POM, the benzoxazines and oligobenzoxazines is successfully generated in POM matrices as confirmed by FTIR and 1H NMR. The process also leads to oligobenzoxazine as identified by GPC to conclude the semi-interpenetrating network of POM and benzoxazines. The polymer obtained exhibits attractive properties such as non-formaldehyde generation, flame retardance, and dimensional stability. The presentation will include other related properties of the semi-interpenetrating polymer obtained, especially in the forms of sheets and nanofibers.

Keywords: Polyoxymethylene, Reactive blending, Benzoxazine, Semi-interpenetrating network.

1. Masamoto, J.; Iwaisako, T.; Chohnno, M.; Kawamura, M.; Ohtake, J.; Matsuzaki, K. *Journal of Applied Polymer Science* **1993**, *50* (8), 1299-1305.
2. Pielichowski, K.; Leszczyńska, A. *Journal of Thermal Analysis and Calorimetry* **2004**, *78* (2), 631-637.
3. Hu, Y.; Ye, L.; Zhao, X. *Polymer* **2006**, *47* (8), 2649-2659.

The Relationship Between Morphology and Impact Toughness of Poly(L-lactic acid)/Poly(ethylene oxide) Blends

Oral presentation

Jin-Ze Li^a, Jerold M. Schultz^b, and Chi-Ming Chan^{*a,c}

^a*Department of Chemical and Biomolecular Engineering
The Hong Kong University of Science and Technology
Clear Water Bay
Hong Kong.*

^bDepartment of Chemical Engineering,
University of Delaware, Newark, Delaware 19716.
USA

^cDivision of Environment
The Hong Kong University of Science and Technology
Clear Water Bay
Hong Kong.

Corresponding author email address: kecmchan@ust.hk

Abstract - The morphology of unannealed and annealed poly(L-lactic acid)/poly(ethylene oxide) (PLLA/ PEO) (80/20) and (50/50) blends were studied using polarized optical microscopy (POM), scanning electron microscopy (SEM) and time-of-flight secondary ion mass spectrometry (ToF-SIMS). Samples were annealed at temperatures between 90 and 125 °C. The size of PLLA spherulites increased dramatically with annealing temperature. SEM analyses of the water-etched PLLA/PEO blend samples and ToF-SIMS analyses of the blend thin films indicated that the PEO content and thickness of the interspherulitic boundary region was higher in the (50/50) blend than in the (80/20) blend. The impact strength of the PLLA/PEO (80/20) blend was higher than that of the neat polymer for all preparation conditions, and for both the impact strength decreased with increasing crystallization temperature (and therefore also with increasing spherulite size). The impact strength of the (50/50) blend was always higher than those of the neat polymer and the (80/20) blend, and increased remarkably with crystallization temperature. The size of the PEO-rich domains within the spherulites was significantly larger in the (50/50) blend than in the (80/20) blend. The size of the intraspherulite PEO-rich domains, the size of the spherulites, and the width and PEO content of the boundary layer all acted to determine the impact toughness of the PLLA/PEO blends. It is suggested that the (50/50) blend exhibits this behavior because it could undergo plastic deformation within and between PLLA spherulites and sustain a higher level of stress in the interspherulitic regions.

Keywords: blends, poly(lactic acid); poly(ethylene oxide); spherulite size; interspherulitic boundary width, impact toughness.

Acknowledgement

The work described in this paper was fully supported by the Research Grants Council of the Hong Kong Special Administrative Region, China (grant nos. 600210 and 600513).

EFFECT OF PRE-ANNEALING ON 3-D ORIENTATION DEVELOPMENT BEHAVIOR DURING SIMULTANEOUS AND SEQUENTIAL BIAXIAL STRETCHING OF POLY(ETHYLENE NAPHTHALATE) FILMS

Oral presentation

T. Abe, W. Takarada and T. Kikutani *

Department of Organic and Polymeric Materials, Graduate School of Science and Engineering
Tokyo Institute of Technology, Japan

Corresponding author email address: kikutani.t.aa@m.titech.ac.jp

Abstract - Effect of pre-annealing on orientation development behavior of poly(ethylene naphthalate) (PEN) films was investigated through in-situ measurement of stress and three dimensional optical retardation during the batch-type simultaneous and sequential biaxial stretching process. Amorphous and non-oriented PEN films were pre-annealed under the conditions of different temperatures and periods before the stretching. Degree of pre-annealing was evaluated through the analysis of crystallinity applying the Differential Scanning Calorimetry (DSC) measurement.

It is well known that naphthalene ring tends to orient parallel to the film surface along with the orientation of molecular chain in the film plane in both uni-axial and bi-axial stretchings of PEN films. The refractive index anisotropy of the resultant films is significantly affected by the planar orientation of naphthalene ring since polarizability in the direction parallel to the planar naphthalene ring is much higher than that in the perpendicular direction. Typical wide-angle X-ray diffraction patterns of PEN films after simultaneous equi-biaxial stretching to the draw ratio of 3 x 3 and after sequential biaxial stretching to the MD (Machine direction) x TD (Transverse direction) draw ratios of 3 x 3.33 are shown in Fig. 1. Difference in the intensity distribution of α -form (010) reflection in the through view clearly indicates the different orientation mode between simultaneous and sequential stretchings. In addition, appearance of α -form (-110) reflection in ND (normal direction) in the edge and end views indicates the planar orientation of naphthalene ring.

Effect of the degree of pre-annealing on 3-D refractive indices for the simultaneous and sequential biaxial stretching is shown in Fig. 2. In case of simultaneous biaxial stretching, refractive index in the MD increased whereas that in ND decreased with the increase of the crystallinity of original film, which corresponds to the degree of pre-annealing. On the other hand, in case of the films of sequential biaxial stretching, refractive indices in MD and TD decreased whereas that in ND increased with the increase of crystallinity. It should be noted that the difference between MD (or TD) and ND refractive indices corresponds to the out-of-plane birefringence. These results indicated that the effect of pre-annealing is opposite for the two different stretching modes, i.e. in case of the simultaneous biaxial stretching, orientation of molecular chain and/or naphthalene ring along the film plane was enhanced, whereas in case of the sequential biaxial stretching, such orientation was suppressed by the pre-annealing.

Keywords: poly(ethylene naphthalate), biaxial stretching, planar orientation, birefringence

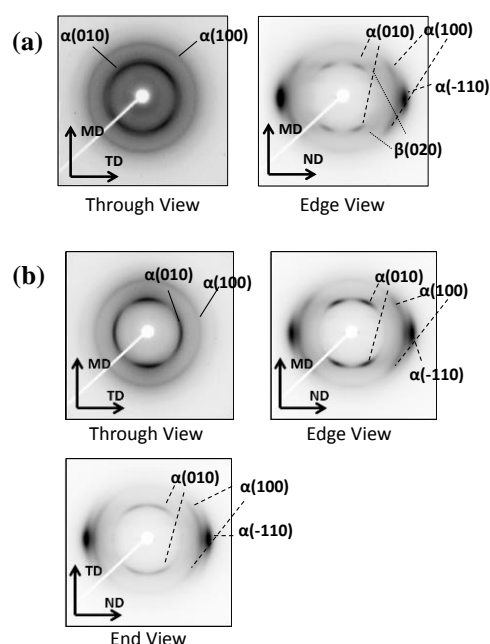


Fig.1 WAXD patterns of (a) simultaneously and (b) sequentially stretched PEN films.

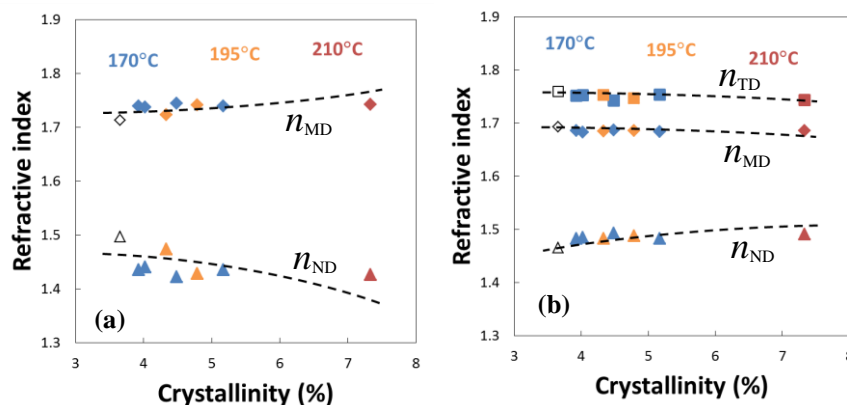


Fig.2 Variations of the 3-D refractive indices of (a) simultaneously and (b) sequentially stretched PEN films with the degree of pre-annealing.

SPINNABILITY AND THEORETICAL ANALYSIS OF THE SPUNBOND PROCESS FOR POLYPROPYLENE

Oral presentation
Toshitaka Kanai^{1*}

¹ *KT Polymer: 5-7-14 Kuranamidai, Sodegaura, Chiba, Japan - toshitaka.kanai@ktpolymer.com*

ABSTRACT:

The spinnability of the spunbond process for polypropylene (PP) was investigated and narrow molecular weight distribution PP had good spinnability. Furthermore, adding low modulus polypropylene (LMPP) to PP could control the crystallization speed and gave good spinnability. A small amount of LMPP was found to stabilize the high speed spinning of PP and very fine fibers were obtained. The theoretical analysis of the spunbond process was set up and applied to PP and its blends. The effect of blending LMPP to high tacticity PP on the spinnability of the spunbond process was investigated. From the calculated results, it was speculated that the improvement of spinnability originated from the suppression of crystallization speed, strain rate in the spinning process and high molecular weight.

Keywords: spunbond, polypropylene, spinnability, crystallization speed

NANOCOMPOSITES BASED ON BIOMASS CHARCOAL WITH MULTIFUNCTION

Oral presentation

Aimiao Qin^{1*}, Ning Tian¹, Lei Liao², Jianwu Sun¹ and Chun Wei¹

¹ College of Materials Science and Engineering, Guilin University of Technology, China

² College of Environmental Science and Engineering, Guilin University of Technology, China

Corresponding author email address: 2005032@glut.edu.cn

Abstract Nanocomposites with multifunction based on bamboo charcoal (BC) and sisal fiber charcoal (SFC) including nano-metal oxide/BC and nano-metal oxide/SFC were successfully prepared via precipitation-impregnation and hydrothermal method, respectively. Structures and morphologies of the nanocomposites were characterized by XRD, SEM, EDS, and etc. The nanocomposites exhibited well properties of adsorption, photocatalysis degradation and energy storage. The effects of experiment conditions on the nanocomposite properties were studied. For removal of organic dyes, the results showed that smaller particle size of biomass charcoal in the composites and at slow pH value of the dye solution had a better ability of absorption and photocatalytic degradation. For example, when the particle size of BC was smaller than or equal to 75 μm , the removal rate of rhodamine B (RhB), methylene blue and acid fuchsin was close to 90% under UV irradiation for 15min, the highest removal rate of nano-ZnO/BC composite for RhB and acid fuchsin was at the pH = 2 and pH = 5.4, respectively. Using as anode materials for lithium-ion batteries, nanostructured metal oxide/SFC composites exited a higher specific capacity and cycle stability, and also showed a synergistic effect on the electrochemical performance. Furthermore, the synthesis conditions such as temperature, heating rate and reaction time had much effect on the performance of nanocomposites based on BC and SFC.

Keywords: Nanocomposite; biomass charcoal; bamboo charcoal; sisal fiber charcoal; multifunction

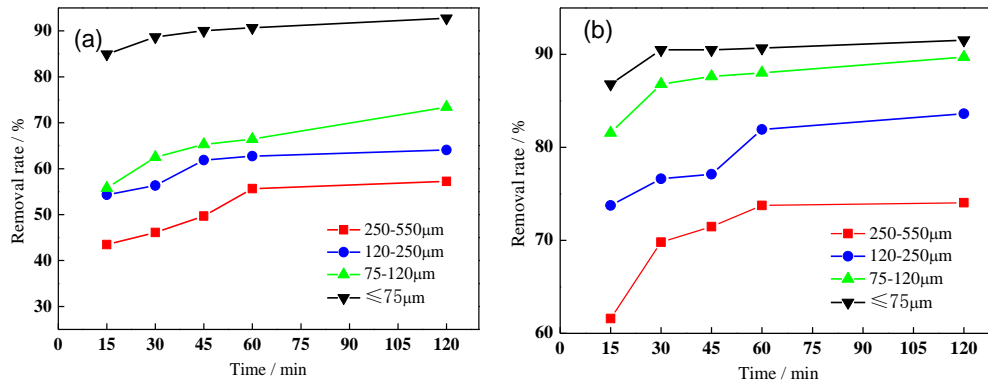


Figure 1 Removal rate of organic dyes by nano-ZnO/BC composites with different particle size of BC: (a) RhB, (b) acid fuchsin.

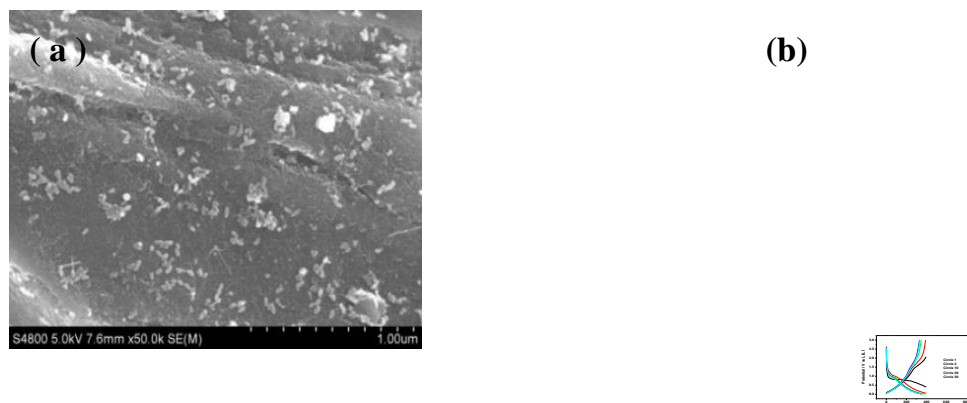


Figure 2 SEM image(a) and discharge/charge curves (b) of iron metal/SFC nanocomposite

EFFECT OF CELLULOSE NANOFIBER ON SCRATCH RESISTANCE OF POLY(VINYL ALCOHOL) COMPOSITES

Oral presentation

S. Konagaya^{1*}, T. Ooshio², H. Furuhashi¹, T. Yamada² and K. Noma³

¹ Graduate School of Engineering, Nagoya University, Japan

² Graduate School of Natural Science & Technology, Kanazawa University, Japan

³ Division of Research and Development, Fujidenolo Co. Ltd., Japan

Corresponding author email address: konagaya@apchem.nagoya-u.ac.jp

Abstract – Recently scratch resistance of the plastic or glass surface has been required to be improved for their application to the touch panels and smart phones. Addition of hard nano-particles such as silica (SiO₂), alumina (Al₂O₃) and carbon nanotube (CNT) to the polymer composites have been studied and actually used for the improvement of scratch resistance [1,2]. The mixtures of such nano-particles with polymer binders and cross-linking agents are usually coated on the glass or plastic substrates in order to improve the scratch resistance.

Cellulose nanofiber (CeNF) is a promising material for the improvement of mechanical properties (tensile strength, modulus) of polymer composites now, since it has high crystallinity and high modulus. The tensile strength of PVA was increased twofold by the addition of 10 wt% CeNF. However there is no study on the effect of CeNF on the scratch resistance of the polymer composites. Then the authors have been studying the effect of CeNF on the scratch resistance of poly(vinyl alcohol) (PVA) composites.

PVA/CeNF composites were prepared from the mixture of CeNF/H₂O dispersion, aqueous PVA solution and a cross-linking agent (CL). The product mixture was coated on the glass substrate and dried at 110 °C for 1 hour. At that time the thickness of the dried PVA composites was adjusted to be around 10µm to get a reproducible data. The scratch resistance (pencil hardness) of the PVA composites was evaluated according to the pencil hardness test (JIS K5600-5-4). The larger the n number of pencil hardness (nH) is, the higher the scratch resistance is.

The pencil hardness of PVA/CeNF composites was increased from 2H to 5H with the increase of CeNF addition to 40 wt%. However the PVA/CeNF composites with 50 wt% CeNF showed lower pencil hardness (4H). It was found out that 30-40 wt% CeNF addition contributed to the enhancement of pencil hardness, but the excess addition of CeNF decreased the pencil hardness. In order to get a higher pencil hardness, CL was applied to the PVA/CeNF composites according to the above procedure. PVA/CeNF/CL (CL/PVA(g/g)= 0.2) exhibited a higher pencil hardness (6H) than PVA/CeNF composites, at the CeNF concentration of 30-40 wt%. It was made clear that CeNF addition was effective for the enhancement of pencil hardness (scratch resistance) of PVA composites.

In this paper the effect of CeNF on the pencil hardness (scratch resistance) of PVA composites will be spoken in detail.

References

- [1] A. Wakahara, J. Jpn. Soc. Colour Mater., 87 [9], 311-316(2014)
- [2] A. Nagasaka, Cabon (Tanso) 2013[No.259], 255-260(2013)

Keywords: Cellulose nanofiber, Poly(vinyl alcohol), Composite, Pencil hardness, Scratch resistance

EFFECT OF CROSS-SECTIONAL CONFIGURATION ON DIE SWELL BEHAVIOR AND SPIN-LINE STABILITY IN BICOMPONENT MELT SPINNING PROCESS

Oral presentation

Y. Chen, W. Takarada* and T. Kikutani

*Department of Organic and Polymeric Materials, Tokyo Institute of Technology, Japan
Corresponding author email address: takarada.w.aa@m.titech.ac.jp*

Abstract – Various kind of bicomponent fibers have been developed to change mechanical properties or add new functionalities to fiber materials. In bicomponent fibers, two or more materials are extruded through single spinneret hole and spun into single filament. Typical cross-sectional configuration of bicomponent fibers are Side-by-side, Seath-Core (S/C), Islands-in-the-Sea (S/I) and Blend. Cross-sectional configuration has an effect not only on the fiber characteristics but also on the spinning behavior or spin-line stability in melt spinning process. In this study, bicomponent melt spinning of polystyrene (PS) and polypropylene (PP) with the composition of 1:1 was performed using a spinning die for the preparation of S/I fibers with 1519 islands in the fiber cross-section and spinning behavior and die swell was investigated in several spinning temperatures.

It was found that the die swell was much larger for the S/I spin-line in comparison with that for the S/C spin-line. With the increase of the extrusion temperature, the die swell tended to be decreased. On the other hand, the die swell of blend spinning increased with the extrusion temperature. The peak position of swelling shifted to downstream in the order of Blend > S/I > S/C. These results suggested that the die swell in the S/C and S/I spinning is governed by the viscoelastic effect whereas that in the blend spinning is caused mainly by the interfacial tension between the two components. Spin-line stability decreased with increasing spinning temperature in Blend spinning whereas spin-line was stable in all spinning temperature in S/I or S/C spinning. This results show that the peak position of swelling has greater impact on spin-line stability than swelling ratio.

Keywords: melt spinning; die swell; interfacial tension.

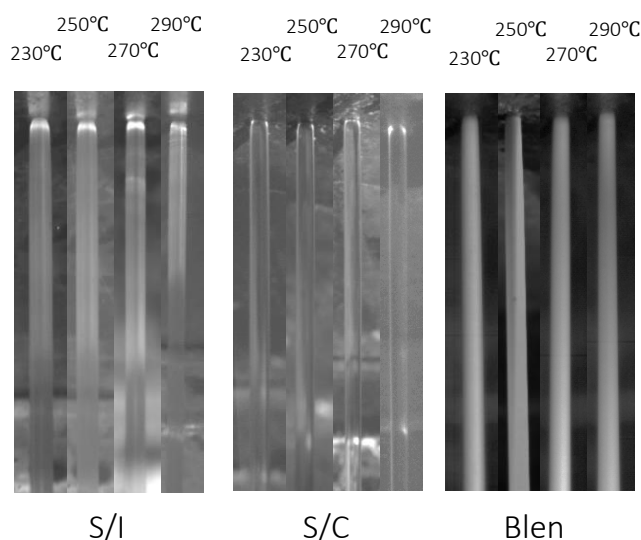


Figure 1. Photographs of free-fall S/I, S/C and blend spin-lines of PP/PS near the spinneret at different extrusion temperatures. For the spinning of blend fibers, S/C type spinneret was used.

POLYMER MELT DIFFERENTIAL 3D PRINTING AND ADVANCED MANUFACTURING

B.H.Chi^{1,2}, Y. An^{1,2}, Z.W. Jiao¹, and W.M. Yang^{1,2*}

¹ College of Mechanical and Electrical Engineering, Beijing University of Chemical Technology, Beijing, China

² State Key Laboratory of Organic-Inorganic Composite, Beijing University of Chemical Technology, Beijing, China

Corresponding author email address: yangwm@mail.buct.edu.cn

Abstract: 3D printing has become one of the most important research fields in the advanced manufacturing technology. In this paper, polymer melt differential 3D printing technology is proposed, this technology can solve problems in the traditional 3D printing, such as materials have special requirements and buckling instability of the filamentous materials. A new polymer melt differential 3D printing device is presented in this paper, this device mainly composed of a melting and plasticizing unit, solenoid valve control unit, three-dimensional motion platform, temperature control unit, pulse pressure controller and other parts. The schematic diagram and photo of the polymer melt differential 3D printing device is shown in Figure 1. The experimental research of printing cartilage tissue engineering scaffold with polyurethane elastomer was made, and the effect of process conditions on the accuracy of printing products was studied. Meanwhile, the advanced manufacturing of the polymer, which is related to 3D printing, is introduced in this paper.

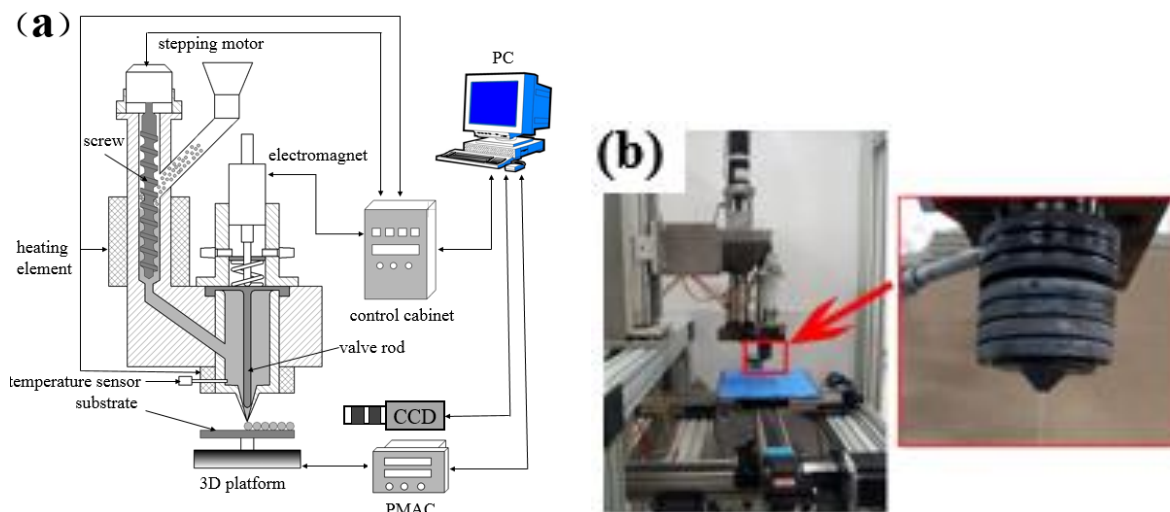


Fig.1 the schematic diagram and photo of polymer melt differential 3D printing experimental system

Keywords: 3D printing; polymer; melt differentiation; advanced manufacturing

GREEN CHEMISTRY: PREPARATION OF ENVIRONMENTALLY-BENIGN GRAFT COPOLYMERS VIA EMULSION SYSTEM

Oral presentation

Kiyoaki Ishimoto^{1*}, Warunee Ariyawiriyanan¹, Amorn Chaiyasat², and Sommai Pivsa-Art¹

¹ *Department of Materials and Metallurgical Engineering, Faculty of Engineering,
Rajamangala University of Technology Thanyaburi, Thailand*

² *Department of Chemistry, Faculty of Science and Technology,*

Rajamangala University of Technology Thanyaburi, Thailand

Corresponding author email address: ishimoto_k@en.rmutt.ac.th

Abstract-

Polymeric material has been a key factor so far, making our daily life comfortable and convenient. On the other hand, our society is nowadays faced with environmental problems caused by these products, such as rapid climate changes due to increasing carbon dioxide levels, the shortage of fossil resource, and the disposal of plastic waste.

In order to take measures to mitigate and resolve these serious issues, it is specific and effective to employ renewable resources as starting materials in materials fields from the viewpoint of green plastic. Much effort has, in fact, been paid to replace the conventional oil-based polymer with biobased polymer (BBP) derived from biomass for building a sustainable society. Poly(lactic acid) (PLA) is the representative of BBP and has been already used in a wide variety of fields. In the former study, the synthesis and characterization of graft copolymers was performed using PLA-containing macromonomers via miniemulsion system. First, macromonomers having a methacryloyl group with different PLA chain length were prepared via ring-opening polymerization of lactide, a six-membered cyclic dimer of lactic acid, in the presence of 2-hydroxyethyl methacrylate as initiator and tin octoate (Sn(Oct)₂) as catalyst. Radical copolymerization of the macromonomers was then carried out with other vinyl monomers via macromonomer technique, or grafting through method to produce graft copolymers with PLA as side chain. The copolymerization in water as solvent provided a stable emulsion system. Additionally, this investigation revealed correlative relationship between the length of PLA and the properties of their products.

The present research was especially focused on biodegradable function graft copolymers have, and designed to examine the properties of their products as well as their behaviors of the monomers used in emulsion system. In this case, it doesn't matter whether a starting material for the synthesis is based on oil resource or renewable biomass. Macromonomers having polymerizable group with various chain length was firstly prepared via ring-opening polymerization of cyclic compounds using an initiator catalyzed by Sn(Oct)₂. Secondly, graft copolymers were synthesized by using the resultant macromonomers and other vinyl monomers in water to characterize their products. These studies would be reported throughout this workshop.

Keywords: Green Chemistry, Macromonomer Technique, Emulsion System

Modification of chemically stable polymeric materials 63. Improvement in the adhesion property of polymeric materials, FRP and CFRPs for car-use

Oral presentation

H. Kanazawa and A. Inada

Department of Industrial Systems, Faculty of Symbiotic Systems Science,
Fukushima University, 1 Kanayagawa, Fukushima 960-1296, Japan: kana@sss.fukushima-u.ac.jp

Abstract Hydrophobic polymeric materials such as polypropylene, polyethylene, PET were modified by a new combination method of physical and chemical processes. The modified materials gave a durable hydrophilic property, and the improvement in adhesion, property. Poly(methyl pentene), silicone resin and engineering plastics of which modification is difficult by corona or plasma discharge treatments were modified well. Especially, polymer composites such as GFRP and CFRP for cars and aircrafts were improved, and the adhesion property of CFRP was increased much more than usual plasma discharge or a peel ply method. Modified polymeric materials were coated with water-based paints. The modified materials gave a high durability as compared with a plasma treatment and the other methods.

Keywords: surface modification, adhesive property, PP, GFRP, CFRP, water-based paint coating, printing in

1. Introduction

Polyolefins such as polypropylene (PP), polyethylene (PE), ultrahigh molecular weight PE (UHMWPE) and poly(methyl pentene) (PMP), etc. are chemically stable and their durable modification is not easy. We tried to combine two or three methods, and found that the combination of some modification techniques was effective for the modification of these stable polymeric materials. The obtained hydrophilic property was not lost for several years. The GFRP and CFRP boards were modified and the adhesion property was compared with usual plasma treatments and a peel ply method.

2. Experimental

2.1 Materials

Polymeric materials were used after washing with methanol. Commercial chemical reagents and hydrophilic reagents were used after a simple purification.

2.2 Adhesives

Poly(vinylpyrrolidone), starch, wood-use bonds, PVAC-water mixture, cyanoacrylate (CA), CA-primer set, tape type epoxy resin adhesives, etc. were used.

2.3 Treatment

Polymeric materials were activated by chemical oxidations or UV, energy irradiations. The activated polymeric materials were treated with chemical reagents

the presence of catalysts.

2.4 Adhesion strength and analysis

A bonding strength of a polymeric material bonded to other materials was measured by a tensile tester, Shimadzu AGS-H5KN.

IR and XPS spectra of materials were observed.

3. Results

3.1 Improvement in the adhesive property of CFRP (epoxy resin)

CFRP (epoxy resin) boards for car and aircraft use are adhered to each other using epoxy resin adhesives. But, the CFRP boards modified by the present KANA method gave the adhesion strength higher than unmodified ones. Table 1 gives the results of the tensile strength test of unmodified-unmodified CFRP boards, plasma-treated-plasma-treated CFRP boards, peel ply treated-peel ply treated CFRP boards, and KANA modified-KANA modified CFRP boards. The highest shear strength was obtained in the adhesion of KANA-modified boards. The adhesion property of plasma treated or peel-ply treated CFRP boards is known to be lost with time. But, KANA treated CFRP boards can be adhered to

Table 1 Adhesion shear strength test of CFRP (epoxy resin) boards adhered using epoxy adhesive and failure styles

specimen	Shear strength (MPa)	Ratio(mod./unm.)	Failure style
unmodified-unmd.	25.4	1.00	interface
plasma-plasma	35.2	1.40	cohesion
peel ply-peel ply	35.0	1.38	cohesion
KANA-KANA	51.3	2.02	cohesion+material

each other even a month after the treatment.

MOLECULAR SIMULATION OF THE EFFECT OF CHAIN TACTICITY ON DEMIXING OF POLYETHYLENE/ POLYPROPYLENE BLENDS

Oral presentation

Visit Vao-soongnern*

Laboratory of Computational and Applied Polymer Science (LCAPS), School of Chemistry, Institute of Science, Suranaree University of Technology, Nakhon Ratchasima, Thailand. E-mail: visit@sut.ac.th

Abstract - The molecular origin of the demixing behavior for 50:50 (wt/wt) polyethylene/polypropylene (PE/PP) with different tacticity of PP at the melts (473 K) was investigated by Monte Carlo simulation of coarse-grained polymer model. *Isotactic* (iPP), *atactic* (aPP) and *syndiotactic* (sPP) polypropylenes were used for blending with PE. Coarse-graining polymer chains were represented by 50 beads, corresponding to $C_{100}H_{202}$ and $C_{150}H_{302}$ for PE and PP, respectively. The simulation was performed on a high coordination lattice incorporating intramolecular interactions from the Rotational Isomeric State (RIS) model and intermolecular interactions Lennard-Jones (LJ) potential function of ethane and propane units. Chain dimensions, the characteristic ratio (C_n) and self-diffusion coefficient (D) of PE in the blends are sensitive to the stereochemistry of PP chains. Compared with neat PE melts, PE dimension was relatively unchanged in PE/iPP and PE/aPP blends but slightly decreased in PE/sPP blends. PP dimension was increased in PE/iPP and PE/aPP but decreased in PE/sPP mixture in comparison with neat PP melts. In addition, diffusion of PE and PP chains in PE/PP mixture was decreased and increased, respectively. Interchain pair correlation functions were used to detect the immiscibility of the mixtures. The tendency of demixing of PE/aPP and PE/iPP blends were weaker than that of PE/sPP blend.

Keywords: Polyethylene, polypropylene, blends, tacticity, molecular simulation

- Ref.** 1. Vao-Soongnern V., Polymer Science - Series A, 56, 928 (2014)
2. Takhulee A. , Vao-Soongnern V., Polymer Science - Series A, 56, 936 (2014)

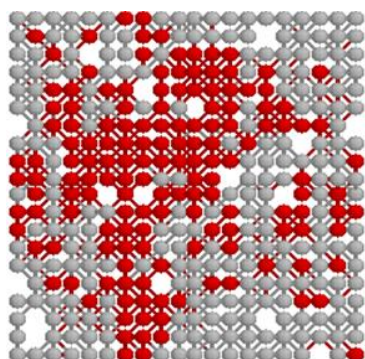


Figure 1 A cross section view of representative snapshots for PE/sPP blends (PE and PP beads are denoted by red and gray color, respectively)

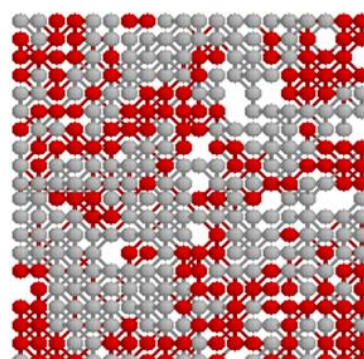


Figure 2 A cross section view of representative snapshots for PE/iPP blends (PE and PP beads are denoted by red and gray color, respectively)

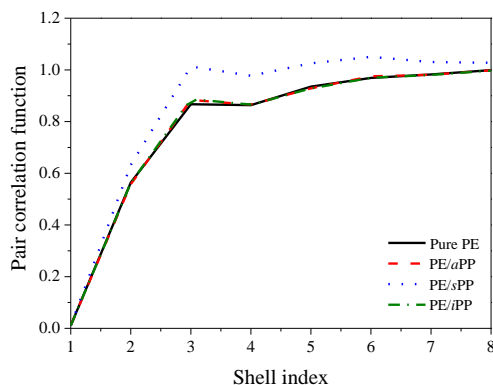


Figure 3 Pair correlation functions, $g_{PE-PE}(i)$, for monomers of PE chains in the pure PE melt and PE/aPP, PE/iPP and PE/sPP blends.

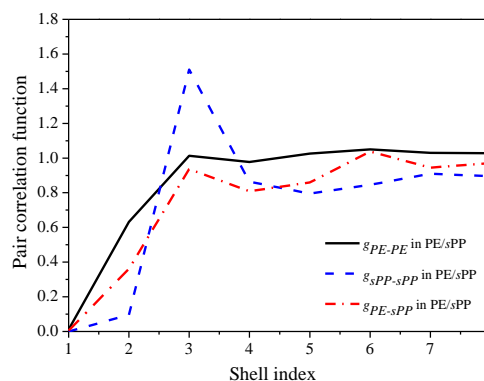


Figure 4 Pair correlation functions, $g_{PE-PE}(i)$, $g_{sPP-sPP}(i)$ and $g_{PE-sPP}(i)$ for 50:50 by weight of PE/sPP blend.

MELT-MIXING BY PITCHED-TIP KNEADING DISKS IN A TWIN-SCREW EXTRUDER

Oral presentation

T. Kajiwara^{1*}, Y. Nakayama¹, H. Takemitsu¹, S. Esaki¹, T. Takeuchi², K. Kimura² and H. Tomiyama²

¹ *Department of Chemical Engineering, Kyushu University, Japan*

² *Research & Development H.Q., The Japan Steel Works Ltd., Japan*

Corresponding author email address: kajiwara@chem-eng.kyushu-u.ac.jp

Abstract –

Twin screw extruders are widely used as a continuous mixing equipment of polymeric materials such as polymer blends and polymer composites. Our research group has been studied on the development of computer simulation technique to predict the materials behavior in a twin-screw extruder and the evaluation method of mixing performance based on the simulation results. The simulation has applied to evaluate the mixing by pitched-tip kneading discs whose tips are pitched to the screw axis. We have studied the performance of mixing elements with different combinations of stagger and tip directions for pitched-tip kneading discs. In this study, we carry out the twin-screw extrusion experiment for a blend of ABS (acrylonitrile-butadiene-styrene copolymer) and AS (acrylonitrile-styrene copolymer). We performed the morphology observation via scanning electron microscope and evaluated the diameter distribution of dispersed rubber particles. We also measured the rheological properties. We compared these results with the mixing performance obtained by the previous simulation, and discussed the melt mixing mechanism by pitched-tip kneading discs and reliability of the numerical simulation.

Keywords: Twin Screw Extruder, Polymer Blend, Numerical Simulation, Rheological Property, Morphology

POLYMER PROCESSING SIMULATION CHALLENGES IN DESCRIBING HIGHLY ELASTIC FLOWS

Oral presentation

Koki Tomioka*

*Department of Advanced Process Development, Nitto Denko Corporation, Japan
Corresponding author email address: kouki_tomioka@gg.nitto.co.jp*

Abstract –

Film casting is a widely used production process in industry. In this process, a molten polymer is extruded into a flat shape through a die, and then stretched in air by using a roll. A uniform film thickness is generally desired. However, the thickness of the film often becomes non-uniform due to phenomena such as draw resonance and die swell. These phenomena are strongly influenced by the viscoelasticity of the molten polymer, and it is desirable to develop mathematical models that can describe this influence.

A major challenge in developing such models is the description of strongly elastic flows. This is also known as the High Weissenberg-Number Problem (HWNP) since the Weissenberg number (product of fluid relaxation time and characteristic shear rate) characterizes the level of elasticity in the flow. The challenge arises because constitutive equations for polymeric liquids are highly nonlinear and very steep stress gradients can develop as a result.

Numerical methods developed before ~2000 only work for values of the Weissenberg less than ~10. Yet in film forming processes the Weissenberg number may be ~100. In the past decade, new methods to overcome these limitations have been developed. These methods are based on preserving the positive definiteness of the polymer conformation tensor, which characterizes the polymer deformation. The presentation will discuss various methods for dealing with the HWNP and their implementation in the computational fluid dynamics package OpenFOAM.

Keywords: Viscoelastic, Extrusion Process, High Weissenberg-Number Problem, Log Conformation Representation

Evaluation of Distributive Mixing in an Internal Mixer by Partially Filled Flow Analysis

Oral presentation

K. Higashi¹, S. Yamada¹, K. Fukutani¹, and Y. Yamane²

¹ *Mechanical Engineering Research Laboratory, Kobe Steel, Ltd., Japan*

² *Industrial Machinery Engineering Department, Machinery Business, Kobe Steel, Ltd., Japan*
Corresponding author email address: higashi.kosuke@kobelco.com

Abstract – Internal mixers are widely used in rubber compounding for tires. It is not sufficiently examined the distributive mixing in the mixer and a relation between a flow in the chamber and the compounding qualities. Therefore, it is important to establish flow analysis technique for developing better performance mixers and rotors. In this study, three-dimensional numerical study has been carried out to investigate the mixing flow in the batch mixers. It is assumed that mixer was partially or fully filled with isothermal rubber in the simulation. Banbury type two-wing rotors were selected as a mixing rotor. Fill factor was changed from 60 to 100 %. Phase difference between two rotors was changed from 0 to 90 deg. Particle tracking method was applied, and flow rate in a cross-section of chamber was also studied for the evaluation of distributive mixing. From the results, it was suggested that the flow through a certain cross section in a chamber does not necessarily enhance the distributive mixing, and that fill factor has significant effect on the distributive mixing. In addition, it was considered that phase difference between two rotors has a correlation with both the flow rate and the distributive mixing.

Keywords: Batch Mixer, Mixing

DYNAMIC MECHANICAL PROPERTIES OF SISAL FIBER CELLULOSE MICROCRYSTAL / UNSATURATED POLYESTER IN-SITU COMPOSITES

Oral presentation

C. Wei^{1*}, D.M. Zeng², J. Lv¹, C.B. Yu¹, Hongxia liu¹, Hongyan Li¹, Aimiao Qin¹

¹ College of Materials Science and Engineering, Guilin University of Technology, Guilin

² Super-Dragon Engineering Plastics Co., Ltd., Guangzhou

Corresponding author email address: 1986024@glut.edu.cn

Abstract: Sisal is a natural material and a potential additive to reinforce composites. In this paper, sisal fiber cellulose microcrystal (SFCM) was obtained from sisal fiber and sisal fiber cellulose microcrystal / unsaturated polyester (SFCM / UPR) in-situ resins were prepared via in-situ polymerization. Moreover, SFCM / UPR composites were produced with methods of rolling and molding. In our previous work, the mechanical properties and tribological properties of SFCM / UPR composites were significantly increased. Based on the previous studies, our further research focuses on the dynamic mechanical properties of SFCM / UPR composites. It is demonstrated that SFCM could significantly improve the dynamic mechanical properties of composites, the effect is closely related with the amount of SFCM, its dispersion in UPR matrix and interfacial interaction. When the content of SFCM was 3 wt%, at 50 °C, the storage modulus of SFCM / UPR composite was 33.22 % higher than that of pure UPR. In addition, the glass transition temperature (T_g) was shifted to a higher temperature by 7.5 °C and loss modulus was decreased by 16.24 %. The equilibrium value of relaxation modulus at 120 min was 30.52 % higher than that of pure UPR composite. Besides, the equilibrium value of creep strain at 120 min was decreased by 41.61 % compared with pure UPR composite.

Keywords: dynamic mechanical properties; sisal fiber cellulose microcrystal; unsaturated polyester; in-situ polymerization; composites

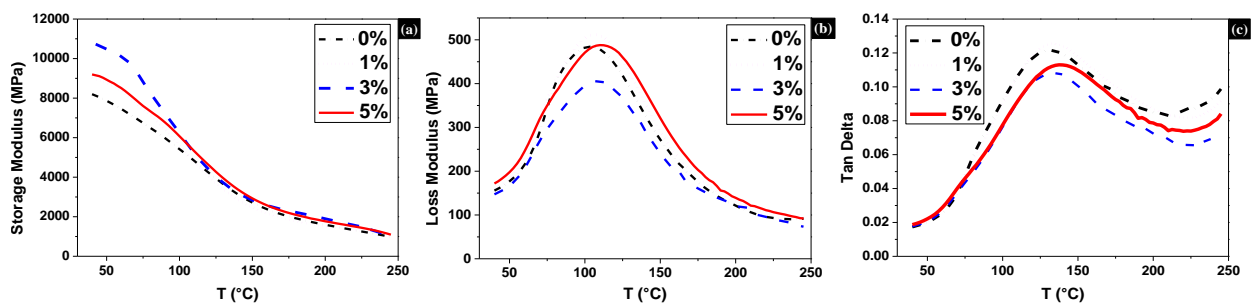


Figure 1. (a) The storage modulus, (b) loss modulus and (c) $\tan \delta$ of pure UPR and SFCM / UPR composites at different temperatures

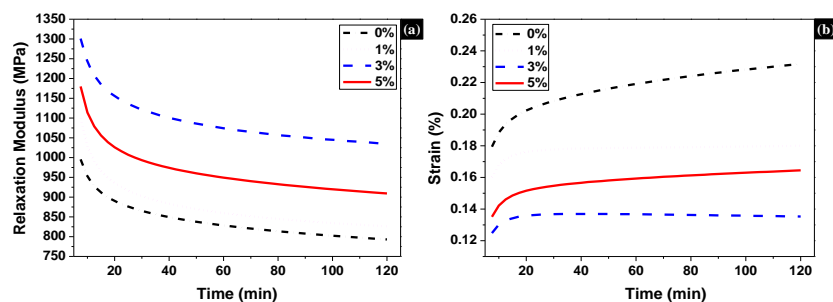


Figure 2. (a) Stress relaxation properties and (b) creep properties of pure UPR and SFCM / UPR composites

MULTI-ELEMENT ANALYSIS OF POLYMER USING WAVELENGTH DISPERSIVE XRF

Oral presentation

H.R. Low

Bruker Singapore Pte Ltd

Corresponding author email address: hou_ran.low@bruker.com

Abstract - XRF analysis can be an integral part for the quality control procedures in polymer production facility to ensure the best polymer quality. With quick and hassle-free sample preparation, a wavelength dispersive XRF can provide critical information about catalyst residues, additive concentrations and even hazardous elements (RoHS) in polymers. Bruker provides unrivaled solution packages that are efficient and reliable for a wide range of polymer chemistry.

Keywords: WDXRF, EDXRF, RoHS, polymer processing.

THE FLAMERETARDANCY STUDY OF PVA USING FOR CARDBOARD BED

Oral presentation

Yoshihiro. Mizutani¹, Yusaku. Mochizuki¹, Masayuki. Okoshi¹ and Hiroyuki. Hamada¹

¹ Department of Advanced Fibro Science, Kyoto Institute of technology, Japan

Corresponding author email address: mizutani@jpacks.co.jp

Abstract - Corrugated cardboards have a truss structure, so these have advantageous in terms of specific strength, workability, price and recycling efficiency. For these properties, corrugated cardboards are used as packing materials. The cardboard came to be often used at the shelters at the time of the disaster by East Japan earthquake disaster. refugees is forced to lie on the floors of the gymnasium directly in Japanese shelters, but the serious second healthy damage and disaster related death. It is thought that the cardboard are effective means to prevent them. In this research we tried to study about the flameretardancy (FR) of a corrugated cardboards using for Polyvinyl Alcohol (PVA).The reason why it is necessary to add the function of FR- corrugated cardboards by fire disaster in Japanese shelters. The coating PVA on the cardboard is possible to be recyclable, because PVA has water solubility. Also the reason using PVA is to protect from the toxicity of flameretardant, which is used to the cardboards. We studied the FR-PVA for different with decomposition point of FR agent. We measured combustion behavior of the PVA with 4 kinds of flameretardant. In the result, we could get the combustion behavior of PVA with each flameretardant.

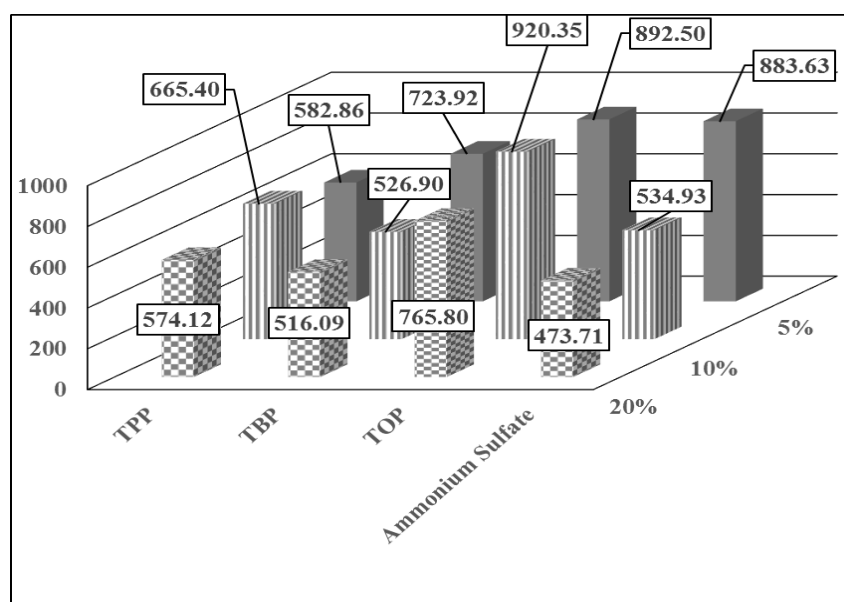


Fig.1 Peak Heat Release Rate

The combustion behavior of cardboard bed was measured by using large combusting furnace. A part of the combusting behavior of cardboard bed was clarified from the experiment and it became important data for our further study.

Keywords: Cardboard, Combustion, Flameretardancy, PVA

..

Size, shapes and superstructures of polymeric materials with a SAXS/WAXS instrument

Author :Sergio Rodrigues *, Pierre Panine, Manuel Fernandez- Martinez, Sandra Desvergne, Frederic Bossan, Ronan Mahé , Peter Høghøj , Xenocs, Sassenage, France

*corresponding author: sergio.rodrigues@xenocs.com

Nanostructured materials hold major expectations but understanding their properties requires the investigation a large number of compositions or process combinations necessitating characterization requirements over broad length scales. Moreover new materials based on a bottom up approach, i.e. self-assembly of complex materials as such as block copolymer are of significant interest for a wide range of applications but still require control and understanding of their morphology, both for fundamental studies or for routine quality verification.

Small Angle X-ray Scattering (SAXS) is a powerful measuring method for investigating nanostructured materials providing information in the range from 1 nm to beyond 150 nm such as nanoscale morphology, mesoscale phase identification, surface to volume ratio of internal structures as few examples. The method requires little sample preparation, is non-destructive and in contrast to microscopy probes a large volume of the sample enabling a statistically meaningful result. However, the same technique can be applied to surface only in the so-called “grazing incidence geometry”. When combined with Wide Angle X-ray Scattering (WAXS) one can also get information on crystalline structure.

Major developments in components and subassemblies achieved the past years offer capabilities for fast routine measurements, screening process parameters or samples. Moreover, most of the time such experiment can be conducted with sample maintained in normal atmospheric conditions, without further preparation, enabling a simplified access to the nanostructure information.

This presentation will summarize major developments on SAXS/WAXS instrumentation emphasizing impact for polymeric materials characterization. High throughput characterization of microinjected semicrystalline polymers will be shown emphasizing the nanostructure and processing relationships. Capability to measure simultaneously nanoscale structure and crystalline features during in-situ studies such as temperature controlled measurements will also be highlighted. More-over, high brightness, ultra-low divergence beam coupled to increased sample to detector distance now enables to extend the probe length to few hundred of nanometers in the UltraSAXS regime, such capability will be discussed with in-situ stretching application example. Finally we will be showing GISAXS measurements on block copolymers as an example of characterization of self-assembled structures.

2D ARRAY NANOHOLE PROCESSING ON ULTRATHIN POLYMER FILMS WITH GOLD NANOPARTICLES

Oral presentation

K. Yamada^{1*}, C. Narita¹ and Y. Tsuboi²

¹*Department of Advanced Fibro-Science, Kyoto Institute of Technology, Japan*

²*School of Science, Osaka City University, Osaka, Japan*

Corresponding author email address: kazushi@kit.ac.jp

Abstract - We present a novel laser processing technique that enables us to form nanoholes ($d < 30$ nm) on a polymer film. The important feature of the present technique is the utilization of a hybrid target, which contains an organic polymer and metal nanoparticles. The Au nanoparticles were fixed to a glass substrate (avoiding aggregation of the nanoparticles) by a technique involving a self-assembled monolayer of 3-aminopropyltrimethoxysilane or ultrathin block-co-polymer film. The film was coated with a thin poly film, and then irradiated with a nanosecond 532 nm pulsed laser light. After laser irradiation for a target, nanoholes with diameters of ca.30 nm were formed, which were allayed two-dimensionally in the observation area. The light excited the resonant plasmon absorption band of the Au nanoparticles. Subsequently, the particles underwent explosive vaporization via a superheated state, resulting in the formation of nanoholes within the film.

We have demonstrated a novel technique for sub-wavelength laser processing, in which nanoholes of several tens-of-nanometers in diameter were formed by utilizing a polymer/metal hybrid film and resonant plasmon absorption. In this presentation, the relevant aspects of the nanohole formation process and the mechanism underlying the process are presented.

Keywords: Laser Ablation, Nano-processing, Gold nanoparticles, Plasmon resonance.

DYNAMIC MECHANICAL ANALYSIS AND HEAT SEAL PROPERTY OF BIODEGRADABLE POLYMER BLENDS AND COMPOSITE FILMS

Oral presentation

S. Thumsorn^{1,2*}, S. Pivsa-Art², K. Yamada², K. Miyata³ and H. Hamada²

¹ Department of Textile Engineering, Rajamangala University of Technology Thanyaburi, Thailand

² Department of Advanced Fibro-science, Kyoto Institute of Technology, Japan

³ Department of Polymer Science and Engineering, Yamagata University, Japan

Corresponding author email address: supaphorn.t@rmutt.ac.th

Abstract - Biodegradable polymers of poly(lactic acid) (PLA) and poly(butylene succinate) (PBS) were compounded with PBS and thermoplastic starch (TPS) in twin screw extruder. PBS contents were from 0-20 wt%. TPS was compounded at the contents of 0-5 wt%. Talc filler was added at the content of 3 phr during compounding the blends. PLA/PBS, PLA/PBS/TPS blends and the composite with talc were fabricated into films using cast film process. The samples were defined to A1, A2 and A3 for PLA/PBS film at 90/10, with TPS 5 wt% and with talc 3 phr, respectively. The other film samples were namely B1, B2 and B3 for PLA/PBS film at 80/20, with TPS 5 wt% and with talc 3 phr, respectively. The films were heat sealed at temperature of 85 °C to 100 °C with varied heat sealed time of 0.5 s and 1.0 s at constant pressure of 0.2 MPa. The effects of blend ratios, TPS contents and talc filler on dynamic mechanical properties, crystallization and peel properties of these biodegradable blends and composite films were investigated. The additional of talc significantly enhanced dynamic mechanical properties and crystallinity of the composite films. The blends and composite films were peeled at the setting heat sealed temperature, except the PLA/PBS blend films. However, the incorporation of TPS decreased peel strength of the polymer blends films while the adding of talc increased peel strength of the PLA/PBS composite films at PBS content 10 wt% when increasing heat seal temperature..

Keywords: biodegradable polymer, crystallization, composite film, heat seal.

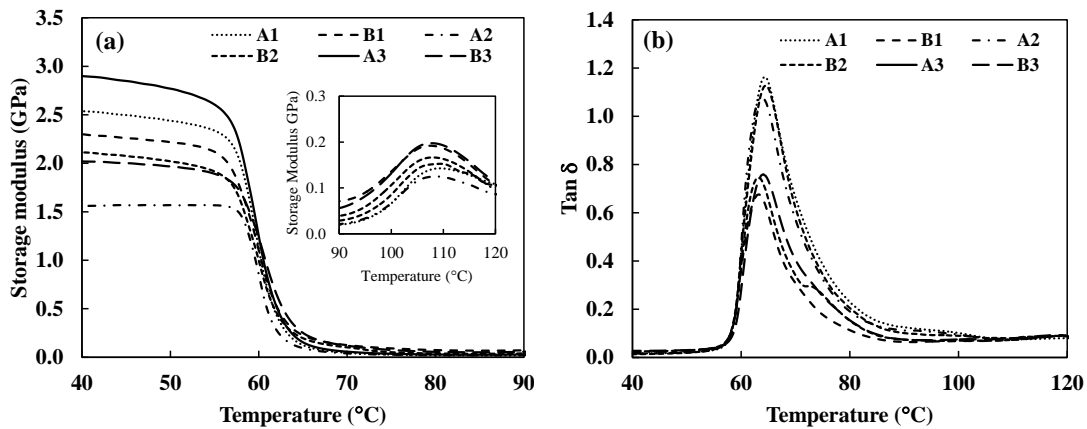


Figure 1. Dynamic mechanical properties (a) storage modulus (b) Tan δ of PLA/PBS films with TPS and talc.

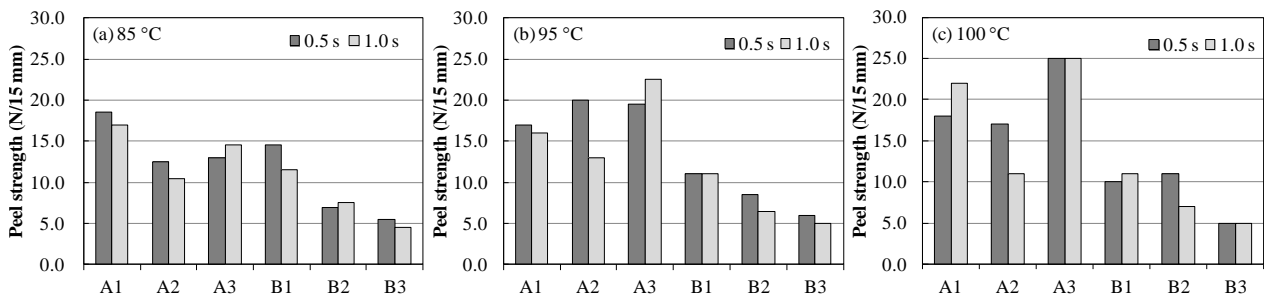


Figure 2. Peel strength of PLA/PBS films with TPS and talc at various heat seal temperatures.

GRAPHENE NANOPATELET/ POLY (BUTYLENE ADIPATE-CO-TEREPHTHALATE) HYBRIDS: PHYSICAL PROPERTIES

Oral presentation

Sima Kashi, Rahul K. Gupta* and Sati N. Bhattacharya

*School of Civil, Environmental and Chemical Engineering, RMIT University, Melbourne, Victoria, Australia
Corresponding author email address: rahul.gupta@rmit.edu.au*

Abstract – Biodegradable Poly (butylene adipate-co-terephthalate) (PBAT) / graphene nanoplatelet (GNP) hybrids were prepared via melt blending by using a Haake internal mixer at six different concentrations of GNPs (0-15 wt%). The effect of the GNP-reinforcements on the mechanical and thermal properties of the hybrids was determined. Measurements demonstrated that addition of GNPs to PBAT significantly improved its Young's modulus. The hybrid with 15 wt% of GNPs exhibited a Young's modulus 5 times higher than that of neat PBAT. However, the thermal stability of pristine PBAT was not much affected by GNP incorporation. Viscoelastic behaviours of the hybrids were characterized by dynamic oscillatory rheological tests using a rotational rheometer. Both storage (G') and loss (G'') moduli of pure PBAT were enhanced by addition of GNPs over the entire frequency range. At high frequencies (>10 rad/s), G' and G'' of PBAT gradually increased with increasing the GNP content of the matrix. The hybrid with 15 wt% GNPs exhibited storage and loss moduli of 3.8 and 3.4 times higher than those of pure PBAT at a frequency of 100 rad/s, respectively. On the other hand, at frequencies below 0.1 rad/s, storage moduli of hybrids with 12 and 15 wt% of GNPs were markedly higher than those of other hybrids and showed a pseudo- plateau trend which is attributed to the formation of 3D network of GNPs. Steady shear measurements were also carried out for PBAT/GNP hybrids. Apparent viscosity of the matrix monotonically increased with the GNP loading and reached 168kPa.s at 15 wt% of GNPs, which was about 10 times higher than pure PBAT's viscosity. Shear thinning flow behaviour was observed for all the samples. As the GNP loading was increased above 6 wt% a stronger shear thinning trend was observed.

Keywords: biodegradable polymer, Graphene nanoplatelet, hybrid

DEVELOPMENT OF STARCH BASED BIO-FILM AND LIFE CYCLE ASSESSMENT

Oral presentation

Zhang Xiwen^{1*}, Zhang Xikui², Yek Wei Ming¹, Tan Yee Shee¹, Munirah Abdul Manan¹, Li Xu²

¹ Singapore Institute of Manufacturing Technology, Singapore

² Institute of Material Research and Engineering, Singapore

Corresponding author email address: zhangxw@SIMTech.a-star.edu.sg

Abstract

PLA and starch are two promising candidates for biodegradable polymer blends. However, hydrophobic PLA and hydrophilic starch are thermodynamically immiscible. This study has developed a thermoplastic starch (TPS)/biopolymer/nanoclay ternary composites film through co-extrusion with nanoclay as both reinforcements and compatibilizer. The biodegradable film (bio-film) has been manufactured through conventional film forming technology for subsequent characterization, mechanical properties and biodegradation investigation. Interphase compatibility, morphology, structure and mechanical properties relationship has been investigated and correlated. After incorporation of nanoclay, the interface between PLA and TPS has improved (*Figure 1*). Tensile strength of nanoclay reinforced PLA/TPS film with up-to 50wt% of TPS can meet the strength requirements of commercial plastic bags (*Figure 2*). Furthermore, biodegradation rate of the can be controlled by changing TPS and nanoclay content.

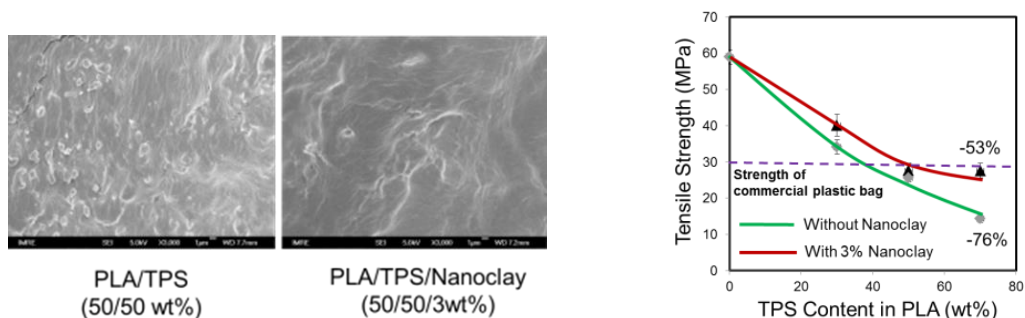


Figure 1. SEM for PLA/TPS films with and without nanoclay. Figure 2. Tensile strength of PLA/TPS biofilms.

Carbon footprint, material cost and energy consumption have been calculated and compared. As a result, bio-film developed in this study achieves lower carbon footprint as compared with the commercial ones (*Figure 3*), i.e. 3.03 kg CO₂e/kg of reduction in average (Compared to commercial LDPE and PP film). The material cost of the bio-film was also reduced around 26% compared to pure PLA film.

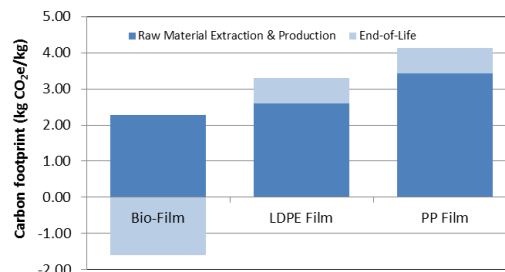


Figure 3 Comparison of Carbon Footprint of Bio-Film with Petrochemical Films

Keywords: PLA, Thermoplastic starch, Biodegradable film, Life cycle assessment

Controlled Urea and Ammonium Sulfate Released from Polylactic acid for Slow Released Fertilizer Application

Sumonman Niamlang, Sommai Pivsa-Art, Apisit Banpean, Navapon Rungruji, Kajana Tarapun

*Department of Material and Metallurgical Engineering, Faculty of Engineering
Rajamangala University of Technology Thanyaburi, Klong 6, Thanyaburi, Pathumthani 12110*

Abstract— This research work aims to fabricate slow release fertilizer from biodegradable plastics. Urea and Ammonium sulfate were selected as model fertilizer for rice. Poly(lactic acid), PLA was selected as the model biodegradable plastic. PLA was synthesized by 2-Steps Direct Polycondensation and confirm the successfully by NMR. Urea/PLA and ammonium sulfate/PLA was prepared in laboratory scale as slow released fertilizer. To investigate to effect of acidity of released condition, the released characteristics of fertilizer from PLA were studied in buffer solution at pH of 4, 5.5 and 8 for 1400 hr. All released conditions show similar behavior, the amount of released fertilizer increases at first stage and becomes saturated after 200 hr. The amount of released fertilizer increases with increasing acidity of buffer solution. At released condition pH 4, hydrolysis reaction of PLA occurred thus fertilizer can easily move out from PLA. Thus these fertilizer can control the amount and rate of released fertilizer by controlling pH condition. The green released fertilizer can be mixed with rapid fertilizer for controlling long term released. Moreover, PLA will not pollute the environmental area because PLA can degrade to natural molecule after 3 months.

Keywords : Polylactic acid, Slow Released Fertilizer, Urea, Ammonium Sulfate.

INFLUENCE OF REACTIVE AGENTS ON FLOW PROPERTY AND MECHANICAL PROPERTIES OF BIODEGRADABLE POLYESTERS

Oral presentation

S. Suttiruengwong^{1*}, P. Rattanaudom¹, S. Mongkolkitikul¹, T. Wongwirat¹, S. Pivsa-Art² and M. Seadan³

¹*Department of Materials Science and Engineering, Faculty of Engineering and Industrial Technology, Silpakorn University, Nakhon Pathom, 73000, Thailand*

²*Department of Chemical and Materials Engineering, Faculty of Engineering, Rajamangala University of Technology Thanyaburi, Klong 6, Thanyaburi, Pathumthani, 12110, Thailand*

³*Department of Physics, Faculty of Science, Silpakorn University, Nakhon Pathom, 73000, Thailand*
Corresponding author email address: suttiruengwong_s@su.ac.th

Abstract - This research aimed to study the influence of two reactive agent systems, peroxides and chain extenders on the flow and mechanical properties of Poly(lactic acid) (PLA), Poly(butylene adipate-co-terephthalate) (PBAT) and Poly(butylene succinate) (PBS). Two different types of peroxide, Perkadox®14S (Di (tert-butylperoxyisopropyl) benzene) and Luperox®101L (2,5-bis (tert-butylperoxy) -2,5-dimethylhexane) were selected and compared. For the chain extender system, Bioadimide®100/Bioadimide®500 and Jorcryl®ADR436 were used. The experiments were carried out in an internal mixer. The torques of all melt-blended samples were recorded. The tensile specimens were then prepared by compression molding and tested according to ASTM D638. For the peroxides system, the results indicated that upon increasing the amount of peroxides (0-0.1 phr), melt flow index values (MFI) decreased regardless the types of the peroxide used. This could be due to the possible crosslinking reaction, leading to the higher melt viscosity. The gel content analysis showed that, in the case of PBS, the gel fractions of around 37% and 30% were obtained with 0.1 phr of Luperox® and Perkadox® respectively. However, no gel contents were found in the case of PLA and PBAT samples. According to the tensile results, the addition of Luperox® in PBS exhibited the better elongation at break compared to Perkadox®, which was 8 folds higher than that of neat PBS. The addition of peroxides in both PLA and PBAT did not change mechanical properties significantly. For the chain extender system, the effect of mixing temperature between 170 °C and 190 °C on the properties of three bioplastics was also investigated. Jorcryl® was kept constant at 0.5 phr and the concentrations of the fixed ratio of Bioadimide®100/Bioadimide®500 (2:1) were varied from 0-2.0 phr. Upon increasing the BioAdimide contents, MFI values of PBS tended to decrease while in the case of PLA and PBAT, these values increased slightly. MFI values did not change significantly when changing the mixing temperatures for all three polymers. The thermal degradation due to high processing temperature could be compensated by the reaction of anti-hydrolysis and chain extended reactions. For mechanical properties, it was found that at the mixing temperature of 190 °C, the modulus and tensile strength of PLA increased by 8.6% and 21.04% respectively compared to that of neat PLA. The elongation at break of PBS at the both mixing temperatures was significantly increase approximately by 20 times compared to that of neat PBS.

Keywords: Reactive agents, Biodegradable plastics, Polyesters, Rheological Property

PHYSICAL DEGRADATION THEORY AND PHYSICAL REGENERATION METHOD FOR RECYCLING OF WASTE PLASTICS

Oral presentation

Nozomi Takenaka, Waka Hayashida, Aya Tominaga, Ryoko Nakano, Hiroshi Sekiguchi, Shigeru Yao*

Dept. of Chemical Engineering, Fukuoka University, 8-19-1 Nanakuma, Jonan-ku, Fukuoka, Japan. 814-0180

Corresponding author email address: shyao@fukuoka-u.ac.jp

Abstract - For recycling plastics, the ideal approach would be to use material recycling, which is reusing without incurring chemical changes, and to employ thermal recycling only for materials that are difficult to reuse, or when material recycling is impractical. However the ratio of material recycling is still remained about 30% for in these 13 years. The reasons are, 1: the physical properties of products made from recycled plastics are inferior to those made from virgin plastics, 2: people believed that the origin of the low physical properties of recycled plastics is thought to be a chemical degradation which arise from the heat, ultraviolet light or oxidation in the process of using, 3: the chemical degradation is thought to be irreversible because it associate with molecular chain session, 4: researchers at university or research institute also think as it is and did not pay attention for plastic recycling.

In this time, we investigated molecular properties of model recycled plastics and mechanical properties of various molding conditions. At that time, we found that the reason of low physical properties is not chemical degradation but physical degradation and physical regeneration is possible. Recently, we found that the theory can extend to the real recycled packaging plastics and we can increase tensile properties of these plastics by choosing molding conditions.

Keywords: Containers and packaging recycle resin, Physical Degradation, Physical regeneration

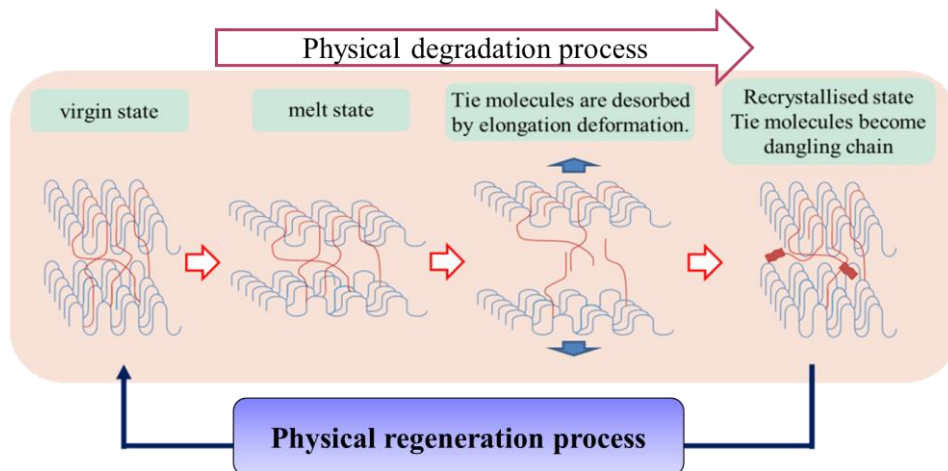


Figure 1 Schematic diagram of physical degradation process of plastics



Figure 2 Shapes of test piece after elongation measurements

MELT TRANSCRIPTION MOLDING PROCESS WITH HIGHER PRECISION AND PRODUCTIVITY FOR THIN THERMOPLASTIC PRODUCTS WITH MICRO- AND NANO-STRUCTURED SURFACE

Oral presentation

K. Furuki^{1*}, A. Naito¹, S.Ochi¹, M.Hara¹, H.Ito¹ and K.Yakemoto¹

¹ The Japan Steel Works, Ltd., Hiroshima Research Laboratory,
Corresponding author email address: kenichi_furuki@jsw.co.jp

Abstract - Thermoplastic devices with fine surface topography are unlimitedly applicable, such as cell culture, sensors of bio-molecules like DNA, hydrophilic/ hydrophobic surfaces, and/or optical devices. To produce micro- and nano-structures in high grade, we developed a melt transcription molding (MTM) process. It consists of plasticizing, coating molten polymer on a mold stamp, compressing and releasing from the mold. The fine patterns on the stamp are transcribed to a molded product. We have shown that MTM is effective to mold thin products ($\geq 50 \mu\text{m}$) with the fine patterns from nanometers to micrometers scale with high aspect ratio (ASP) up to 20 (**Fig.1, 2**). However, the issue was the cycle time is still long, compared to that of an injection molding process. In this study, we developed shortened cycle time while keeping high transcription performance using the following methods:

- (1) A new die with modified design was developed to obtain smoother surface of coated polymer under lower stamp temperature. By using it, the roughness was greatly improved even under the stamp temperature 30°C lower than the previous die (**Table 1**). The heating and cooling time was shortened due to lowered stamp temperature.
- (2) A new coating process control was developed for better thickness uniformity. The coating velocity was controlled to make the transient flow of molten polymer change at the start of coating (**Fig.3**). In case of the coated area of $W80 \times L100 \times \text{Thickness } 0.1\text{mm}$, the thickness distributions were controlled less than $10\mu\text{m}$ (**Fig.4**).
- (3) When the compression starts early at lower stamp temperature, then the thermal expansion of polymer increases the cavity pressure and enhances the transcription. In case of the polystyrene (PS) products, 14 chips on the product with the patterns of ASP 5 were uniformly transcribed (Transcription ratio $> 98\%$) in the cycle time 75s.
- (4) High speed coating ($\sim 100 \text{ mm/s}$) was adopted to reduce the enthalpy loss of molten polymer due to less heat radiation. This enabled to mold 2mm thickness products of polycarbonate (PC) ($T_g=146^\circ\text{C}$) at the stamp temperature 145°C .

When PC product was transcribed at 145°C , it could be released at the same temperature. As a result, heat and cool of the stamp was eliminated, and the shortest cycle time 37.7s was attained in case of PC products with the thickness 2mm (**Table 2**).

Key word : Thermoplastics, Transcription, Nanometer, Surface

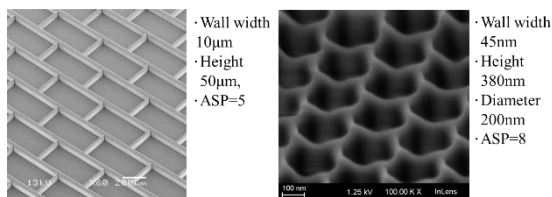


Fig.1 SEM image of micro grids made of PS.

Fig. 2 SEM image of nano holes made of PMMA.

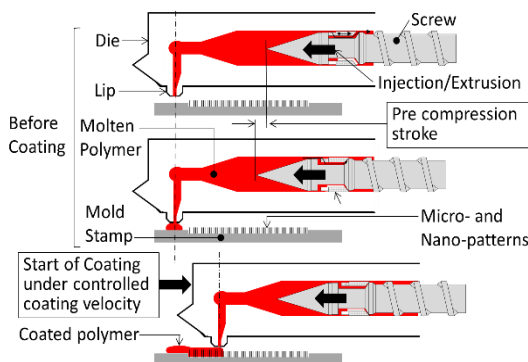


Fig.3 Schematic illustration of the coating operation of MTM.

Table 1 Comparison of the roughness(Ra) of polymer coated by using previous die and new one.

		Stamp temperature	
		160°C	130°C
Surface roughness of coated polymer Ra	Previous die	1.60µm	7.01µm
	New die	0.62µm	0.61µm

· Ra is the arithmetic average of the absolute values $R_a = \frac{1}{n} \sum_{i=1}^n |y_i|$
· Material used : PC, Molten polymer temperature : 275°C

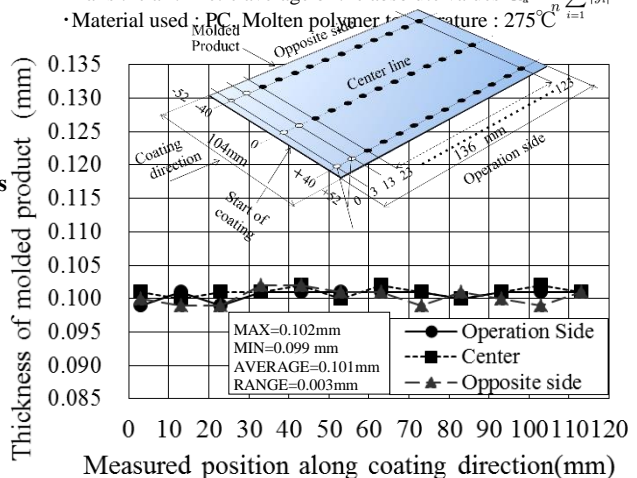


Fig.4 The thickness distribution of a PMMA product.

Stamp	close	open	Releasing	time		
Stamp	9.3s	7.6s	10.0s	7.7s	3.1s	37.7s

ADHESION BEHAVIOR OF "WARM-OFF" TYPE ACRYLIC PSAS

Oral presentation

S. Yamaguchi^{1,2}, S. Kawahara¹, R. Shibahara³, S. Tabuchi³ and H. Murakami^{4*}

¹ Nitta Corporation, Nara, Japan

² Department of Science and Technology, Graduate School of Engineering, Nagasaki University, Nagasaki, Japan

³ Department of Advanced Engineering, Graduate School of Engineering, Nagasaki University, Nagasaki, Japan

⁴ Division of Materials Science, Graduate School of Engineering, Nagasaki University, Nagasaki, Japan

Corresponding author email address: hiroto@nagasaki-u.ac.jp

Abstract - Pressure-sensitive adhesives (PSAs) whose adhesion can be controlled by external stimuli are useful for temporary attachment in industrial processes. Especially, the adhesion controls with a change in temperature and exposure to light are of interest. A side-chain crystalline acrylic PSA possesses a "cool-off" function, because the crystalline unit undergoes a reversible order-disorder transition with a change in temperature. Below the transition temperature, the PSA behaves as a hard plastic. Above the transition temperature, the crystalline unit changes to an amorphous state and become soft and flexible, leading to an appearance of tackiness. In contrast, an acrylic PSA containing a low-molecular weight acrylic copolymer with the long alkyl side-chain crystalline unit as a "warm-off" component (WOC) shows a "warm-off (WO)" function in which the PSA loses its adhesion above the transition temperature. However, no detail mechanism of the WO function is understood. In this presentation, we describe i) adherend dependence of the WO tapes, ii) *in-situ* optical microscope observation of the interface between the PSA tape and adherend, and iii) design of WOC. From these results we propose a possible mechanism of WO function.

Keywords: Acrylic PSA, Side-chain Crystalline Copolymer, Warm-off Function

SOLID ELECTROLYTE FUNCTION OF SIDE-CHAIN CRYSTALLINE BLOCK CO-POLYMER

Oral presentation

Yusuke Sano, Ryoko Nakano, Hiroshi Sekiguchi, Shigeru Yao*

Dept. of Chemical Engineering, Fukuoka University, 8-19-1 Nanakuma, Jonan-ku, Fukuoka, Japan. 814-0180

Corresponding author email address: shyao@fukuoka-u.ac.jp

Abstract - Side-Chain Crystalline Block Co-Polymer (SCCBC), which is composed of a side-chain crystalline monomer unit and a functional monomer unit (which can confer solvent-compatibility, polarity, etc.), can be adsorbed to a polyethylene crystal through crystalline supramolecular interaction. By using this interaction, we can modify not only the surface but also the inner pores of a porous polyethylene membrane to give various properties. In this study, we used a monomer with ethylene oxide repeating units as a functional unit, and evaluated its potential as a solid electrolyte for use in a Li ion secondary battery. The properties of the solid electrolyte were excellent compared to those of a non-modified porous membrane at low temperature. In addition, the solid electrolyte did not show temperature-dependence, and the Li⁺ ion conductivity remained nearly constant throughout the temperature range of 30 °C to 60 °C. However, at high temperature (above 70 °C), the conductivity began to decrease. This characteristic may make it useful for sensing temperature and for self-controlling thermal runaway.

Keywords: Solid electrolyte, Filling Membrane, Side-Chain Crystalline Block Co-Polymer, Crystalline Supramolecular Interaction

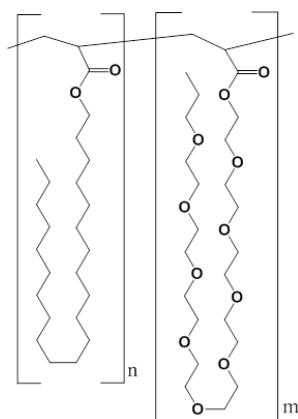


Figure 1. Typical chemical structure of side-chain crystalline block copoly-

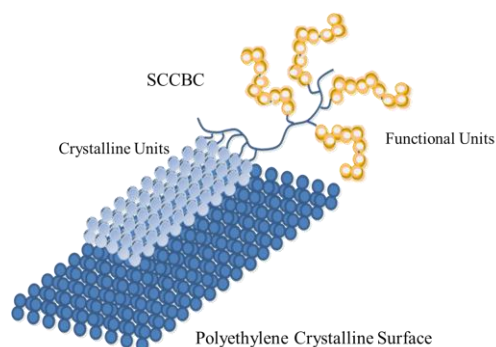


Figure 2. Schematic of the crystalline supramolecular interaction mechanism of the adsorption of SCCBC on a polyethylene surface. The side-chain crystalline units are adsorbed onto the PE crystalline surface and construct a pseudo crystal.

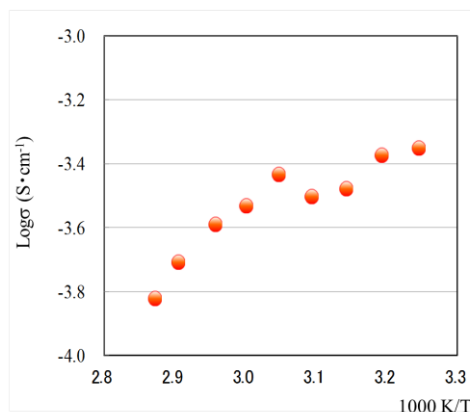


Figure 3. Temperature-dependence of Li⁺ ion conductivity of a mod-PE2 membrane used as a solid electrolyte.

DURABILITY AND PROPERTIES OF JUTE FIBER TREATMENT IN GREEN FILLED RUBBER

Oral presentation/~~Poster presentation~~ **(Please select one)**

W.Ariyawiriyanan^{1*}, P. Pantamanatsopa¹ and H.Hamada²

¹ *Department of Materials and Metallurgical Engineering, Rajamangala University of Technology Thanyaburi, Thailand*

² *Department of Advanced Fibro-Science, Kyoto Institute of Technology, Japan*

**Corresponding author email address: warunee@rmutt.ac.th*

Abstract – Optimal conditions for jute fiber surface treatment, durability and properties green filled rubbers have been investigated. In this study, dilute NaOH solution and HANR latex were used as surface cleaning agent and coupling agent, respectively. Surface treatments of jute fiber were carried out in the presence of NaOH solution, HANR, and NaOH solution together with HANR. For jute fiber samples treated with HANR and NaOH solution together with HANR, thickness of latex coated layer was controlled by variation of dipping times and %DRC of HANR. It was found that the thickness of latex layer coated on jute fibers using HANR with 10-50 %DRC were not affected by the dipping times while this is not the case for HANR with 60 %DRC. The jute fibers treated using HANR with higher %DRC provided higher durability than those treated using NaOH solution and NaOH solution/HANR. The mechanical properties of untreated and treated jute fibers were examined. Only higher elongation was obtained from treated jute fibers with an increase of %DRC., The tenacity of all treated jute fibers was lower than that of the untreated jute fibers. Therefore, in this study, the treated jute fibers used as reinforced agent for natural rubber were prepared using NaOH/HANR with 10 % DRC. SEM micrographs revealed that spaces between jute fibers treated using NaOH/HANR and natural rubber was much closer than that of untreated jute fibers. This was due to miscibility between HANR coated layer and natural rubber leading to an increasing of interfacial adhesion between jute fiber and natural rubber. As expected, the tensile strength obtained from composite rubbers reinforced using treated jute fibers were higher than that of composite rubbers reinforced using untreated jute fibers.

Keywords: jute fiber, natural rubber, durability, surface treatment

FIGURES CAN BE USED BUT THE LENGTH OF THE ABSTRACT SHALL BE KEPT WITHIN ONE A4 PAGE

PERCOLATION MODEL FOR REINFORCEMENT EFFICIENCY OF CARBON NANOTUBES IN THERMOPLASTIC COMPOSITES

Oral presentation

Zhenyu Jiang^{1*}, Hui Zhang², Jingfeng Han¹, Zejia Liu¹, Yiping Liu¹, Liqun Tang¹

¹ School of Civil Engineering and Transportation, South China University of Technology, Guangzhou 510640, China

² National Center for Nanoscience and Technology, Beijing 100190, China

Corresponding author email address: zhenyujiang@scut.edu.cn

Abstract - Considerable experimental work on carbon nanotube-reinforced composites has shown that the reinforcement efficiency of carbon nanotubes (CNTs) starts to be lower than the theoretical expectation when CNT loading is above a critical value. This critical value is considered to coincide with the electrical percolation threshold of CNTs within hosting polymers, which is related to the onset of formation of percolating CNT network. Based on this concept, a percolation model is proposed to describe the sharp decrease in the reinforcement efficiency of multiwalled CNTs dispersed in thermoplastics around the percolation threshold, which is estimated via a numerical simulation of randomly curved CNTs generated according to the statistics on geometrical features of CNTs in transmission electron microscope images. The percolation model, integrated into the well-known Halpin-Tsai equations, is verified using the experimental data of a wide variety of thermoplastics reinforced with multiwalled CNTs obtained by different research groups. The developed mechanical model achieves a good agreement with the measured moduli of nanocomposites, and demonstrates an excellent prediction capability over a wide range of CNT loading up to 13 vol%, as shown in Figure 1.

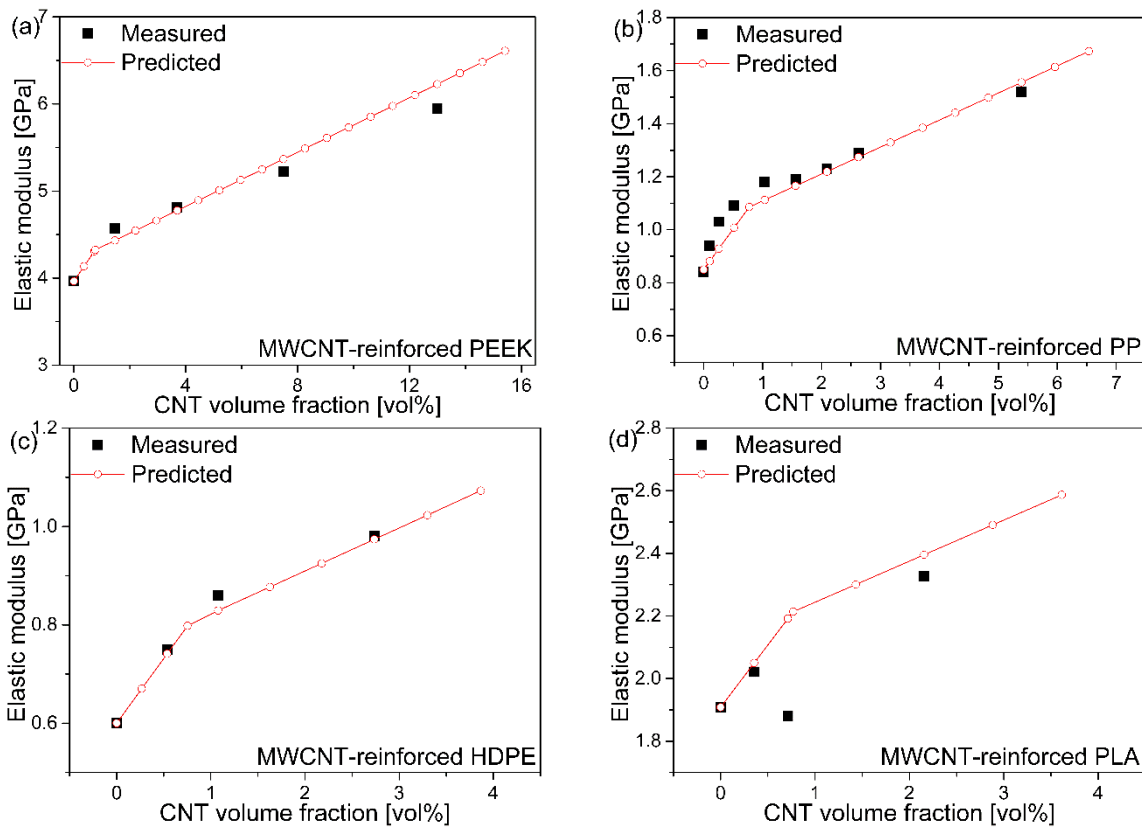


Figure 1. Measured moduli of MWCNT-reinforced thermoplastics (including (a) PEEK, (b) PP, (c) HDPE, and (d) PLA) and the results predicted using the proposed model.

Keywords: Carbon nanotubes; Thermoplastics; Modelling; Percolation threshold; Mechanical properties

EVALUATION OF GRASS FIBER REINFORCED ENGINEERING PLASTICS FOR WATER HEATER

Oral presentation

Kazuhisa Igawa¹, Atsushi Takeda², Kazushi Yamada², and Hiroyuki Nishimura²

¹ Residential Energy System Development Department, Osaka Gas Co., Ltd., Osaka, Japan

² Department of Advanced Fibro-Science, Kyoto Institute of Technology, Kyoto, Japan

Corresponding author email address: hnishimu@kit.ac.jp

Abstract

Although grass fiber reinforced engineering plastics are widely used for parts of the water heater in Japan, it is not sufficient for evaluation of long-term performance of them under hot water environment. In this study, the long-term performance of glass fiber reinforced polyphenylene sulfide (PPS), modified polyphenyleneether (mPPE), and polypropylene (PP) were investigated for thermal resistance due to hot water immersion and hot air exposure. The acoustic emission analysis was conducted to investigate the cause of an initial change in mechanical properties by the three point bending test. The tensile test and the Izod impact test were also conducted.

Figure 1 (a) and (b) show the tensile strengths of the glass fiber reinforced PPS after hot air exposure and hot water emersion at 80, 100, 120 °C. Although the tensile strength of the glass fiber reinforced PPS was almost constant with the elapsed time after hot air exposure, the tensile strength of the glass fiber reinforced PPS gradually decreased with the elapsed time. The reduction of the tensile strength was attributed to the interfacial debonding between a glass fiber and a matrix resin after hot water immersion.

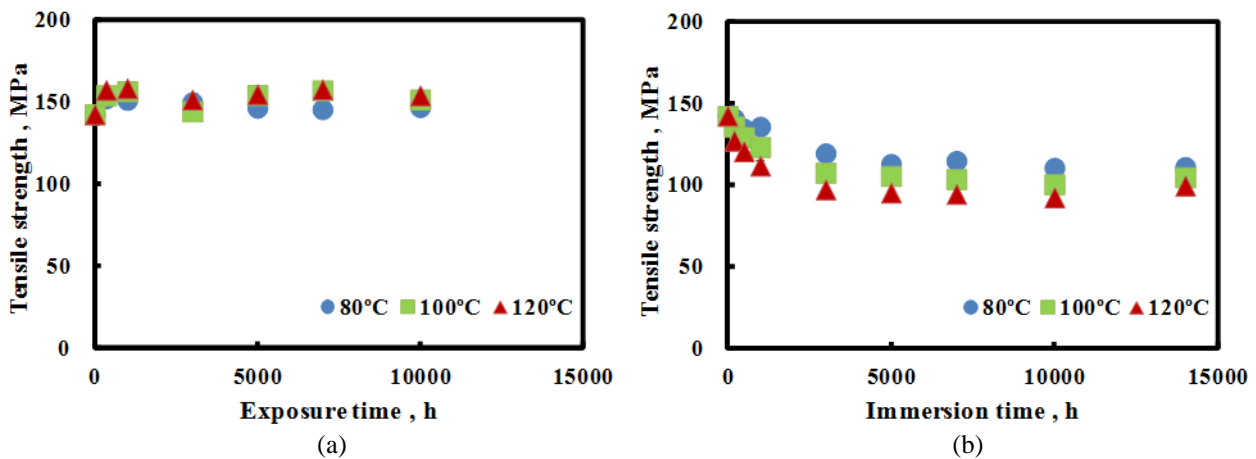


Figure 1 Tensile strengths of glass fiber reinforced PPS (a) in hot air and (b) in hot water at 80, 100, 120 °C.

Keywords: GFRP, water heater, PPS, hot water immersion, hot air exposure, interfacial strength

Studies of Mechanical Properties of High Density Polyethylene/Vietnamosasa Pusilla Fiber Composite for Decoration Applications

Oral Presentation

Supranee Suadaow¹, Sumonman Naimlang^{1*}

¹Department of Material and Metallurgical Engineering, Faculty of Engineering, Rajamangala University of Technology Thanyaburi, Klong 6, Thanyaburi, Pathumthani 12110

E-mail: sumonman.n@en.rmutt.ac.th*

Abstract

A vietnamosasa pusilla, VP is a weed which has high growth rate and toughness. The development of high density polyethylene (HDPE)/VP composite for decoration applications was studied in this research work. VP fiber was prepared by immersing dried VP leaf in 5%w/w of NaOH for 24 hr. Immersed VP leaf was then immersed in 5%w/w of HCl for 10 hr. The extracted VP fiber was dried in oven at 60 °C for 24 hr. Extracted VP fiber was grinded and sieved. VP fiber was mixed with HDPE by two roll mill. The HDPE/VP composite was fabricated by compression molding at 250 MPa and 190 °C. To investigate the effect of amount of VP on mechanical and physical properties of composite, HDPE/VP composites at various amount of VP (0, 1, 5, 10 and 20 %w/w) were prepared. The brown like HDPE/VP composite was produced for decoration application. The tensile strength increase with increasing amount of VP fiber because VP fiber act as filler in composite system.

Keywords: High density polyethylene; Vietnamosasa pusilla fiber; Decoration application

FIBER STRUCTURE DEVELOPMENT IN HIGH-SPEED MELT SPINNING OF SHEATH-CORE BICOMPONENT FIBERS CONSISTING OF ALIPHATIC COPOLYESTERS OF DIFFERENT COPOLYMER COMPOSITION

Oral presentation

Qing Qin, Wataru Takarada and Takeshi Kikutani*

*Department of Organic and Polymeric Materials, Graduate School of Science and Engineering,
Tokyo Institute of Technology, Japan*

Corresponding author email address: kikutani.t.aa@m.titech.ac.jp

Abstract - Poly(3-hydroxybutyrate-co-3-hydroxyhexanoate) (PHBH) is one of the PHB based co-polymers known as a melt-processable aliphatic co-polyester. Difficulty arises in the processing of PHBH because its glass transition temperature is below the room temperature while its crystallization rate is extremely low. Especially for the PHBH with high 3-hydroxyhexanoate (3HH) composition the fibers did not crystallize in the spin-line and stuck together on the take-up bobbin as shown in Fig.1 (a) even though stress-induced crystallization was expected to occur at high take-up velocities. Therefore, in this research, sheath-core bicomponent spinning was carried using PHBH with low 3HH composition of 5.4 mol% as the sheath component and that with high 3HH composition of 10.4 mol% as the core component. There was no sticking among fibers on the take-up bobbin and well separated fibers were collected at high take-up velocities as shown in Fig.1 (b). Structure of individual components as well as mechanical properties of the bicomponent fibers were investigated. WAXD patterns of the as-spun bicomponent PHBH fibers prepared at extrusion temperature of 180 °C are shown in Fig.2. The as-spun fibers prepared at 0.5 km/min showed α -form crystals of no orientation. The crystalline orientation increased gradually with an increase in the take-up velocity and the appearance of equatorial reflection corresponding to highly oriented β -form crystals was confirmed at the take-up velocity of 5 km/min. Birefringence measurement of the sheath and core components using an interference microscope revealed that the molecular orientation of the sheath component of low 3HH content was high while that of the core component of high 3HH content was extremely low even at high take-up velocities especially when extrusion temperature was high. This result corresponds to the overlapping of the crystalline reflections of highly oriented and low oriented α -form crystals. In any case, the processability of PHBH with high 3HH composition was improved through the bicomponent spinning with low 3HH composition PHBH and the fibers with fairly high mechanical properties were obtained.

Keywords: high-speed melt spinning, bicomponent fiber, crystalline orientation

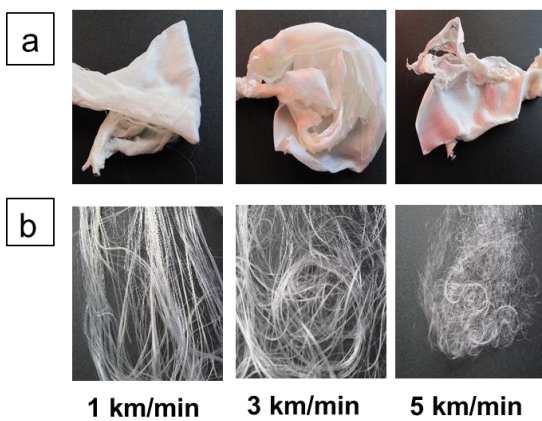


Fig. 1 Photographs of as-spun PHBH fibers prepared at 180°C: (a) single component PHBH fiber of high 3HH composition, (b) bicomponent PHBH fibers

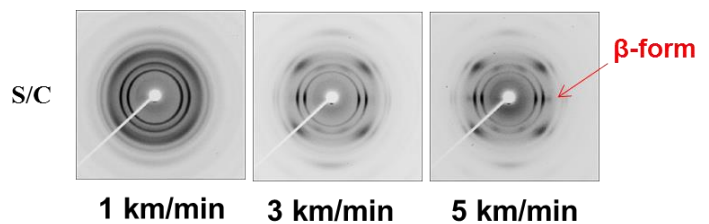


Fig. 2 WAXD patterns of as-spun bicomponent PHBH fibers consisting of PHBHs of low and high 3HH composition as the sheath and core components, respectively. The fibers were prepared at the total throughput rate of 10 g/min and extrusion temperature of 180 °C.

FIBER-BREAKAGE EVALUATION OF MELTS PASSING THROUGH CHECK-RING BASED ON NEWLY-DEVELOPED HEATING CYLINDER WITH MULTI-PORTS FOR IN-PROCESS SAMPLING

Oral presentation

S.Ma^{1*}, K.Shibata², H.Yokoi³

¹ *Institute of Industrial Science, The University of Tokyo, Japan – masai@iis.u-tokyo.ac.jp*

² *TOYO MACHINERY & METAL CO., LTD., Japan – k-shibata@toyo-mm.co.jp*

³ *Institute of Industrial Science, The University of Tokyo, Japan – hiyokoi@iis.u-tokyo.ac.jp*
4-6-1, Komaba, Meguro-ku, Tokyo, 153-8505, Japan

Abstract - In the injection molding of long fiber reinforced resins, the greatest challenge in realizing high strength molded products is minimizing the breakage of fibers during the plastication process inside the heating cylinder and during flow inside the mold. The breakage of fibers during the plastication process and while they are flowing past the check-ring (CHR) is a common problem faced at the manufacturing site. But to date, no systematic research has been carried out. In the past, static visualization experiments applied to the analysis of such breakage based on the screw cooling and pulling-out method, which requires complicated work. For this reason, the authors developed a heating cylinder with multi-ports on the wall for extracting the melted resin from the cylinder inside to perform in-process sampling of the resin. In this study, the new device was used to sample melted resin before and after CHR and investigate the effects of the shapes of the CHR on glass fiber breakage. From the experiment result, it is clearly demonstrated that the breakage of fiber can be minimized to the extent when there is enough space (large d , large λ , small θ , no claw) for melted resin to gently flow and pass the CHR. In addition, it was confirmed that the length of CHR does not affect glass fiber breakage significantly.

Keywords: Glass fiber reinforced resin / Inprocess multi-port sampling / Fiber-breakage evaluation/ Check-ring

1. Introduction

In recent years, long fiber reinforced resins are drawing widespread attention in various industries as a metal substitute with good impact-resistance and high rigidity, and which is lightweight. However, the tendency for fibers to break easily is a problem, and minimizing this breakage is becoming an increasingly important task in the plastication process. During the plastication process, the glass fiber reinforced pellet is dropped into the hopper, and melted while being transported to the nozzle by the screw. It must pass through the check-ring(CHR), before the injection from the nozzle. The influence of the CHR on the fiber length is a common problem faced at most molding sites, but to date, systematic studies have not been performed to investigate the degree of this influence by the CHR. The screw pulling-out method is one possible means of investigating this. Frozen samples of melted resin can be collected before and after the CHR, and then the fiber length distribution can be measured by the ashing method. However, because there is a need to repeat the same experimental procedures to cool down the cylinder and pull out the screw for sampling frozen resins per each experimental condition, such as different screw rotational speeds, CHR configurations, etc., which are extraordinarily time-consuming and complicated works. For this reason, the authors developed a heating cylinder with multi-ports on the wall for drawing the melted resin inside the cylinder to

perform in-process sampling of the resin. The extruder with sampling cylinder¹⁾ developed in previous studies were referred to build the sampling device. In this study, the melted resin before and after the CHR was sampled using this device to investigate the effects of the CHR shape on the glass fiber breakage. The summary is reported below.

2. Experimental Device and Molding Conditions

The developed multi-port sampling cylinder²⁾ was then mounted on an injection molding machine Si-80V (mold clamping force of 80tonf, screw diameter of 36mm, TOYO MACHINERY & METAL CO., LTD.). The laser microscope used was the LEXT OLS4000 (Olympus Corp.). The resins used were long glass fiber reinforced PP containing 50wt% glass fiber (L-5050P; Prime Polymer Co., Ltd). The glass fiber diameter used was 13 μ m and the fiber length (set value) was 8mm. The cylinder temperature was set at 230/230/230/220/210 $^{\circ}$ C from the nozzle side. Fig. 1 shows the newly-developed heating cylinder mounted with a sampling device and Fig. 2 shows the fundamental structure. The valve pin built into the inner wall surface of the cylinder is open to convey the melted resin to the outside through the connecting pipe. Fig. 3 shows the relationships between the screw with compression ratio of 1.8 (FF1) and cylinder axial coordinate. Fig. 4 shows the

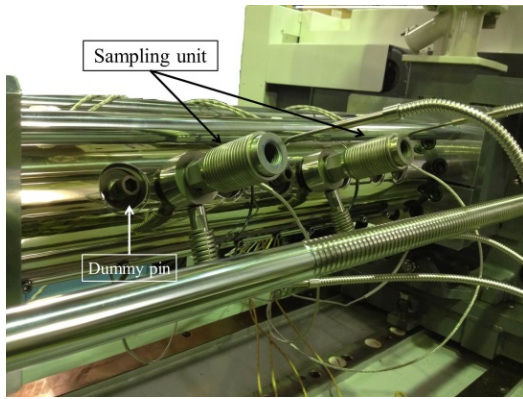


Fig.1 Appearance of in-process multi-port sampling cylinder

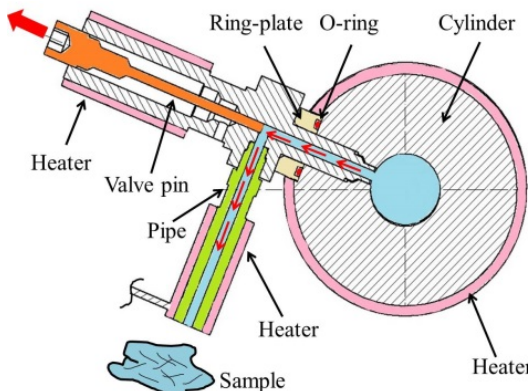


Fig.2 Fundamental structure of in-situ sampling equipment from heating cylinder

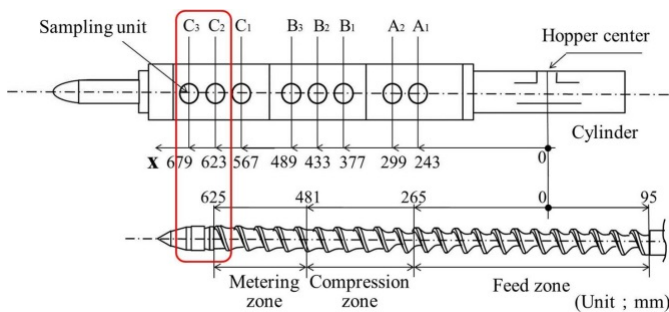


Fig.3 Relationships between screw and cylinder axial coordinate

schematic diagram of the CHR including characteristics such as (1) CHR length L , (2) contact face angle θ , (3) CHR stroke λ , (4) radial clearance between CHR and screw head d and (5) number of claws n . In our experiments, the nine CHR shapes shown in Table 1 were used while varying these characteristics. The experiments were conducted by moving the screw backward by 68mm in order to set the CHR between C2 and C3 and compare the fiber length before and after the CHR. After melting conditions stabilized, samples were taken at the rotation speed of 150rpm, and the glass fibers were extracted by ashing the resin. Fiber length was measured by a microscope to evaluate the fiber length distribution.

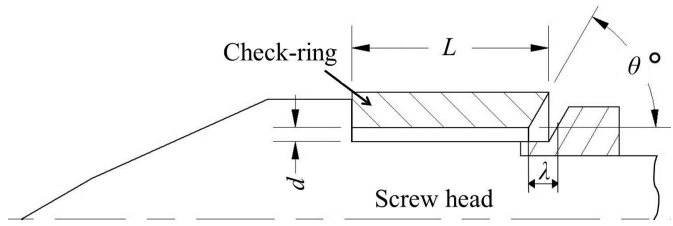


Fig.4 Schematic of check-ring configuration

Table 1 Check-ring profiles

No.	Type0	Type1	Type2	Type3	Type4	Type5	Type6	Type7	Type8
$L(\text{mm})$	28	35	28	28	28	28	28	28	28
$\theta(^{\circ})$	60	60	45	90	60	60	60	60	60
$\lambda(\text{mm})$	1.8	1.8	1.8	1.8	2.3	2.8	1.8	1.8	1.8
$d(\text{mm})$	2	2	2	2	2	2	1.5	2.5	2
n	0	0	0	0	0	0	0	0	2

 : Changed parameter

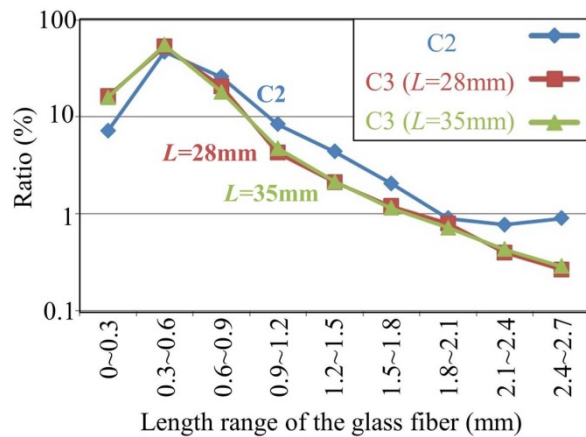
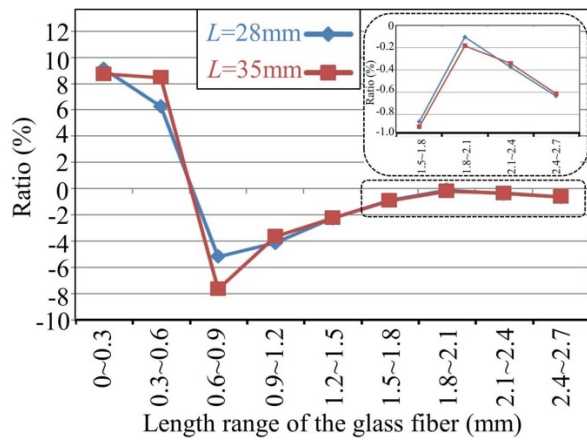


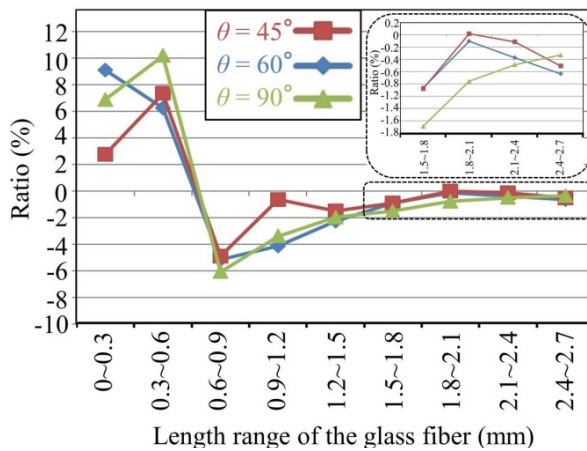
Fig.5 Comparison of glass fiber length distribution between samples of C2, Type0 and Type1

3. Experiment Results and Discussion

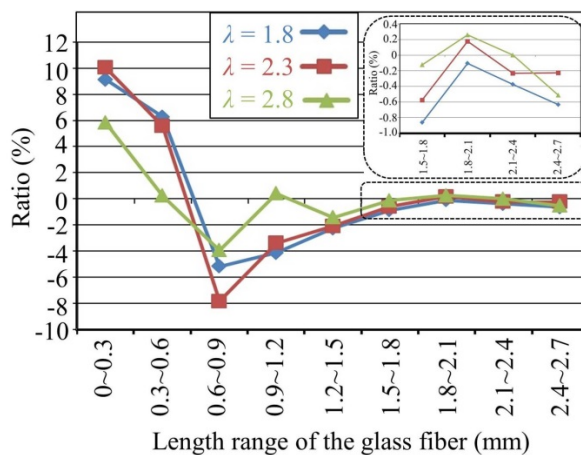
In preliminary experiments²⁾, among the full-flight screws with different compression ratios, FF1 showed the best effect for minimizing the breakage of fiber particularly at high rotation speeds. For this reason, FF1 was adopted in the following experiments to provide plasticized resin with the longest fiber length until just before reaching the CHR. The results of the experiments also confirmed that the fiber length distribution of the sample taken immediately after the CHR at C3 is nearly the same as that taken from the nozzle. We particularly focused our evaluation on fibers shorter than 2.7mm (fiber length exceeding 2.7mm is 3% or less at the maximum.).



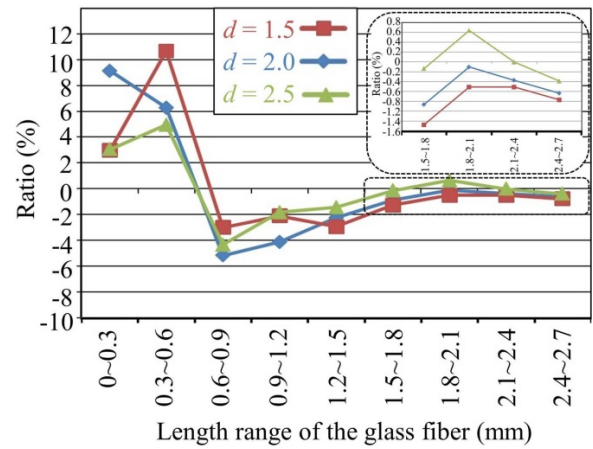
(a) CHR length L



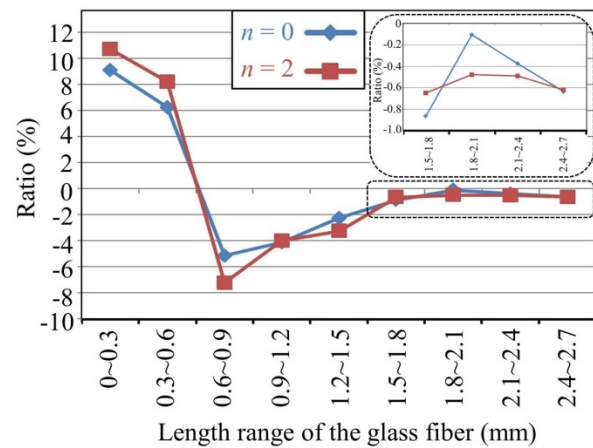
(b) Contact face angle θ



(c) CHR stroke λ



(d) Radial clearance between CHR and screw head d



(e) Number of claws n

Fig.6 Deviation of the fiber length distribution of samples at C3 from those at C2 (before check-ring)

1) CHR length L :

Fig.5 shows the effects of CHR length on the fiber length distribution before and after the CHR. The vertical axis is the logarithmic scale. Since the C2 data is common to all the conditions and the effects on fiber breakage can be evaluated from the deviations of C3 from the distribution of C2, the

influence of all the conditions was evaluated by the deviation from C2 as follows. Fig. 6 summarizes the results. Comparing the fiber length distribution before and after the CHR in Fig.6 (a), the presence of fibers shorter than 0.6mm increases dramatically and suddenly decreases when the fiber length is longer than 0.6mm, continuing to decrease until the

fiber length is 1.8mm long. When CHR is 35mm long, it does not affect fibers longer than 1.2mm, but fibers shorter than 0.9mm shows the tendency to break.

2) Contact face angle θ :

Fig. 6 (b) shows the effects of the contact face angle θ on the fiber length distribution. Like Fig.6(a), it changes drastically from increase to decrease when the fiber length is around 0.6mm in length regardless of θ . It seems that when θ increases, the fiber existence ratio increases when fiber length is shorter or around 0.6mm. The deviation to C2 (before the CHR) approaches zero when the fiber length is 0.9mm and θ is 45°, when the fiber length is 1.8mm and θ is 60°, or when the fiber length is 2.4mm or longer and θ is 90°. The fibers were found to not break easily in the above range. The experimental results showed that when the inflow angle θ changes suddenly, which is the inlet to the inside of CHR, the mutual restraint and fiber curvature between long fibers tend to increase. The localized shear rate in the corner also increases. These results suggest that the breakage of fiber may be promoted when they pass CHR at a higher angle.

3) CHR stroke λ :

Fig. 6(c) shows the effect of λ on the fiber length distribution. Although there is not too much difference of the fiber length distribution between $\lambda=1.8$ and $\lambda=2.3$ mm, it was confirmed that fibers longer than 0.9mm hardly break when $\lambda=2.8$ mm. It was also found that long fibers are also less likely to break if there is sufficient clearance for the melted resin to pass through CHR.

4) Radial clearance between CHR and screw head d :

Fig.6 (d) shows the effect of d on the fiber length distribution. Compared to the slight increase when $d=2.5$ mm, when $d=1.5$ mm, the area in which the fiber length is shorter than 0.6mm increases conspicuously, indicating that the fiber breaks easily. However, when the fiber is longer than 0.6mm and d equals to 1.5mm, breakage is promoted, causing significant decrease in each fiber length range. On the other hand, when $d=2.5$ mm, the minus range decreases and fibers longer than 1.5mm seems to break less easily. These results indicate that the space between the CHR and screw head is the flow path of the melted resin, which may serve as an important controlling factor for maintaining the fiber length uniform.

5) Number of claws n :

Fig.6 (e) shows the effect of the number of CHR claws on the fiber length distribution. When there are claws, the fiber length distribution shows that

Table 2 Weight-average (L_w) of fiber lengths and the ratio of fibers with length longer than 2.7mm (Sampled at C2&C3)

Sampling port; CHR Type No.	L_w (mm)	Ratio (%)	Sampling port; CHR Type No.	L_w (mm)	Ratio (%)
C2; <Before CHR>	1.54	2.96	C3; Type4 ($\lambda=2.3$ mm)	1.18	1.48
C3; Type0 (Standard)	1.06	1.06	C3; Type5 ($\lambda=2.8$ mm)	1.26	2.19
C3; Type1 ($L=35$ mm)	1.09	1.15	C3; Type6 ($d=1.5$ mm)	0.77	0.39
C3; Type2 ($\theta=45^\circ$)	1.11	1.31	C3; Type7 ($d=2.5$ mm)	1.34	2.44
C3; Type3 ($\theta=90^\circ$)	0.78	0.29	C3; Type8 ($n=2$)	1.00	0.71

the deviation does not converge to zero for any fiber length of more than 0.6mm, which means that fiber breakage is promoted. Particularly when the fiber length ranges from 0.6 to 1.5mm, the fiber breakage ratio increases. When CHR has claws that co-rotate with the screw head, the melted resin flows into the gap of the CHR stroke. The shearing action always works on the inlet in the orthogonal direction. It is assumed that long fiber breaks easily because of the narrow gap at the CHR outlet side caused by the fitting clearance between the claws and screw head.

6) Comparison of influential factors:

The weight average fiber length L_w is calculated by the formula (1). Table 2 compares L_w and the ratio of fibers longer than 2.7mm. α indicates the broken state, especially for long fibers. Both L_w and α are correlated roughly. From the comparison between L_w of C2 and α based on the different shapes of CHR, the fiber length is most affected when $d=2.5$ mm and $\lambda=2.8$ mm, and subsequently affected by $\lambda=2.3$ mm and $\theta=45^\circ$. Conversely, it was confirmed that fiber breakage occurs when $\theta=90^\circ$, $d=1.5$ mm and CHR with claws. The comparison of α shows that glass fibers break intensively when $\theta=90^\circ$ and $d=1.5$ mm.

$$L_w = \frac{\sum n_i L^2}{\sum n_i L} \quad (1)$$

4. Conclusion

In this study, the authors successfully evaluated fiber breakage using different shapes of CHR which melted resin passes, using the sampling device. The results clearly demonstrated that fiber breakage can be minimized when there is enough space (large d , large λ , small θ , no claw) for melted resin to gently flow and pass the CHR. The length of the CHR does not have considerable influence.

Reference

- 1) T.Nishio ; et al : KOBUNSHI RONBUNSHU, 47(4), p.331 (1990)
- 2) S.Ma; H.Yokoi : AWPP 2013, India, CD (2013).

STUDY ON FEEDSTOCK OF METAL INJECTION MOLDING

Oral presentation

N.Kayamori^{1*}, and T. Tanaka¹

^{1*} Applied Materials Engineering Laboratory, Department of Science and Engineering, Doshisha University, 1-3, Tatara Miyakodani, Kyotanabe, Kyoto, 610-0321, Japan
duo0533@mail4.doshisha.ac.jp

Abstract –Recently, Metal Injection Molding (MIM) has been focused as a method of metal parts manufacturing, because hard material such as titanium and so on, and products with complicated shape can be manufactured by MIM. There are four processes in MIM. They are consisted of compounding, injection molding, defatting and sintering. In the compounding process, kneader is generally used. However, kneader is poor productivity for batch type. Hence, twin screw extruder which is good in productivity for continuous processing was focused in this study. However, the dispersion state of the feedstock compounded with twin screw extruder is worse than the one made by conventional kneading machine. So, the improvement of the dispersibility of feedstock manufactured by twin screw extruder is necessary in our experiment. Therefore, as the purpose in this study, relationship of mixing condition and dispersibility of feedstock was investigated because dispersibility of metal powder depend on the mixing condition in twin screw extruder. Mixing condition refers to rotation speed, mixing temperature, and feed rate.

As the material of MIM, water atomized 316L stainless powder was used. The binder system consists of polypropylene, paraffine wax, camauba wax and stearic acid.

The X-rays CT scanning that the aggregation of metal powder could be observed three-dimensionally was used as an evaluation method of the dispersion state of feedstock. The example about image of X-ray CT scan is showed in fig.1. The metal powder area is indicated white color, and the resin area is indicated the black color. In the image of the X-ray CT scanning, area-equivalent circle diameter of metal powder was calculated from a white area. This area-equivalent circle diameter is used for evaluation index of dispersibility of feedstock. Additionally, segregation of metal powder is appeared in the image (Fig.1). The index of segregation level is used CV index about density of feedstock. This CV index also used for evaluation index of dispersibility of feedstock. If CV index becomes low, the dispersibility of feedstock is improved.

As a result, first, the relationship rotation speed and area-equivalent circle diameter and CV index was showed in Fig.2. The increase rotation speed decrease area-equivalent circle diameter and CV index. That is showed improvement of dispersibility of metal feedstock. Second, the relationship temperature and area-equivalent circle diameter and CV index was showed in Fig.3. The reduction of mixing temperature decrease area-equivalent circle diameter and CV index. That is showed improvement of dispersibility of feedstock. Third, the relationship feed rate and area-equivalent circle diameter and CV index was showed in Fig.4. The reduction of feed rate decrease area-equivalent circle diameter and CV index. That is showed improvement of dispersibility of feedstock.

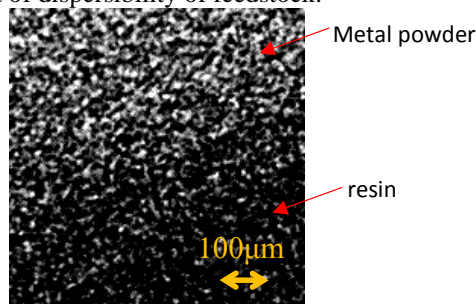


Fig.1

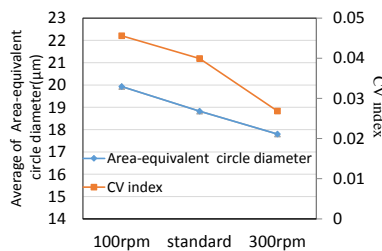


Fig.2

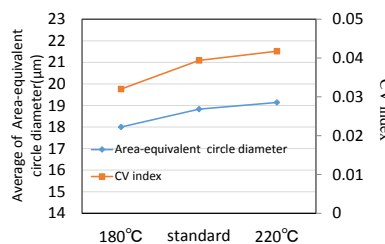


Fig.3

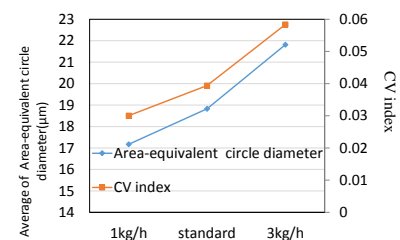


Fig.4

Keywords: Metal Injection Molding, dispersibility, twin screw extruder, compounding

EFFECT OF TITANIUM DIOXIDE ON THE INTERFACE OF POLY(LACTIC ACID) BETWEEN SHEATH-CORE FIBERS

Oral presentation

N. Roungpaisan^{1*}, N. Srisawat¹, N. Suwannamek², C. Prahsarn²

¹*Department of Textile Engineering, Faculty of Engineering, Rajamangala University of Technology Thanyaburi, Pathumthani 12110, Thailand*

²*National Metal and Materials Technology Center, 114 Paholyothin Rd., Klong Luang, Pathumthani 12120, Thailand*
**E-mail: nanjaporn_r@rmutt.ac.th*

Abstract – The sheath/core(S/C) cross sectional is the one of bicomponent fibers. One of polymer is a center fully surrounded by second component(sheath). The shape was designed for improving surface special function while the strength can provide at core region. Sheath/core bicomponent fiber were prepared by Hill Lab Scale Bicomponent Extruder Fed Spinning Machine, using different amount of TiO₂ (1, 1.5, and 2% w/w) at the sheath region was diluted by TiO₂-PLA masterbatch and neat PLA at core region which spun together into one fiber. With various ratio(S/C) 0/100, 10/90, 30/70, 50/50 and 70/30, respectively. Cross-sectional features and fracture of the fiber, as well as morphologies at sheath and core interfaces, of the TiO₂-PLA/PLA fibers were investigated, using optical microscope and scanning electron microscope. The strength of the color(K/S) of the TiO₂-PLA/PLA fibers was measured, using spectrometer to determine the coloring effect of titanium dioxide content by CIELAB system. Crystallinity and mechanical properties were studied x-ray diffraction and tensile testing. In order to adjust the strength of color value, we can lower sheath/core ratio from 70/30 to 50/50 which contain TiO₂ in the sheath part 1.5-2%. However, for mechanical property, the optimum TiO₂ loading is 1-1.5% and the S/C ratio is 10/90-30/70. These conditions presented the better tensile property than neat PLA.

Keywords: Sheath-core bicomponent, polylactic acid, interface of phase

Study on Fabricating Carbon Nano Fiber by Cotton Candy Method

Oral presentation

Ryo Takematsu¹, Akihiro Tada², Masayuki Okoshi¹, Hiroyuki Inoya¹ and Hiroyuki Hamada¹

¹Department of Advanced Fibro-Science, Kyoto Institute of Technology, Matsugasaki, Sakyo-ku, Kyoto, 606-8585, Japan

²OHGI TECHNOLOGICAL CREATION CO., LTD. 4-13, 3-chome, Nakano, Otsu City, Shiga Prefecture 520-2114

Corresponding author email address: takematsu4@yahoo.co.jp

Abstract

Recently, it has been possible to make a preparation of nano fibers in the technology field¹. Nano fibers have several excellent properties such as mechanical properties and adhesive properties. Therefore, nano fibers are expected to apply in various field including energy sector, electronics sector, medical sector and so on.

Several methods for fabricating nano fibers were reported by researchers, and among which electrospinning method is one of the most famous methods². The electrospinning method can fabricate the nano fibers by dissolved resin in the solution with a high voltage. In the result, it is possible to make the nano fibers to stretch the dissolved resin by electrostatic repulsion. But the electrospinning method results in large cost because of keeping the high voltage during the produce. Besides, the electrospinning method does not have enough stretching process. Therefore, the nano fibers fabricated by electrospinning method are low crystallinity and weak mechanical properties.

In this research, We introduce the novel method that called Cotton Candy Method (CCM). Polyacrylonitrile (PAN) that was precursor of carbon fiber was solved in N-methylpyrrolidone (NMP). This solution was blown and stretched by air. After that stretched nano fiber was caught in water. NMP is good solvent for PAN, but water is poor solvent for PAN. This simple process can fabricate PAN nano fibers. Since the CCM does not need a high voltage, this novel method is expected to produce in large volume in a low cost way. In addition, the carbon nano fiber was fabricated by carbonizing PAN nano fiber. Fig. 1(a) shows SEM observation of PAN nano fiber, Fig.1 (b) shows that of carbon nano fiber by CCM. From results of SEM observation, average diameter of nano fiber by CCM was determined about 300 nm. CCM has a great potential for nano fiber industry.

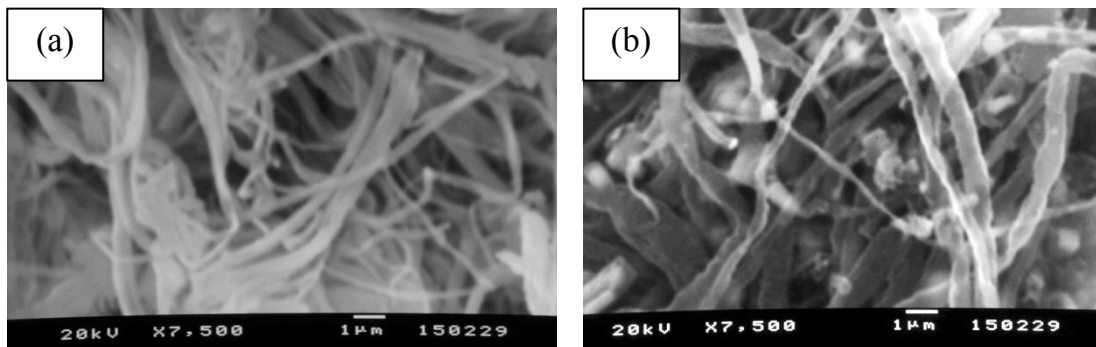


Fig.1 (a) PAN nano fiber, (b) Carbon nano fiber

Reference

- (1). S. Petrik, Industrial Production Technology for Nanofibers, NANOFIBERS – PRODUCTION, PROPERTIES AND FUNCTIONAL APPLICATIONS, Pages3-17, 2011
- (2). J.M Deitzel, J Kleinmeyer, D Harris and N.C Beck Tan, The effect of processing variables on the morphology of electrospun nanofibers and textiles, Polymer, Volume 42, Issue 1, January 2001, Pages 261–272

Keywords: nano fiber, carbon fiber, Polyacrylonitrile

Development of Poly(lactic acid)/Gelatin/Shellac Blend for Green Composite Film from

Kewalee Nilgumhang¹, Anin Memon², Sumonman Naimlang^{1*}

¹*Department of Material and Metallurgical Engineering, Faculty of Engineering, Rajamangala University of Technology Thanyaburi, Klong 6, Thanyaburi, Pathumthani 12110*

²*Department of Industrial Engineering, Faculty of Engineering, Rajamangala University of Technology Thanyaburi, Klong 6, Thanyaburi, Pathumthani 12110*

Abstract— Polylactic acid (PLA) is one of the most interesting biodegradable polymers and commercially produced thermoplastic that is derived from renewable resources. However, the limitation of PLA is the stiffness and brittleness. In this research, PLA/Gelatin/Shellac blends films were fabricated to improve the flexibility of blend film. To study the effect of gelatin and shellac, the PLA/Gelatin/Shellac blend films were fabricated at various blending ratio (%w/w of PLA: Gelatin: Shellac is 90:10:0, 80:10:10, 70:10:20, 60:10:30, 90:0:10 and 70:20:10 for PLA:GEL:SH 90:10:0, PLA:GEL:SH 80:10:10, PLA:GEL:SH 70:10:20, PLA:GEL:SH 60:10:30 and PLA:GEL:SH 70:20:10, respectively.) The yellow-orange PLA/Gelatin/Shellac blends films were successfully prepared. The tensile strength of blend films increase with increasing amount of shellac and gelatin. These blend films will be new class of green film without non-toxic substance which can degrade in composed environment.

Keywords— Shellac, Biodegradable plastic, Poly(Lactic acid), Gelatin, Solvent Casting.

ANALYSIS ON CRYSTALLIZATION BEHAVIOR OF EQUI-BIAXIALLY STRETCHED AMORPHOUS POLY(ETHYLENE TEREPHTHALATE) FILMS

Oral presentation

S. Shibata, W. Takarada¹ and T. Kikutani^{1*}

Department of Organic and Polymeric Materials, Graduate School of Science and Engineering,
Tokyo Institute of Technology, Japan

Corresponding author email address: kikutani.t.aa@m.titech.ac.jp

Abstract – To investigate the effect of biaxial stretching on crystallization rate, amorphous poly(ethylene terephthalate) (PET) films with various degrees of molecular orientation were prepared through the simultaneous equi-biaxial stretching of amorphous and isotropic PET films to various draw ratios at 90 °C. Crystallization and melting behaviors of the films were analyzed using the fast scanning chip calorimetry (FSC) and the conventional differential scanning calorimetry (DSC). In the FSC measurement, significant data fluctuation caused by the thermal shrinkage of the oriented films was observed at around the glass transition temperature T_g as shown in Fig. 1 (a). We found however that it is possible to shrink the film without crystallization through heating the oriented films up to 120 °C and immediately cooling down to a temperature below T_g at high heating and cooling rates. Eventually, data fluctuation in the FSC measurement was satisfactorily suppressed as shown in Fig. 2(b). Based on this technique, measurement of the cold crystallization behaviors was conducted at various heating rates applying the time-temperature profiles including the pre-thermal treatment as shown in Fig.2. The models for crystallization kinetics proposed by Ozawa¹⁾ and Nakamura²⁾ were combined to calculate the non-isothermal crystallization rate of un-stretched and stretched PET films. The results analyzed from the DSC and FSC measurements are shown in Fig. 3. Even after applying the thermal shrinkage, the highly stretched films showed crystallization rate more than 1000 times higher than that for the un-stretched film.

Keywords: poly(ethylene terephthalate), crystallization rate, molecular orientation

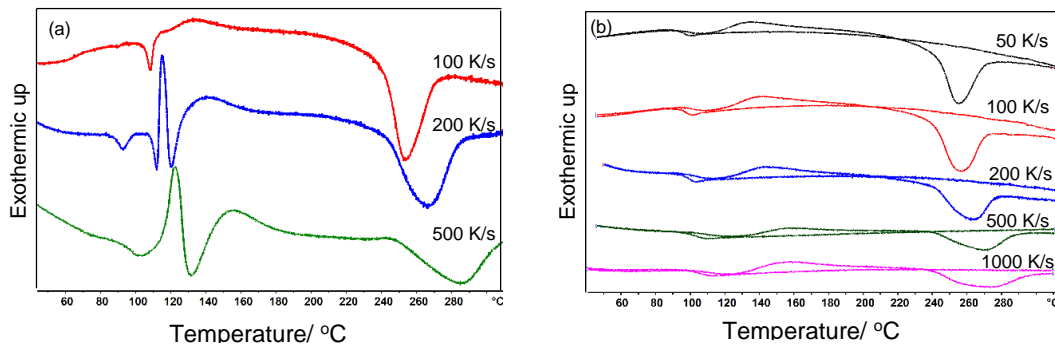


Fig. 1 (a) FSC thermograms without pre-thermal treatment and (b) those after pre-thermal treatment for PET films stretched to the draw ratio of 2.5×2.5.

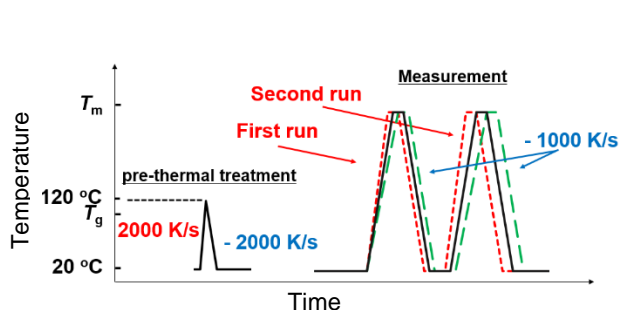


Fig. 2 Time-temperature profile for analysis of cold crystallization behavior of stretched PET films.

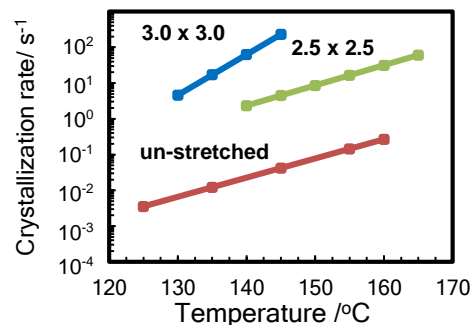


Fig. 3 Non-isothermal crystallization rate for PET films of various MD×TD draw ratios analysed from the results of DSC and FSC measurements.

Reference

- 1) T. Ozawa, *Polymer*, **12**, 150 (1971)
- 2) K. Nakamura, K. Katayama, T. Amano, *J. Appl. Polym. Sci.*, **17**, 1031 (1973)

Preparation of The Carbon Nano Fiber Using Cotton Candy Method

Oral presentation

Akihiro Tada¹, Ryo Takematsu², Hiroyuki Inoya², Masayuki Okosi² Hiroyuki Hamada²

¹ OHGI TECHNOLOGICAL CREATION CO., LTD. 4-13, 3-chome, Nakano, Otsu City, Shiga 520-2114, Japan

² Department of Advanced Fibro-Science, Kyoto Institute of Technology, Matsugasaki, Sakyo-ku, Kyoto, 606-8585, Japan

Corresponding author email address: tada.akihiro@ohki-techno.com

Abstract

Carbon based nanomaterials (fullerene and carbon nanotube, etc.) have been actively studied since the 1980s. These have the potential of attractive applications such as specific shape and physical properties. Therefore a variety of research and development have been expanded. However, carbon-based nanomaterials produced by the vapor deposition, it is necessary to reduce the cost under the production line.

In this study we focused on carbon nano fiber in the carbon-based nanomaterials. Carbon Nano Fibers (CNF) are expected to various applications. However, the CNF have a high cost. Therefore We are trying to make a preparation of precursor of the CNF using Cotton Candy Method (CCM). CCM is a method of forming a fiber with only air injection. Therefore it is possible to make a cost saving by CCM, because it does not require heating and the electric field.

In this study, We have been planing to make a preparation of the CNF by using the CCM.

The fiber diameter is about 270nm of the CNF by using CCM. The process of carbonization is two steps. The one stage is process of producing a flameproofed fiber. Under the process conditions is temperature 250 °C, rate of temperature rise 5 °C / min, holding time 1 h, oxygen concentration of 20% atmosphere. The other stage is process of producing a carbon nanofiber. Under the process conditions is temperature 1000 °C, rate of temperature rise 7 °C / min, holding time 10 min, Nitrogen atmosphere.

The nanofiber after the carbonization process (carbon nanofiber) is shown in Figure1. Fig.1 shows the SEM image of carbon nanofiber. The Result of the SEM image diameter of about 270 nm of carbon nanofiber and keep fiber form after carbonization process.

Fig.2 shows the raman spectrum of the CNF. The spectrum consists of two broad peak around 1590 and 1370 cm⁻¹: the G band and D-band respectively. The G-band is due to E_{2g} symmetry corresponding to the bond stretching vibration of the in-plane pairs of sp² site, and the D-band is due to A_{1g} symmetry corresponding to the breathing vibration of 6-fold aromatic rings. The intensity ratio, I(D)/I(G) and G band position have been reported to depended on the sp² content in carbon nanofiber. The I(D)/I(G) and G-band position of our carbon nanofiber were about 3.5 and 1575 cm⁻¹, suggesting that the main bonding configuration of carbon atoms is sp². Comparing this result with the general carbon fibers is considered to have the same carbon structure from that nearly the same peak was obtained.

In the Future, we are planning to study on the carbonization treatment method and the carbon nanofiber characterization.

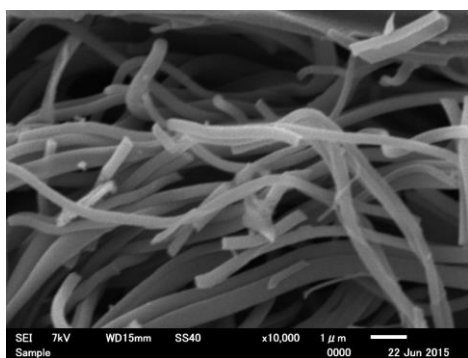


Fig.1. SEM image of carbon nanofiber.

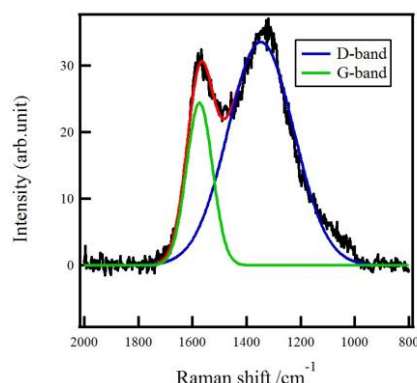


Fig.2 Raman spectra of carbon nanofiber

Keywords: nano fiber, carbon fiber, cotton candy method,

DEVELOPMENT OF PEEK- NANO- SiC COMPOSITES FOR HIGH PERFORMANCE COATING AND ADHESIVE APPLICATIONS

Oral presentation/Poster presentation

Ajay Kumar Kadiyala and Jayashree Bijwe

Industrial Tribology Machine Dynamics & Maintenance Engineering Centre (ITMMEC), Indian Institute of Technology Delhi, Hauz Khas, New Delhi, 110016 India.

Abstract –

Polyetheretherketone (PEEK) as a high performance polymer having excellent mechanical properties and their fairly good retention at high temperature, good chemical resistance and high long-term working temperatures. It is considered to be one of the most prospective polymers for biomedical applications, the automotive industry, electronics, spacecraft design etc. The efforts for performance enhancement are continuously being done by the researchers and nano-composites are most favoured area now a days. However, developing nano- composites based on PEEK with uniform distribution of nano-particles (NPs) is most challenging since it cannot be processed using solution method where probe sonication technique can be employed.

In the present work a novel emulsion based dispersion of PEEK and SiC nano filler is reported first time. The emulsion was then dried in oven to remove the solvents. The coating was carried out on a stainless steel substrate by using electrostatic powder spray technique. The composites were characterized using FTIR-ATR, XRD, SEM, DSC, TGA, Contact angle and Raman spectroscopic measurements. The scratch hardness and scratch adhesion of the composites showed significant improvement with addition of 1% SiC, while 15 % micro SiC proved to be best performer. The adhesion strength results also showed almost two times improvement with addition of SiC particles and the adhesive strength was retained to a significant level up to 300 °C. The fracture analysis of adhesives joints showed very good interaction between filler and matrix interface, which lead to improvement in adhesive strength properties.

Keywords: nanocomposite, PEEK emulsion based composites, high temperature adhesives.

BIODEGRADABLE AND RENEWABLE POLY (LACTIDE)-LIGNIN COMPOSITES: SYNTHESIS, INTERFACE AND TOUGHENING MECHANISM

Oral presentation

Yang Sun,^a Liping Yang,^b Xuehong Lu^c and Chaobin He^{a,d,*}

^a Department of Materials Science & Engineering, National University of Singapore, 9 Engineering Drive 1, Singapore 117576. Email: msehc@nus.edu.sg

^b Institute of Chemical and Engineering Science, Agency for Science, Technology and Research (A*STAR), 1 Pesek Road, Jurong Island, Singapore 627833

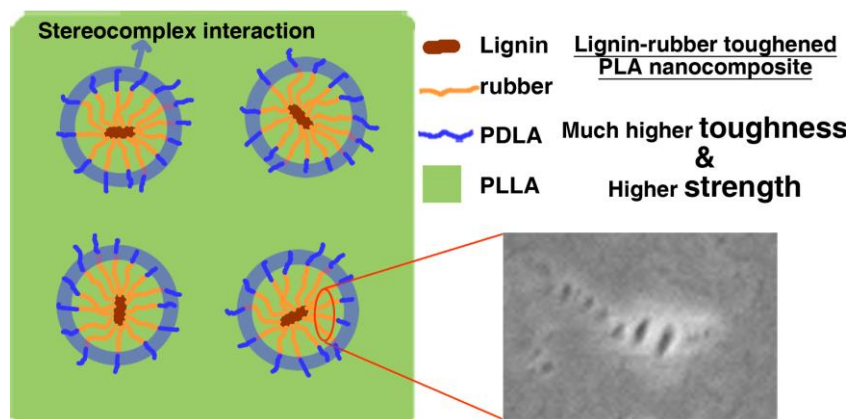
^c School of Materials Science and Engineering, Nanyang Technological University, Block N4.1, Nanyang Avenue, Singapore 639798

^d Institute of Materials Research and Engineering, Agency for Science, Technology and Research (A*STAR), 3 Research Link, Singapore 117602. Email: cb-he@imre.a-star.edu.sg

Corresponding author email address: msehc@nus.edu.sg; cb-he@imre.a-star.edu.sg

Abstract - Poly (lactide) (PLA)-lignin composites were fabricated by blending lignin-g-rubber-g-poly (D-lactide) copolymer particles and commercial poly (L-lactide) (PLLA) in chloroform. To synthesize the copolymer, poly (ϵ -caprolactone-co-lactide) (PCLLA) rubbery layer was formed *via* lignin-initiated ring opening copolymerization of ϵ -caprolactone/L-lactide mixture, followed by the formation of poly (D-lactide) (PDLA) outer segments *via* polymerization of D-lactide. The PDLA segments may contribute to strong interfacial interactions between lignin-rubber-PDLA and PLLA matrix by stereocomplexation which was observed using differential scanning calorimetry (DSC), Fourier transform infrared spectroscopy (FT-IR) and wide angle X-ray scattering (WAXS). The quasi-random structure of PCLLA and the formation of outer PDLA segments were characterized by nuclear magnetic resonance (NMR). A T_g of ~ 36 °C for PCLLA was detected by DSC, which confirms the rubbery characteristic of the synthesized copolymer. The resulting renewable and biodegradable composites exhibited a six-fold increase of elongation at break and a simultaneous improvement of tensile strength and Young's modulus albeit to a lesser extent. Light scattering, WAXS, small angle X-ray scattering (SAXS) and scanning electron microscope (SEM) studies suggested that good lignin dispersion, rubber-initiated crazing and strong filler-matrix interactions due to stereocomplexation are the effective mechanisms behind the excellent mechanical performances.

Keywords: Poly (lactide), lignin, nanocomposite, toughening, interface



HIGH EXPANSION OPEN-CELL POLYLACTIDE (PLA) FOAM FROM BLENDS WITH FIBRILLAR POLYTETRAFLUOROETHYLENE (PTFE)

Oral presentation

S. Ishihara, and M. Ohshima

Department of Chemical Engineering, Kyoto University, Kyoto, Japan 615-8510

Corresponding author email address: ishihara.shota.85r@st.kyoto-u.ac.jp

Abstract – Polymer blends of Polylactide (PLA) and fibrillar polytetrafluoroethylene (PTFE) were foamed by foam injection molding with core-back operation. PTFE has a fibrillar morphology in the PLA and increases shear and elongational viscosities, which suppressed bubble growth and increased bubble nucleation rate. By controlling the core-back distance, the open-microcellular foam with 80 % open cell content (OCC) of fibrillar structure was produced.

Keywords: Core-back Foam Injection Molding, Open Cell Foam, Polylactide, Polytetrafluoroethylene

1. INTRODUCTION

There have been many investigations of PLA foam aiming to lower the material cost by weight reduction and replace the traditional petroleum-based plastics by the biodegradable polymer. However, PLA was considered as a difficult polymer to be foamed because of its slower crystallization rate and lower melt tension [1].

In this study, blending the fibrillar PTFE, viscoelastic properties were modified and microcellular foams with higher expansion and open cell content were prepared in core-back foam injection molding process. The effect of PTFE on cell structure was investigated

2. EXPERIMENTAL

PLA (TP-4000, Unitika), whose melt flow rate is 3 g/10 min and D-isomer concentration was 1.5 %, was used as received. Acrylic modified PTFE (Metablen A3000, Mitsubishi Rayon) was added to PLA. N₂ gas (99.7 %, Izumi Sangyo) was used as blowing agent. PLA/PTFE blend foams were prepared by varying the PTFE content as well as expansion ratio in core-back foam injection molding process. The cell structure was observed by SEM (Mighty-8, Technex).

3. RESULTS AND DISCUSSION

Fig. 1 shows cellular structure of cross-sectional area perpendicular to the core-back direction of twofold expansion PLA/PTFE foams. The cell size of PLA/PTFE foams was reduced by addition of PTFE.

It is known that PTFE has fibrillar morphology in PP or PLA. Due to this morphology, entanglement of polymer chain was enhanced and shear viscosity and elongational viscosity were increased. Then, the bubble growth was

suppressed and bubble nucleation was enhanced. As a result, cell structure became uniform and fine.

Fig. 2 shows cellular structure of cross-sectional area parallel to the core-back direction of threefold expansion PLA/PTFE (97/3) foam. By increasing expansion ratio (core-back distance), fibrillar structures were obtained and OCC was increased to 80%

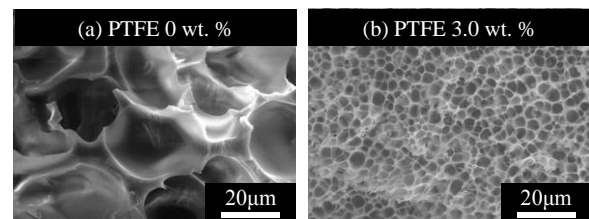


Fig. 1 SEM images of cross-sectional area of twofold expansion PLA/PTFE foams prepared at foaming temperature, 95 °C, and different PTFE contents, (a) 0 and (b) 3.0 wt. %

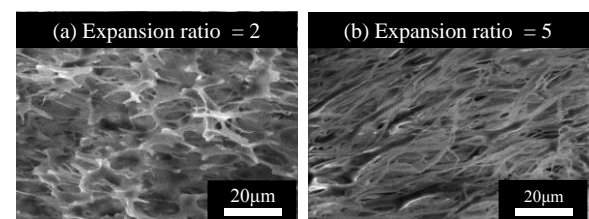


Fig. 2 SEM images of PLA/PTFE foams at the same foaming temperature (110 °C) and weight fraction of PTFE (3.0 wt. %), but different expansion ratios (a) 2 and (b) 5

4. CONCLUSION

High expansion open cell PLA foams were obtained by blending fibrillar PTFE.

REFERENCE

1. L. T. Lim et al., Prog. Polym. Sci., Vol. 33 pp. 820-852 (2008).

MEASUREMENT OF DEMOLDING RESISTANCE IN INCLINE DIRECTION TO TEXTURING CAVITY SURFACE USING 3-COMPONENT FORCE TRANSDUCER

Oral presentation

D. KATAYAMA¹, S. OWADA², and H. YOKOI³

¹ Institute of Industrial Science, The University of Tokyo - d-ktym@iis.u-tokyo.ac.jp

² Institute of Industrial Science, The University of Tokyo - showada7@iis.u-tokyo.ac.jp

³ Institute of Industrial Science, The University of Tokyo - hiyokoi@iis.u-tokyo.ac.jp

4-6-1, Komaba, Meguro-ku, Tokyo, 153-8505, JAPAN

Abstract - Transcription defects occurring on the textured surface of plastic molded products are due to the complicated combination of various factors. One of the main factors is the lateral force working on the textured patterns as a result of the shrinkage of resin or demolding at the incline surface. In this study, we proposed a method which measures demolding resistance generated during demolding in the incline direction. The measurement mold we used mounts a cavity block drive mechanism and 3-component force transducer, which allow measurement of the demolding resistance including the lateral force during demolding at inclined angle (inclined demolding) to the textured surface. We conducted demolding resistance measurement experiments using PS, a cavity with textured surface, and the demolding incline angle set to 45 degrees. The results showed that the demolding resistance in the melt flow direction increases proportionately to the mold gap, and then starts to decrease gradually after a certain threshold. We were able to specifically clarify the changes in the demolding resistance where the peak increases with increasing holding pressure. In addition, the magnified observation of the surface of the molded product confirmed that the anisotropy of the reflected light and the deformation of textured shapes remain after demolding, suggesting that in inclined demolding, these two defects should be caused by forcibly sliding along the inclined demolding direction in between the bumps of molded products and textured cavity surfaces.

Keywords: Injection molding, Demolding resistance, Textured surface, Inclined demolding

Introduction

During the texturing process in injection molding, many different patterns with concave and convex shapes such as stain-embossed finish and grain leather patterns are formed on the product surface. Transcription defects of these textured surfaces often occur, whereas many of the factors have not been analyzed in detail. The authors therefore conducted visualization analysis of the demolding process on stain-embossed finish to investigate the correlation with the transcription rate distribution of molded products. In a previous study, it was revealed that anisotropy occurs due to the deformation of the textured shapes during the demolding process as a result of the shrinkage of the molded product¹. Generally, the textured surfaces of molded products are positioned at the inclined surface to the mold opening direction. For this reason, like the results reported above, most of the demolding process is carried out by inclined demolding to the textured cavity surface. This is thought to cause defects such as non-uniform transcription of textured patterns on the molded products observed after demolding. With the aim to analyze the correlation between demolding defects and demolding resistance, in this study, we have developed a new mold for measuring inclined demolding resistance, based on the measurement mold used for measuring the demolding resistance in the mold opening direction in a previous report². We also conducted molding experiments to analyze the

correlation between the inclined demolding process and surface characteristics of the molded product. The following discusses the results.

Experimental Device

Fig.1 shows the experiment device developed in this study. The movable side of the mold is mounted with an elevating mechanism which can move the cavity block upward. As a result, during the demolding of the molded sample, demolding movements are generated in the parallel direction to the textured surface by the rise of the elevating mechanism when the mold opens in the perpendicular direction to the parting face as shown in Fig.2. The combination of these two movements realizes inclined demolding. At the stationary mold side, a transducer (washer type 3-component force transducer 9067, Kistler Japan Co., Ltd.) is mounted in the preloaded state between the movable block B (textured cavity surface) and base block C. This enables measurement of the force generated on the textured surfaces as in the melt flow direction (X-component), and the force working in the thickness direction (Z-component). The cavity has a rectangular shape with textured surface (Fig.3), and the runner has a submarine gate. This structure allows inclined demolding of only the molded product separated from the runner part during demolding. Table 1 shows the molding conditions for measuring demolding resistance when the demolding angle is set at 45 degrees in the direction perpendicular to the

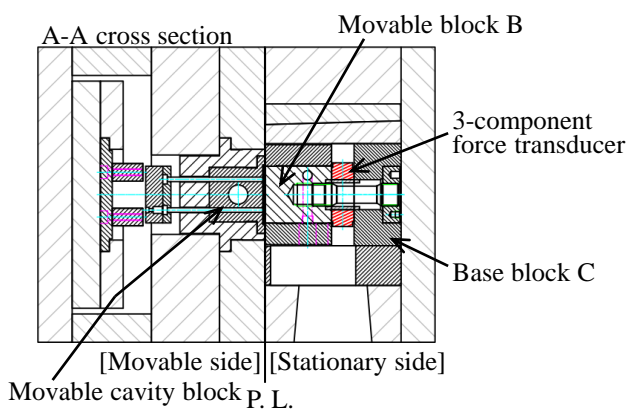
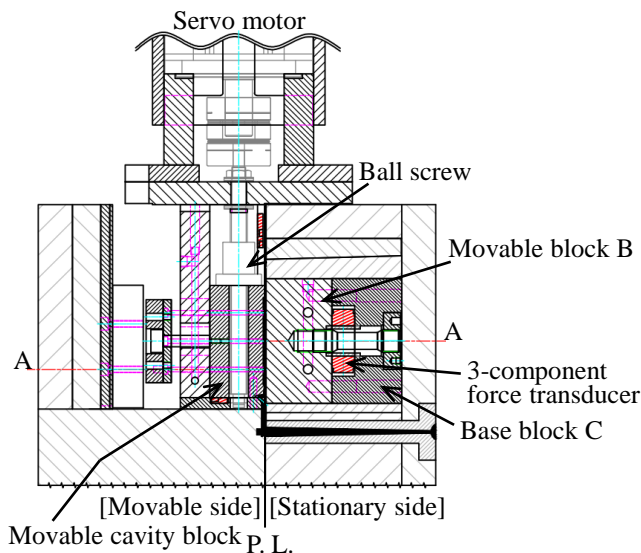


Fig.1 Fundamental structures of measurement mold of demolding force.

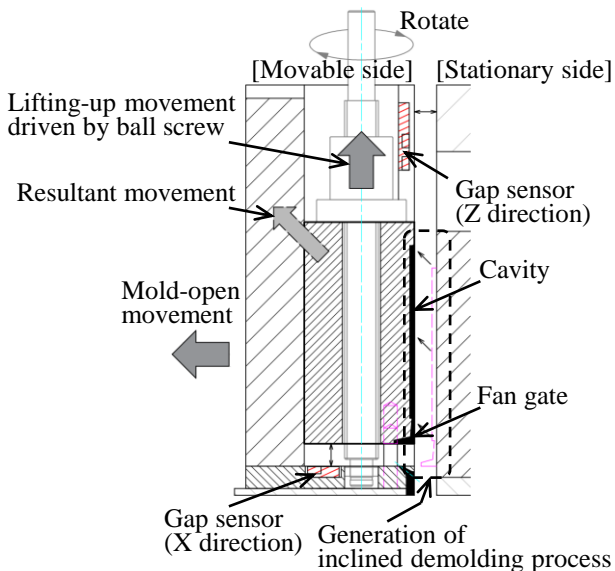


Fig.2 Schematic process of inclined demolding between molded product and cavity surface on stationary side.

cavity surface. The molding machine used was the NEX100 (NISSEI PLASTIC INDUSTRIAL CO., LTD.). Stain-embossed finish of Ra 10 μ m was used as the textured surface.

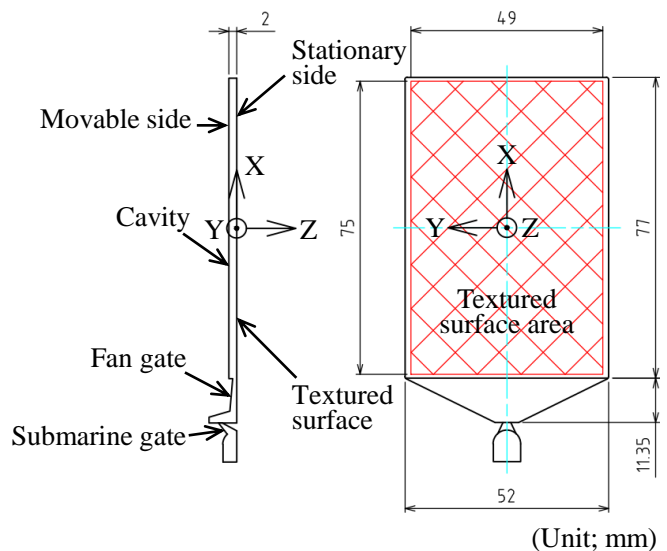


Fig.3 Cavity shape with textured surface.

Table 1 Molding conditions.

Injection molding machine	NEX110 (NISSEI PLASTIC INDUSTRIAL CO., LTD.)
Resin	GPPS 679 (PS Japan Corporation)
Cylinder temp. [°C]	220 – 230 – 230 – 220 – 210 – 60
Injection rate[cm ³ /s]	20
Mold temp. [°C]	60
Holding pres. [MPa]	30, 50
Textured surface	TH115 (TANAZAWA HAKKOSHA CO.,LTD.)
Demolding incline angle [deg]	45

Result and Discussion

Figs.4 to 8 show the measurement curves of the 3-component forces obtained from molding experiments. Figs.4 to 6 demonstrate the graphs of the 3-component forces at the holding pressure of 30MPa. Fig.4 shows the 3-component force measurement curves of all processes from P1 to P4 taking the x-axis as the time axis. P1 to P4 indicate the injection process, pressure holding process, cooling process, and demolding process. After the pressure holding process finished, the screw moves back so that the metering process can start. Fig.5 enlarges only the demolding process together with the mold gap (Z-gap). Fig.6 shows the 3-component force of the same demolding data taking the x-axis as the mold gap. The rising amount of the cavity block (X-gap) is also demonstrated. Figs.7 and 8 correspond to Figs.5 and 6 but with holding pressure set to 50MPa.

As the mold open mechanism of the molding machine used in this experiment is operated by a toggle mechanism, it is clear that the X- and Z-components in Fig.5 are exhibiting complicated behaviors. After the high pressure mold-clamping operation is canceled at t1, the mold starts to open from t2, and demolding completes at t6. Mold opening operations pause at t3, and resume at t4. For this reason, the mold gap (Z-gap) does not increase monotonously. In contrast, when the mold gap is expressed using the x-axis, the

X-component increases proportionately with the Z-gap and X-gap from t2 to t5 as shown in Fig.6. The X-component becomes maximum at t5, and starts to decrease until demolding completes at t6. For this reason, the surface of the molded product and textured cavity surface continue to contact until t5 (Z-gap = 56 μ m), after which partial demolding starts from t5. It is thought that the gradual decrease in the demolding resistance reflects the progress of partial demolding to the whole cavity surface.

When the holding pressure is increased to 50MPa, the slope of the X-component becomes 3.5 times that of 30MPa as shown in Fig.8. The peak value also increases by 3.2 times. It means that the increase in the restraint force between the molded product and textured surface of the mold has been specifically measured.

In a precedent study, the demolding resistance of the L&S micropattern was successfully measured, where a large demolding resistance was obtained in the perpendicular direction to the cavity surface²⁾. In contrast, such large resistances are not found in the Z-component measurement of textured surfaces in this experiment (demolding resistance is taken to be negative value). This means that with this textured pattern made up of the tapered face and curved face,

the demolding resistance in the perpendicular direction of the textured surface should be very small compared to the demolding resistance in the diagonal direction.

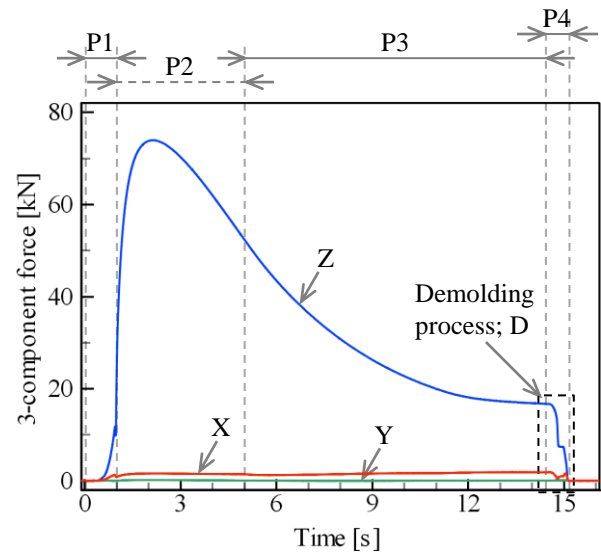


Fig.4 Change curves with time of 3 component forces measured in all the processes from filling start to end of demolding (Holding pressure: 30MPa).

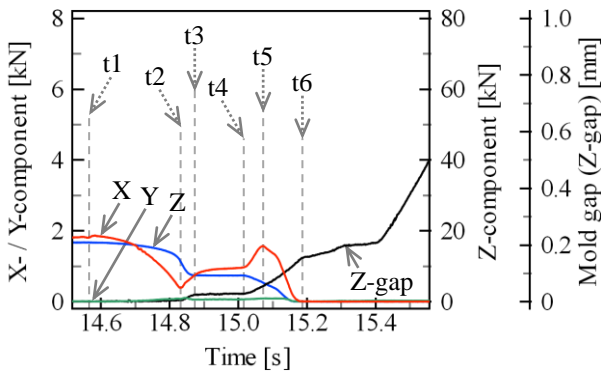


Fig.5 Detailed curves with time around the demolding process corresponding to D in Fig.4 (Holding pres.: 30MPa).

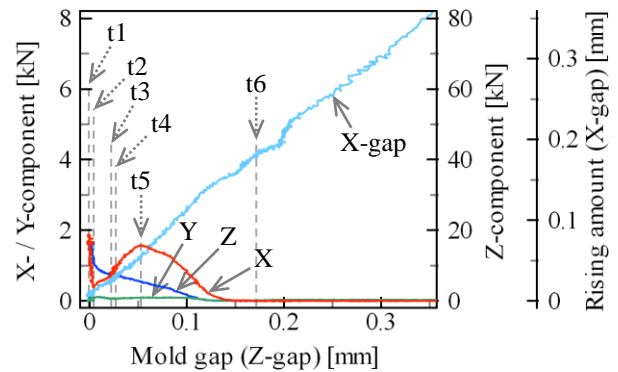


Fig.6 Change curves of indicated property with mold gap (Z-gap) during the demolding process (Holding pres.: 30MPa).

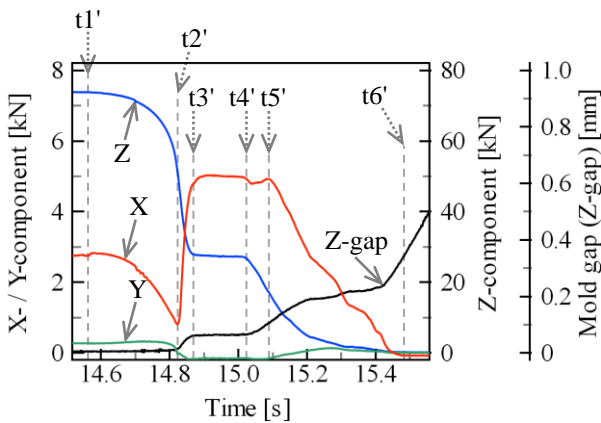


Fig.7 Detailed curves with time around the demolding process (Holding pres.: 50MPa).

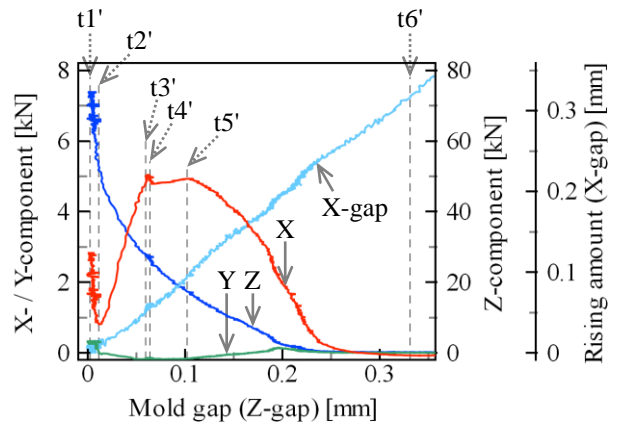


Fig.8 Change curves of indicated property with mold gap (Z-gap) during the demolding process (Holding pres.: 50MPa).

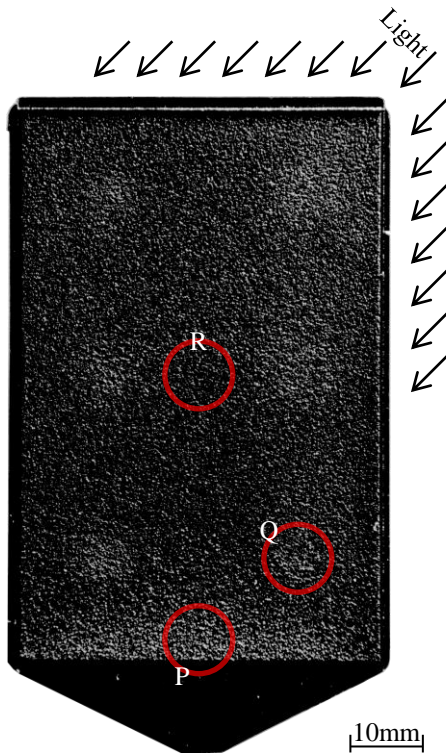


Fig.9 Overall appearance of the molded sample (Holding pres.: 50MPa).

Fig.9 shows a photo of the external view of the product molded at the holding pressure of 50MPa. When the photo was shot, the light was shone from the top right of the figure. For this reason, the area around the fan gate P and back of the ejector pin Q are whitish, confirming that the anisotropy of the reflected light has occurred. Next, the P and Q areas and general surface R were magnified, observed, and compared under a laser microscope. Fig.10 shows the results. In the P and Q areas, damaged areas S can be seen elongating in the up and down directions on the textured pattern. These areas show a consistent incline angle between 14 to 18 degrees. The same damage was found on the textured surface formed using the holding pressure of 30MPa, but it was minor. Taking into account that the peak value of the X-component of the demolding resistance at the holding pressure of 50MPa is 3.2 times that of 30MPa, it was concluded that these anisotropies of the reflected light differ in degree according to the different fixed states depending on the molding conditions and positions. In the inclined demolding process, anisotropy is thought to have been generated by the scratches from rubbing by the textured pattern on the resin transcribed surface being moved diagonally upwards by the textured pattern on the mold.

Conclusion

Experiments on the measurement of inclined demolding force were conducted using a newly

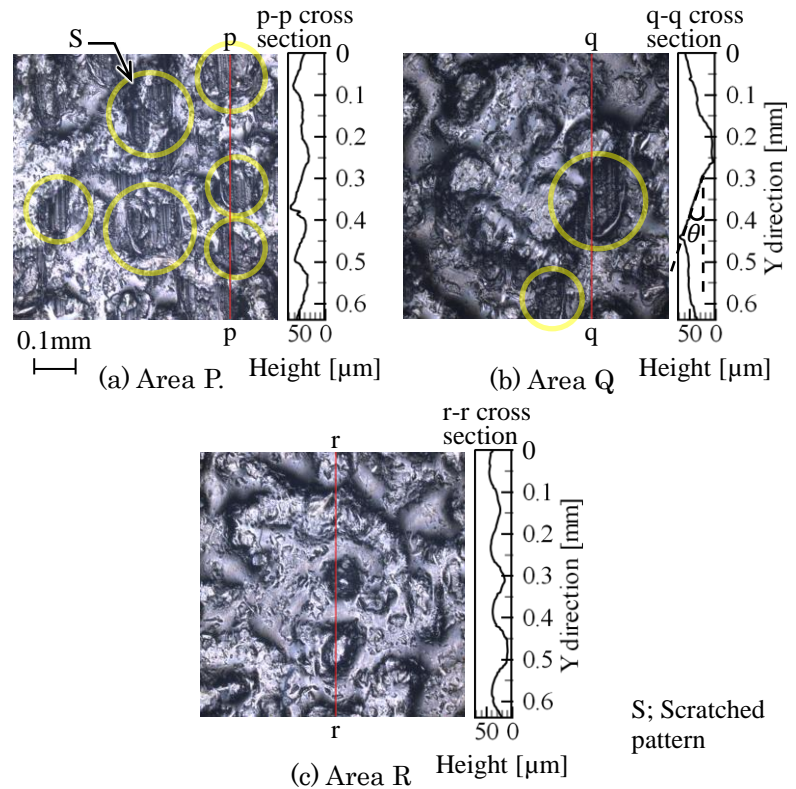


Fig.10 Observation of the molded surfaces and cross-sectional profiles by a laser-microscope.

developed measurement mold mounted with a 3-component force transducer. It was found that demolding resistance including the resistance along the cavity side can be measured. In molding experiments using PS and demolding incline angle of 45 degrees, the X-component, a force working in the melt flow direction, was found to increase proportionately with the mold gap amount and with the rising amount of the cavity block, confirming that the increase in the holding pressure causes the X-component peak value to increase sharply. In addition, it is assumed that the X-component decreases with the mold gap amount, resulting in the progress of partial demolding. Furthermore, magnified observation of the surface of the molded product revealed that the demolding progresses with the transcribed shape of the textured pattern interfering with the mold textured surface. This causes part of the textured surface to deform, resulting in the anisotropy of the reflected light.

Reference

- 1) N. Masuda, H. Yokoi, Analysis on the Generation Process of Irregular Brightness Change Pattern Appeared on Textured Molding Surfaces, AWPP 2014 Proceeding, #1225, 2014.
- 2) T. Ueda, H. Yokoi, Measurement of Demolding Resistance in Direction Vertical to Transcribed Surface without Bending Deformation of Molded Product, AWPP 2014 Proceeding, #1227, 2014.

PREPARATION OF POLY(LACTIC ACID) NANOFIBER BY COTTON CANDY METHOD

Oral presentation

R. Wongpajan¹, S. Thumsorn^{1,2}, H. Inoya¹, M. Okoshi¹ and H. Hamada¹

¹ Department Advanced Fibro-Science, Kyoto institute of Technology, Japan

² Department of Textile Engineering, Rajamangala University of Technology Thanyaburi, Thailand

Corresponding author email address: cussu_think@hotmail.com

Abstract - Poly(lactic acid) (PLA) is well known for biodegradable polymer, which is synthesized from renewable resources such as tropical and corn starch. According to environmental consideration, biodegradable of PLA is promising for applied in various kinds of industrial applications. This research is focus on preparation of PLA nanofibers by cotton candy method. The barrel temperatures were varied from 230, 240, 250, 260 and 270 °C. PLA was fed and subsequently spun through the spinneret, which has controlled the air pressure of 0.2, 0.3, 0.4 and 0.5 MPa and hot air at the spinneret. The screw speed was set at 10 rpm. The effect of barrel temperature on morphology, thermal properties and crystallization behavior of PLA nanofiber was investigated. Morphology of nanofiber is determined by scanning electron microscope (SEM). Thermal properties and crystallinity are examined using differential scanning calorimetry (DSC). Figure 1 shows morphology of PLA nanofiber at 260 °C and 270 °C that were obtained with magnification of 10,000. The diameters of PLA nanofiber are 1.0991 and 1.6376 μm for 260 °C and 270°C, respectively. It was found that the fiber diameter at 260 °C was smaller than that of 270 °C. However, PLA nanofiber size was not uniformity. The DSC results show clearly glass transition and cold crystallization temperature in the nanofiber at 270 °C, which indicated that this nanofiber was slow crystallization during process. On the other hand, it can be seen higher intensity of melting temperature in the nanofiber at 260 °C. It was considering that the nanofiber at lower processing temperatures would be smaller diameter and would be presented higher crystallinity than that of higher temperature. The effect of air pressure on morphology and thermal properties of PLA nanofibers are elucidated.

Keywords: poly(lactic acid), nanofiber, extrusion, high pressure, hot air

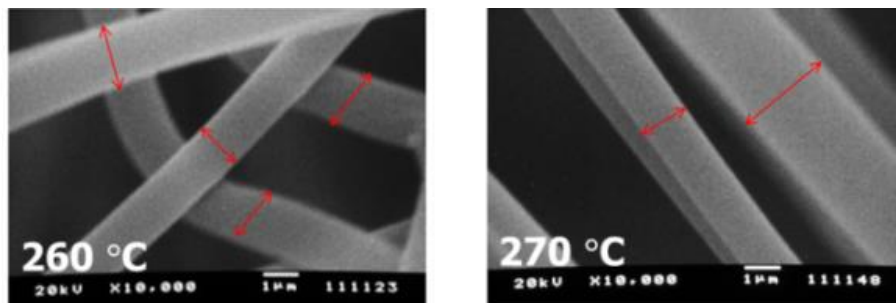


Figure 1 Longitudinal SEM photographs of the PLA nanofiber.

CONTROL OF GLASS TRANSITION TEMPERATURE IN IMMISCIBLE RUBBER BLEND

Oral presentation

N. Kuhakongkiat, K. Yoshida, S. Nobukawa and M. Yamaguchi*

School of Materials Science, Japan Advanced Institute of Science and Technology, Japan

1-1 Asahidai, Nomi, Ishikawa, JAPAN 923-1291

Corresponding author email address: m_yama@jaist.ac.jp

Abstract – Interphase transfer phenomenon was used to control the glass transition temperature, T_g , of immiscible rubber pair as a function of ambient temperature. In this study, the laminated sheets composed of ethylene-propylene rubber (EPR) and poly(isobutylene) (PIB), in which di-(2-ethylhexyl) adipate (DOA) is added, are separated after annealing at various temperatures.

Figure 1 shows the temperature dependence of tensile loss modulus E'' at 10 Hz for pure rubbers and the rubbers with 10 phr of DOA. It is found that T_g of each rubber, defined as the peak temperature of the E'' curve, shifts to lower temperature by the addition of DOA, demonstrating that DOA acts as a plasticizer for both rubbers. Furthermore, a single peak of E'' for both blends suggests that DOA is miscible with each rubber.

Figure 2 shows E'' for separated sheets after annealing at $-20\text{ }^\circ\text{C}$ and $40\text{ }^\circ\text{C}$ for 5 days. It is demonstrated that T_g of EPR shifts to low temperature after annealing at $-20\text{ }^\circ\text{C}$ and high temperature at $40\text{ }^\circ\text{C}$. Correspondingly, T_g of PIB also changes by the annealing procedures.

These experimental results suggest that DOA shows interphase transfer even in a blend of EPR and PIB, having phase-separated structure. When EPR is a matrix, the blend is flexible in winter season due to a large amount of the plasticizer in the matrix, and vice versa in summer season.

Keywords: Immiscible rubber, Liquid transfer, Plasticizer

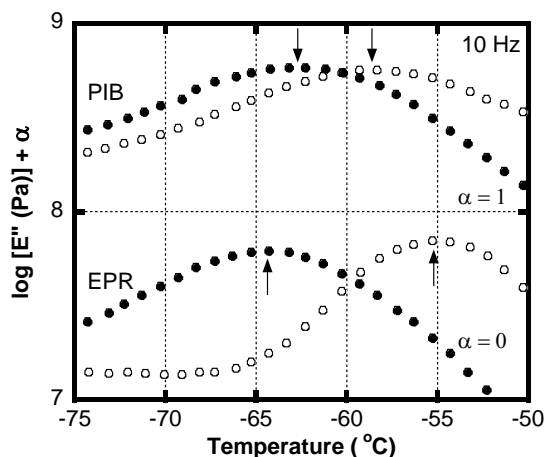


Figure 1 Temperature dependence of the tensile loss modulus E'' for the samples of (open symbols) pure rubber and (closed symbols) rubber containing 10 phr of the DOA; (top) PIB and (bottom) EPR

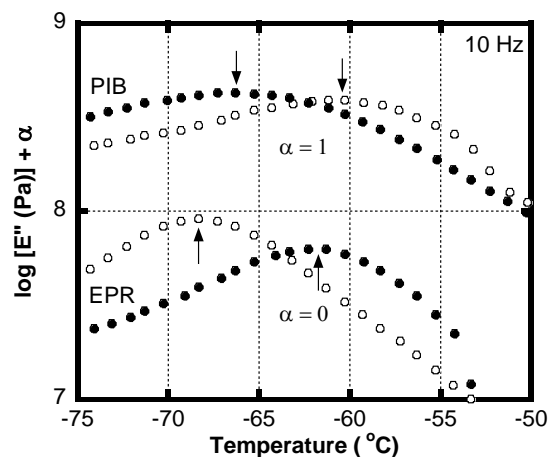


Figure 2 Temperature dependence of tensile loss modulus E'' for the samples after annealing at (closed symbols) $-20\text{ }^\circ\text{C}$ and (open symbols) $40\text{ }^\circ\text{C}$; (top) PIB and (bottom) EPR

PP/LLDPE HYBRID IN AXIAL POWDER FLOW APPARATUS

Oral presentation

E. Junsri^{1*}, N. O-Charoen¹ and H. Hamada²

¹*Department of Materials and Metallurgical Engineering, Faculty of Engineering, Rajamangala University of Technology Thanyaburi, Pathum thani 12110*

²*Department of Advanced Fibro Science, Kyoto Institute of Technology, Sakyo-ku, Kyoto, Japan 606-8585*
Corresponding author email address: ektinai.js@gmail.com

Abstract - In this study, the axial powder flow apparatus was used in molding the hybrid polymers between polypropylene copolymer and linear low-density polyethylene (LLDPE). Materials were prepared in powder form by pulverizer and mixed by dry blend method at ratio 50 : 50 (wt%). The variations of temperature inside the mold and state changes of PP/LLDPE hybrid were investigated. Differential scanning calorimeter (DSC) and Optical microscope (OM) use to determine thermal properties and phase separation in the hybrid respectively. Mechanical properties of the hybrid was monitored by compressive strength method. The results showed that the mechanical properties of the hybrid decreased when compared with PP and LLDPE pure. The result from melt flow index (MFI) of the hybrid shown that LLDPE improves the flow properties in PP. However, the PP/LLDPE hybrid was successfully in processability using the axial powder flow apparatus at ratio 50 : 50 (wt%) with the internal air temperature 170 °c and rotational speed 7 rpm.

Keywords: Polypropylene, Linear low-density polyethylene, Rotational molding, Two-layer structures.

THE FLAMERETARDANCY STUDY OF CORRUGATED CARDBOARD USING FOR CARDBOARD BED

Oral presentation

Yusaku. Mochizuki¹, Yoshihiro. Mizutani¹, Masayuki. Okoshi¹, Hiroyuki. Hamada¹

¹ Department of Advanced Fibro Science, Kyoto Institute of Technology, Japan

Corresponding author email address: mczk0520@gmail.com

Abstract - Recently Corrugated Cardboard is available for not only packing materials but we use the cardboard for furniture and cots at refuges. The reason why the cardboard has the characteristics of lightness, high strength, cheapness and recycle ability. In particular, there is the strong needs to add flameretardancy to cardboard bed for prevention of second disaster. Our purpose in this study is to add the flameretardancy to the cardboards with keeping the recycle ability. The cardboard of combusting behavior was measured by using a calorimeter. We used Ammonium Sulfate, Tri-Octyl Phosphate (TOP) and Tri-Butyl Phosphate (TBP) as flameretardant. Also we used 3 kinds of commercial flameretardant to compare with Ammonium Sulfate, TOP and TBP. As the result, Ammonium Sulfate showed great flameretardancy to cardboards. By adding Ammonium Sulfate to cardboard, It is possible to decrease exponentially the Heat Release Rate (HRR).

[Fig.1] [Fig.2]

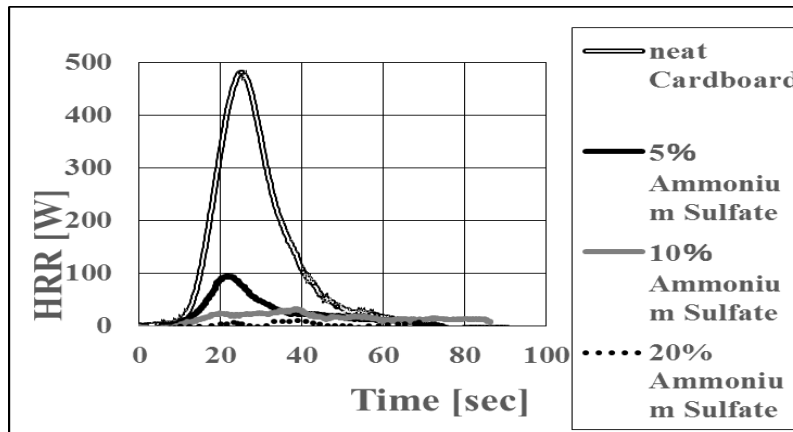


Fig.1 HRR of Ammonium Sulfate

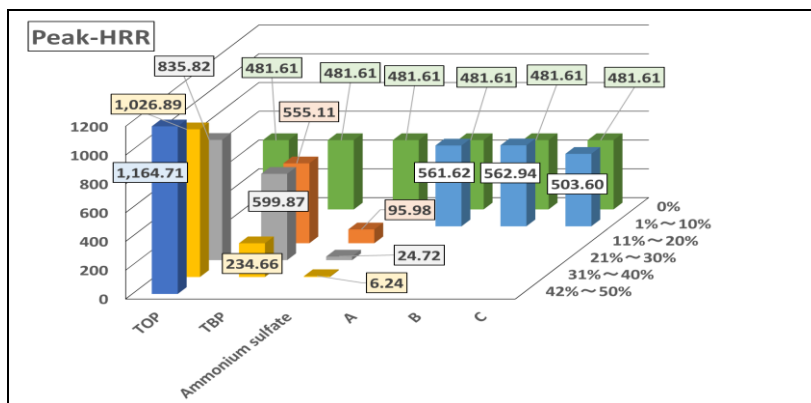


FIG.2 PEAK-HRR OF EACH FLAMERETARDANT

We are planning to use the cardboard bed. Therefore we are trying to add the flameretardancy for cardboard. The combustion behavior of cardboard bed was measured by using large combusting furnace. A part of the combusting behavior of cardboard bed was clarified from the experiment and it became important data for our further study..

Keywords: Cardboard, Combustion, Flameretardancy, PVA.

POLY(LACTIC ACID)/POLYPROPYLENE BLENDS FOR COSMETIC CASE PRODUCTS

Oral presentation

J. Kordsa-Art¹, R. Wongpajan², H. Hamada² and S. Pivsa-Art^{1*}

¹*Department of Materials and Metallurgical Engineering, Faculty of Engineering,
Rajamangala University of Technology Thanyaburi, Pathumthani, Thailand*

²*Department of Advanced Fibro Science, Kyoto Institute of Technology, Kyoto, Japan
Corresponding author email address: sommai.p@en.rmutt.ac.th*

Abstract - Cosmetic cases are conventionally produced from polypropylene (PP) or Acrylonitrile-butadiene-styrene (ABS) copolymers. However, these polymers are non-degradable and their wastes cause problems to environment. Addition of environmental friendly material to the petroleum-based polymer will reduce the amount of non-degraded parts. Poly(lactic acid) (PLA) is a biodegradable polymer having high potential for industrial applications from its mechanical property. Blending of PLA and PP increased the biodegradable part of the polymer blends. But due to phase separation of PLA and PP, we studied the effects of a compatibilizer for the blends. The polymer blends were prepared with PLA:PP ratios of 100:0, 80:20, 60:40, 50:50, 40:60, 20:80 and 0:100 with addition of 1, 3 and 5 wt% of polypropylene-*graft*-maleic anhydride (PP-*g*-MAH) as a compatibilizer. The product samples were prepared with injection molding process and subjected to thermal, mechanical properties chemical properties morphology analysis and percent of compatibility of PP-*g*-MAH. The thermal analysis confirmed that addition of PP-*g*-MAH has no effect on crystalline melting temperature of the polymer components but the impact strength was increased. The highest impact strength was found with PLA:PP ratio 40:60 with 3 wt% of PP-*g*-MAH. The results are in agreement with morphology study of polymer blends confirmed the adhesion of PLA and PP by assistance of PP-*g*-MAH. The addition of more amount of PP-*g*-MAH resulted in high polarity of a compatibilizer and decreased the compatibility with PLA. The tensile strength of polymer blends increased with increasing amounts of PLA. The research results confirmed the application of polymer blend system with injection molding process.

Keywords: Poly(lactic acid), Polypropylene, Polypropylene-*graft*-maleic anhydride, Cosmetic case

Analysis of Dispersive Behavior and Mixing State of Filler Mixed into SBR and BR

Oral presentation

Shonosuke Kaneko^{1*}, Asahiro Nagatani² and Tatsuya Tanaka¹

¹ Department of Mechanical Engineering, Doshisha University, Japan

² Hyogo Prefectural Institute of Technology, Japan

Corresponding author email address: duo0527@mail4.doshisha.ac.jp

Abstract - Rubber products which are consisted of other polymers or fillers such as carbon black (CB) are made by internal mixer. This process is called mixing process. And it is known that this process affects the later product quality greatly. Mixing and dispersion process cannot be seen directly because internal mixer is a sealed type mixer. Generally, the mixing state is examined based on relationship a torque (or electricity power) and mixing time curve (i.e. mixing chart). Method to decide mixing time is an important problem in rubber mixing technique.

In addition, it was known to be decided by a unit work as for the Mooney viscosity in the mixer, even if the volume of mixer is different by past document^[1]. It was revealed that this relationship is established in the case of the different number of revolutions. Then, it is assumed that the internal mixer has the role as the viscometer. The viscosity depends on shear speed and temperature in the case of shearthiny materials. Therefore temperature was remarked as a judgment of mixing time. In other words, the state of the mixing or dispersion state can be estimated from relations of the shear stress and the temperature. In this study, relationship with parameter which is provided from internal mixer and filler dispersion in rubber or the viscosity was investigated.

As experiment, SBR, BR, CB, silica was used for materials. These are used for raw materials of the tire. After testing with a smaller internal mixer, a larger internal mixer was used for discussing the difference of volume. The dispersion state of compound mixed by larger mixer dose not equal to the one of smaller mixer because of the difference of power capacity and heat transfer. Laboplastmil (toyoseikiseisakusyo) has 0.1L capacity and MIXTRON (Kobe Steel) has 1.63L capacity were used for mixing. All materials were introduced into the mixer at the same time. The torque, mixing time, consumption electricity and temperature of the materials were measured during mixing. The evaluation of the filler dispersion was performed by TEM, viscoelastic examination. The viscosity was measured Mooney viscometer and capillary rheometer.

As a result, relationship instantaneous electric power and total electric power was showed in Fig1. And the relationship the parameter which divided instantaneous electric power by the number of revolutions and total electric power curve was piled up even if the number of revolutions was changed (Fig2). When the number of revolutions was changed, the average shear stress calculated from the shear rate in the tip clearance and the fill factor was the same level. And It was revealed that the relationship the reciprocal of temperature and the logarithm of the shear stress were proportion in the end part of mixing.

[1] O'CONNOR,G.E., Putman, J.B. : Rubber Chem. Thecnol.,57, 799 (1978)

Keywords: mixer, dispersion, rubber, shear stress, viscosity

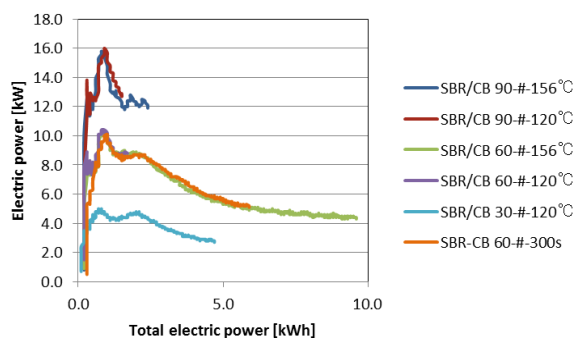


Fig1. Instantaneous power — Total power curves

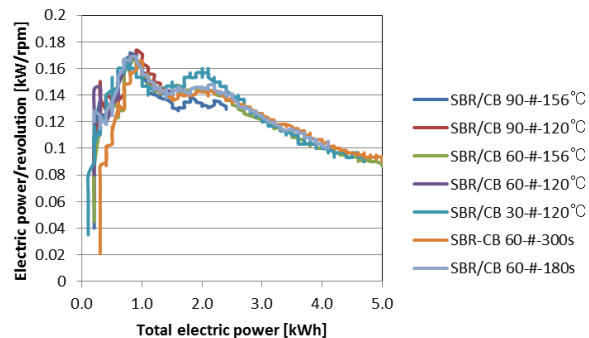


Fig2. Converted curves in consideration of the number of revolutions

MEASUREMENT OF THREE-DIMENSIONAL TEMPERATURE DISTRIBUTIONS INSIDE CAVITY FILLING MELTS USING INTEGRATED THERMOCOUPLE SENSOR

Oral presentation

S. Ishida, N. Masuda, H. Yokoi*

Institute of industrial Science, The University of Tokyo, 4-6-1 Komaba, Meguro-ku, Tokyo, 153-8505, Japan

**Corresponding author email address: hiyokoi@iis.u-tokyo.ac.jp*

Abstract Integrated thermocouple sensors capable of high precision measurement of temperature distribution inside melts filling into the cavity have such drawbacks as complicated measurement work, difficulty to change the sensor position, and poor sensor durability. In this study, the authors developed a measurement mold capable of moving these sensors to anywhere in the cavity, and maintaining the sensors at both the stationary and movable sides of the mold. Experiments were then conducted to clarify that the mold is capable of three-dimensional measurement of temperature distribution by moving the sensors gradually from the center of the cavity to the side of the cavity. In molding experiments using a rectangular cavity with a thickness of 3mm and PP, it was found that cooling effects along the cavity wall are promoted at low injection rate, and that the closer the sensor moves to the cavity side, the temperature drops more sharply. On the other hand, at high injection rate, shear heating effect becomes more conspicuous as the sensor moves toward the side, resulting in the sudden increase in the temperature. Such dramatic temperature changes were confirmed to be limited to the area near the side of the cavity wall to the area where the wall thickness is 2 to 3 times more (about 7 to 10 mm).

Keywords: Injection molding, Gap-width temperature profile, Flowing melt, Integrated Thermocouple Sensor

1. Introduction

In injection molding, the clarification of the distribution of resin temperature in the mold is an important research task for understanding various molding phenomena. Some of the authors developed a method of measuring temperature distribution inside melts filling into the cavity by patterning pure metals made of copper and nickel on a thin board, and forming a row of thermocouples at high integration rate, installing the sensors perpendicularly to the mold cavity face and parallel to the flow direction of the melt, and have been conducting studies on the measurement of temperature distribution along the thickness of the cavity under various conditions¹⁾⁻⁴⁾. As the sensors are supported only at one end, asymmetrical force works on the sensor face near the cavity side, causing the sensors to turn over and become damaged. For this reason, there is a need to support the sensors on both ends from the stationary and movable sides in non asymmetrical flow fields. In preceding studies, some of the authors conducted experiments in which the complicated job of removing the support block of the movable mold for every shot was carried out. To change the position of the sensors, the cavity has to be rebuilt each time. Thus, in this study, the authors developed a measurement mold which allows the sensors to be moved to any position inside the cavity, and the sensors to be supported at both the stationary and movable sides of the mold. Measurement experiments were then conducted on continuous molding using this mold to clarify temperature distribution inside the cavity three-dimensionally, and the results confirmed

the usefulness of the method. The study and results are reported below.

2. Experimental System and Method

2.1 Integrated thermocouple sensor

Fig.1 shows the basic structure of the BT resin substrate integrated thermocouple sensor used in this study. For the base material, BT resin reinforced with fiberglass cloth was used to provide increased durability compared to the polyimide base. On both sides of a 100 μ m thick base, both Cu and Ni were patterned, and a coupling section was made using a through-hole. Sixteen measuring points were set, 0.25mm apart.

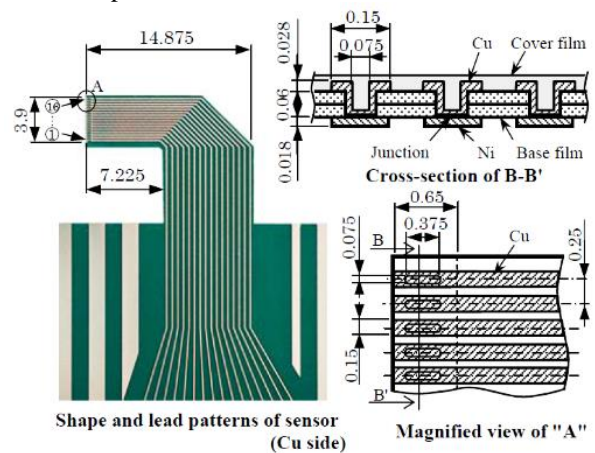


Fig. 1 Basic structure of BT resin-based sensor (Unit: mm)⁴⁾

2.2 Basic Structure of Measurement Mold

Fig. 2 shows the basic structure of the measurement mold developed in this study. The integrated thermocouple sensors were sandwiched between the two blocks A and B of the stationary side mold, and connected to the special compensating lead wire. The measurement block has a structure which enables the sensors to be moved to any positions along the cavity width using the adjustment bolts installed on both sides of the mold base, and the sensors positions to be managed using the contact displacement sensor (AT-V, made by KEYENCE). The movable side of the measurement mold installed with two cavity blocks C and D with left-right symmetrical screw holes. These cavity blocks C and D can be opened/closed by rotating the shaft extended to outside the mold. This open/close mechanism is linked to the mold closing action by the cams and positioning pins installed on both sides of the stationary side cavity blocks. The sensor positions are always corresponding to the open/close central positions of blocks C and D. For this reason, after the mold is tightened, blocks C and D move symmetrically and support the sensors on both sides.

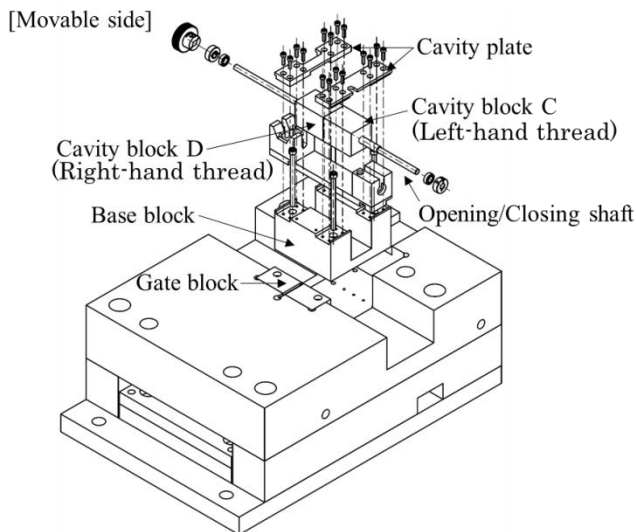
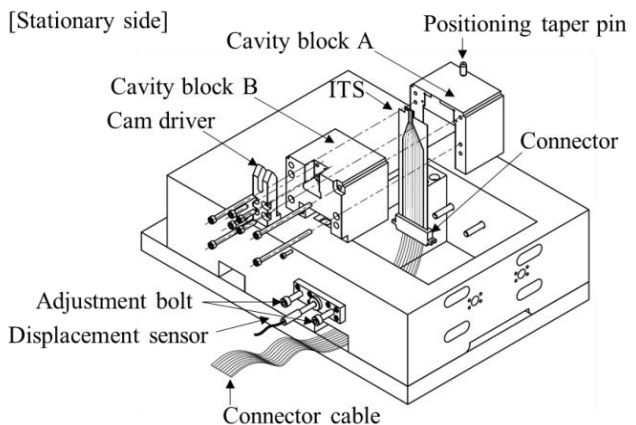


Fig. 2 Schematic structure of mold

2.3 Measurement Method

Fig.3 shows the shape of the cavity used and the measurement positions of the sensors. The cavity size is 120x50mm and 3mm thick. A well cavity is provided at the end of the cavity. An indirect inner pressure sensor (Type 9221 made by Kistler) is installed under the ejector pin inside the runner to measure the pressure. Fig.4 shows how the sensor supported on both ends is installed. Taking the position of the stationary side cavity face to be 0 mm in respect to the 3 mm thickness of the cavity, 11 measurement positions No.2 (0.25mm) to No.12 (2.75mm) were set on the coupling. Taking the center of the cavity to be $x=0$, the sensors were moved along the cavity width to measure at positions $x=0, 5, 10, 15, 18, 20, 21, 21.5, 22$ mm in this order. The injection molding machine used was NEX110 (screw diameter of $\varnothing 36$ mm, NISSEI PLASTIC INDUSTRIAL CO., LTD.). The resins used was PP (J106, Prime Polymer Co.,Ltd.) and the molding conditions are shown in Table 1. The injection rates were set at 10, 55, and 100cm³/s.

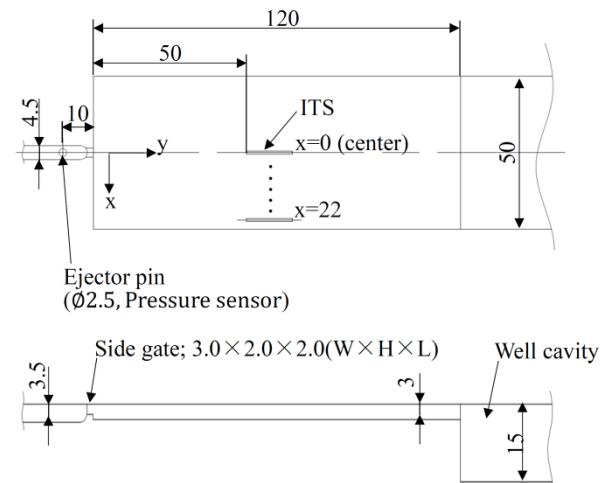


Fig. 3 Cavity shape (Unit: mm)

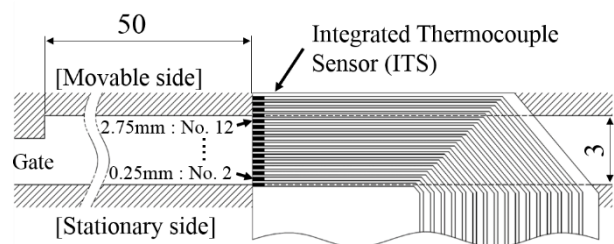


Fig. 4 Sensor installation method (Unit: mm)

Table1 Molding conditions

Resin	PP J106 (Prime Polymer Co., Ltd.)
Injection rate[cm ³ /s]	10, 55, 100
Cylinder temp. [°C]	220-230-230-220-210
Mold temp. [°C]	40
Charging stroke (mm)	62

3. Experiment Results and Discussion

Fig. 5 shows the bird's eye view of the results of temperature distribution along the thickness of the cavity just before injection molding ends at the various injection molding rates. It was confirmed that temperature distribution along the thickness of the cavity can be continuously measured while moving the sensor from the center of the cavity to the side of the cavity.

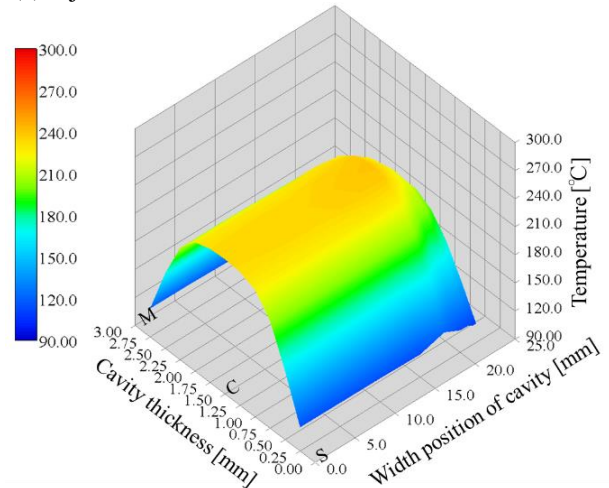
At the injection rate of $10\text{cm}^3/\text{s}$, the temperature dropped from $x=20\text{mm}$ to $x=22\text{mm}$. Under low injection rates, cooling is promoted due to the long filling time. The temperature near the wall drops along the thickness of the cavity, and cooling effects are the highest near the side of the wall along the width of the cavity because this area is enclosed by walls in three directions. For this reason, cooling is promoted, resulting in a sharp drop in the temperature. On the other hand, at high speed conditions above the injection rate of $55\text{cm}^3/\text{s}$, temperature starts to increase around $x=18\text{mm}$, and the change is larger towards the side of the wall. At high injection rates, shear heating effects become conspicuous near the wall. On the other hand, the shortening of the filling time is thought to enhance the cooling effects.

Fig.6 shows the temperature distribution along the thickness of the cavity at each injection rate, $x=0, 20, 22\text{mm}$ to compare the temperature distribution profiles. When $x=0\text{mm}$ (center of the cavity), the temperature distribution is a radial shape at the injection rate of $10\text{cm}^3/\text{s}$. Its shape starts to change to a trapezoid when the injection rate increases to 55 and then $100\text{cm}^3/\text{s}$.

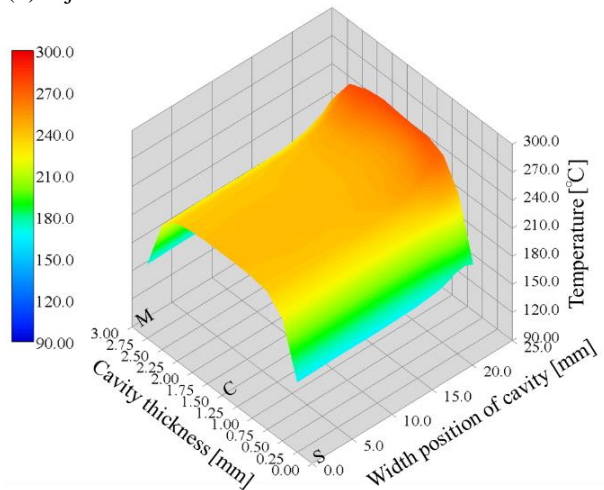
At $x=20\text{mm}$ to 22mm , the temperature decreases in the radial shape at $10\text{cm}^3/\text{s}$. On the other hand, at high injection rates of 55 and $100\text{cm}^3/\text{s}$ and when $x=20\text{mm}$, the temperature distribution changes to a horn shape where the temperature near the wall along the thickness of the cavity starts to increase from the center of the cavity. At $x=22\text{mm}$, the temperature rises throughout the whole area and is especially conspicuous at the center. The temperature distribution profile gradually changes to a trapezoid shape again. This may be because temperature increased throughout the whole area as a result of the shear heating effects from three directions, namely two walls along the thickness of the cavity, and the side wall of the cavity. In particular, the temperature peaked selectively at the horn area. The rise in temperature is thought to correspond to the preceding flow of the edge known as ear flow. The area with conspicuous temperature change at the side of the cavity was found to be about 7 to 10mm ($x=18\text{-}15\text{mm}$) away from the cavity side, and correspond to the edge which is 2 to 3 times thicker.

In particular, temperature distribution along the thickness was asymmetrical near the side. This may be because the closer the sensor is to the wall, the more the sensor tends to deform during measurement, causing measurement error. The sensor strength is therefore an issue that must be resolved.

(a) Injection rate $10\text{cm}^3/\text{s}$



(b) Injection rate $55\text{cm}^3/\text{s}$



(c) Injection rate $100\text{cm}^3/\text{s}$

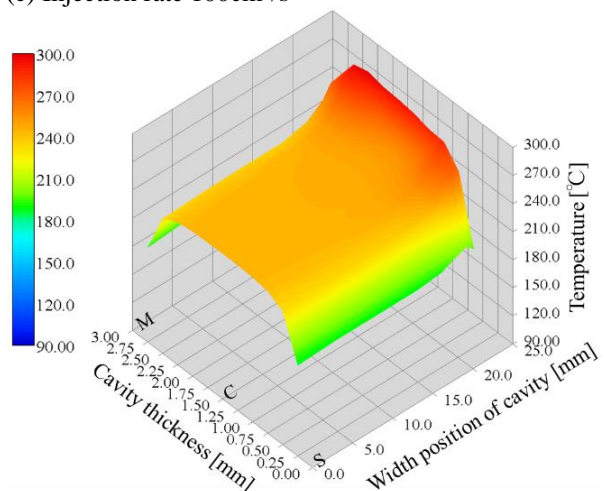


Fig. 5 Temperature distributions inside cavity filling melts (S: Stationary side, M: Movable side, C: Center of cavity thickness)

4. Conclusion

- (1) The results of measurement experiments confirmed that the developed mold is able to continuously measure temperature distribution along the thickness of the mold by moving the measurement position from the center of the cavity to the side of cavity.
- (2) Cooling effects were promoted at low injection rates, and the temperature decreased sharply the nearer the measurement positions were to the cavity side along the width. It was also confirmed that at high injection rates above $55\text{cm}^3/\text{s}$, temperature increasing effects by the shear heating along the width of the cavity increased.
- (3) The areas where the temperature change along the cavity thickness was large were confirmed to be the areas where the melt flowed from the cavity side to the side of the cavity measuring 7 to 10 mm (2 or 3 times greater than the thickness).

References

- 1) Yokoi, Murata, and Tsukakoshi: Seikei-Kakou, 8, 107 (1996)
- 2) Murata, Abe, and Yokoi: Seikei-Kakou, 14, 257 (2002)
- 3) Murata, Abe, and Yokoi: Seikei-Kakou, 15, 706 (2003)
- 4) Yokoi, Murata, Takahashi, Anbe, and Nakamura: JSPP'09 Tech. Papers, 157(2009)

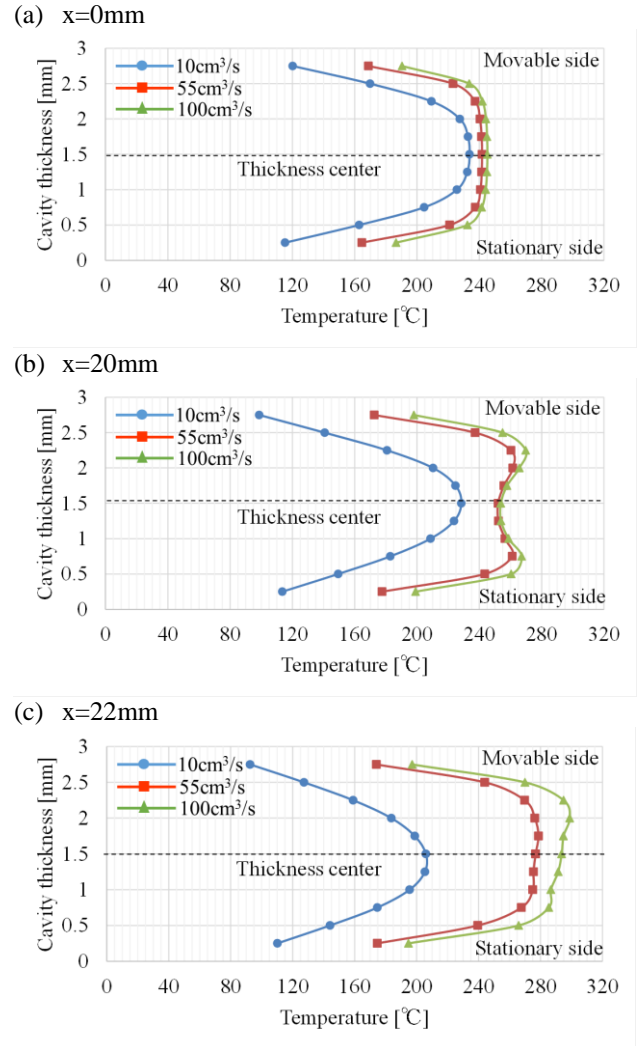


Fig. 6 Temperature profile along cavity thickness for several cavity width positions at end of filling process

A HIGHLY EFFICIENT REEL TO REEL HOT EMBOSsing PROCESS FOR FABRICATION OF POLYMER MICROLENS ARRAY

Poster presentation

C.Y. Chang* and J.H. Chu

Department of Mold and Die Engineering, National Kaohsiung University of Applied Sciences, Taiwan

Corresponding author email address: cychang@kuas.edu.tw

Abstract - Reel-to-reel (R2R) hot embossing is a promising process for fabrication of micro structures on polymers with high accuracy and high through-put. This paper reports a novel and high effective method for fabrication of polymer microlens array devices based on reel to reel film transfer and gas assisted hot embossing process. Therefore, a novel reel to reel hot embossing system with gas pressure capacity has been designed, constructed and tested. As shown in Fig. 1, the system are composed of a reel to reel mechanism with tension roller, a closed chamber, a nitrogen tank with a pressure regulator and valves, a heating/cooling plate with vacuum pump. In this study, a large area thin steel mold with micro-circular holes array pattern is fabricated by photo-lithography and wet chemical etching process. The roll of plastic film/ thin steel mold stack is placed in a closed chamber and hot plate is heated to processing temperature which is above the T_g of the plastic material. During the heating process, vacuum pressure is applied to the film to prevent the film from creasing. When the processing temperature is reached, the nitrogen gas is introduced into the chamber to exert gas pressure over the film, forcing the film in close contact with the thin steel mold. Under proper processing conditions, the softened polymer will just partially fill the micro-circular holes on the surface of thin steel mold and due to surface tension form a convex lens surface. After the cooling process, the nitrogen gas is vented, the chamber is opened. The microlens array pattern on the surface of plastic film is removed from the thin steel mold. After the reel to reel hot embossing process. The roll of large area polymer microlens array device can be fabricated, as shown in Fig. 2. Finally, the effects of processing conditions on the shape and quality of fabricated polymer microlens array were investigated. The geometrical and optical properties of the fabricated polymer microlens arrays were measured and proved satisfactory. This technique shows great potential for fabrication of polymer microlens array with high productivity and low cost.

Keywords: Reel to reel hot embossing, polymer microlens array

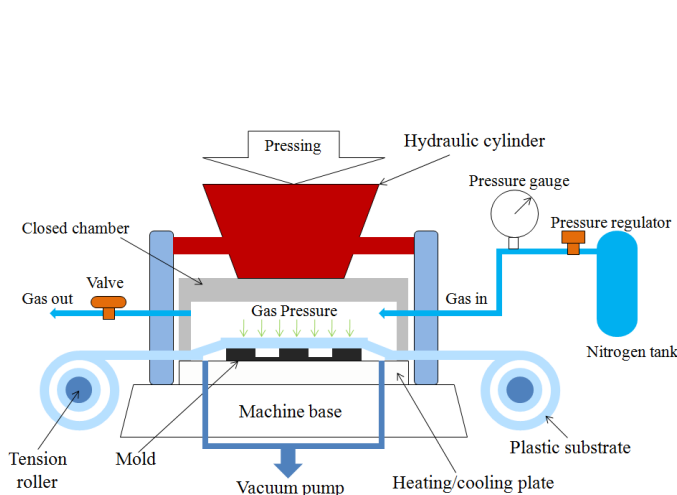


FIGURE 1



FIGURE 2

Modification of chemically stable polymeric materials 64. Improvement in the hydrophilic and adhesion properties of polymeric materials and FRPs

Poster presentation

H. Kanazawa and A. Inada

*Department of Industrial Systems, Faculty of Symbiotic Systems Science,
Fukushima University, 1 Kanayagawa, Fukushima 960-1296, Japan: kana@sss.fukushima-u.ac.jp*

Abstract Hydrophobic polymeric materials such as polypropylene, polyethylene, PET were modified by a new combination method of physical and chemical processes. The modified materials gave a durable hydrophilic property, and the improvement in adhesion, property, water-based paint coating or ink-jet printing. Poly(methyl pentene), silicone resin and engineering plastics of which modification is difficult by corona or plasma discharge treatments were modified well. Polymer composites such as GFRP and CFRP for cars and aircrafts were improved., and the adhesion property was increased. The modified materials gave a high durability as compared with a plasma treatment and the other methods.

Keywords: surface modification, adhesive property, polypropylene, GFRP, CFRP, ink-jet printing

1. Introduction

Many techniques were carried out to modify the surface property of polyolefins. However, their durable improvement is not obtained. For instance, when PE or PP materials are treated by a plasma or a corona discharge treatments, these materials become water wettable. But the modified property is lost with time. We found that the combination of some modification techniques was effective for the modification of chemically stable polymeric materials. The obtained hydrophilic property was not lost for several years. In addition, a water-based paint coating on the modified materials, and a solvent-bonding are examined.

2. Experimental

2.1 Materials Polymeric materials were used after washing with methanol. Commercial chemical reagents and hydrophilic reagents were used after a simple purification.

2.2 Adhesives Poly(vinylpyrrolidone), starch, wood-use bonds, PVAC-water mixture, cyanoacrylate (CA), CA-primer set, tape type epoxy resin adhesives, etc. were used.

2.3 Treatment Polymeric materials were activated by chemical oxidations or UV, energy irradiations. The activated polymeric materials were treated with chemical reagents in the presence of catalysts.

2.4 Adhesion strength and analysis A bonding strength of a polymeric material bonded to other materials was measured by a tensile tester, Shimadzu AGS-H5KN.

IR and XPS spectra of materials were observed.

2.5 Ink-jet printing Epson and Canon printers were used with water-based ink.

3. Results

3.1 Modification of silicone resin and poly(methyl pentene) (PMT) resin.

Silicone rubber has a high water-repellency and its modification is very difficult. We investigated the technique. A part of silicone rubber sheet modified by the present method (KANA method) gave a durable water wettability (Fig. 1).

Polymethylpentene (PMP) is one of the most difficult materials to be modified. PMP-made vessels were modified by the present method; the inner wall of the modified one is wettable with water (Fig.2).



Fig. 1 Modified silicone rubber sheet wetted with water.



Fig.2 Water-wettability of unmodified (left) and modified (right) PMP resin vessels.

CONTROLLED GROWTH OF MOF-BASED HYBRID NANOMATERIALS

Poster presentation

Jiating He, Ray Chin Chong Yap, Siew Yee Wong, Yu Zhang, and Xu Li*

*Institute of Materials Research and Engineering, A*STAR, 2 Fusionopolis Way, Innovis, #08-03, Singapore 138634*

Corresponding author email address: x-li@imre.a-star.edu.sg

Abstract - Microporous metal-organic frameworks (MOFs) consisting of metal ions assembled together with organic ligands have become a popular topic due to their large internal surface area, tunable chemical property and variable cavities, leading to diverse applications in gas storage,¹⁻⁴ chemical separation^{5,6} and drug delivery.^{7,8} In order to enhance their performance for different applications, MOFs have been incorporated with other functional nanomaterials to form hybrid nano-structures.^{9,10} Incorporation of functional nanoparticles into MOFs is an effective methodology to confer novel physical properties which will bring about new opportunities for future applications. For example, hybrid nanoparticles composed of metal nanoparticles and MOF can be incorporated in polymer substrate to adsorb and scavenge unflavoured gases or dyes.

Typically, precursors of MOFs are deposited onto pre-synthesized seed nanoparticles uniformly in solution and MOFs will grow from the modified seed nanoparticles. For such binary hybrid motifs, three kinds of structures can be obtained in general: concentric core-shell, eccentric core-shell and Janus nano-hybrids. Concentric core-shell nano-hybrids are the most common configurations, as a result of simple over-coating of MOFs on seed nanoparticles to form a uniform shell or granular domains in colloidal systems.^{11,12} Compared to concentric core-shell configurations, eccentric core-shell and Janus structures which are absent of centro-symmetry demonstrate higher diversity and complexity. Especially with Janus structures, the exposed surfaces of both components are expected to exhibit their original surface activities as well as integrated surface activities.

Here, we report a facile strategy that can control the growth of zeolitic imidazolate framework (ZIF-8) materials on the surface of metal nanoparticles at room temperature. The selective growth is driven by surface functionalization of metal nanoparticles via competitive ligand adsorption. Both hydrophilic and hydrophobic ligands are employed to adsorb and assemble on surface of metal nanoparticles, resulting in anisotropic surface domains on nanoparticles with different affinities to ZIF-8 precursors. Ligand ratio is proved to be a key factor to manipulate the coverage of ZIF-8 on the metal nanoparticles, leading to formation of MOF-based nano-hybrids with tunable structures, such as concentric core-shell, eccentric core-shell and Janus nano-hybrids. The capability to direct ZIF-8 growth by controlling the ligand assembly on the metal nanoparticle surfaces opens up new opportunities in the synthesis of MOF-based complex nanostructures. The resulting nano-hybrids to be incorporated in polymer films to be applied in fixed-bed catalysis.

Keywords: hybrid nanoparticles, metal-organic framework

1. Murray, L. J.; Dinca, M.; Long, J. R. *Chem. Soc. Rev.* **2009**, *38*, 1294.
2. Dinca, M.; Dailly, A.; Liu, Y.; Brown, C. M.; Neumann, D. A.; Long, J. R. *J. Am. Chem. Soc.* **2006**, *128*, 16876.
3. Dinca, M.; Long, J. R. *Angew. Chem. Int. Ed.* **2008**, *47*, 6766.
4. Rosi, N. L.; Eckert, J.; Eddaoudi, M.; Vodak, D. T.; Kim, J.; O'Keeffe, M.; Yaghi, O. M. *Science* **2003**, *300*, 1127.
5. Li, J.-R.; Kuppler, R. J.; Zhou, H.-C. *Chem. Soc. Rev.* **2009**, *38*, 1477.
6. DeCoste, J. B.; Peterson, G. W. *Chem. Rev.* **2014**, *114*, 5695.
7. Ferey, G. *Chem. Soc. Rev.* **2008**, *37*, 191.
8. Yaghi, O. M.; O'Keeffe, M.; Ockwig, N. W.; Chae, H. K.; Eddaoudi, M.; Kim, J. *Nature* **2003**, *423*, 705.
9. Lu, G.; Li, S.; Guo, Z.; Farha, O. K.; Hauser, B. G.; Qi, X.; Wang, Y.; Wang, X.; Han, S.; Liu, X.; DuChene, J. S.; Zhang, H.; Zhang, Q.; Chen, X.; Ma, J.; Loo, S. C. J.; Wei, W. D.; Yang, Y.; Hupp, J. T.; Huo, F. *Nat. Chem.* **2012**, *4*, 310.
10. Zhang, W.; Wu, Z.-Y.; Jiang, H.-L.; Yu, S.-H. *J. Am. Chem. Soc.* **2014**, *136*, 14385.
11. Huang, X.; Zheng, B.; Liu, Z.; Tan, C.; Liu, J.; Chen, B.; Li, H.; Chen, J.; Zhang, X.; Fan, Z.; Zhang, W.; Guo, Z.; Huo, F.; Yang, Y.; Xie, L.-H.; Huang, W.; Zhang, H. *ACS Nano* **2014**, *8*, 8695.
12. Zhong, H.-x.; Wang, J.; Zhang, Y.-w.; Xu, W.-l.; Xing, W.; Xu, D.; Zhang, Y.-f.; Zhang, X.-b. *Angew. Chem. Int. Ed.* **2014**, *53*, 14235.

EVALUATION OF STRUCTURE-PHYSICAL PROPERTIES OF REACTIVE MOLDED POLYAMIDE 6 AND ITS FRTP

Poster presentation

Hiroto Suenaga¹, Kentaro Taki², Hiroshi Ito^{1}, and Takashi Inoue¹*

1 Graduate School of Science and Engineering, Yamagata University, Japan

2 Graduate School of Natural Science and Technology, Kanazawa University, Japan

Corresponding author email address: ihiroshi@yz.yamagata-u.ac.jp

Abstract -Recently, fiber reinforced thermoplastics (FRTP) has attracted attention in the automotive and aviation fields. However, the thermoplastic resin is used as the matrix of FRTP is very difficult to the fiber bundles impregnate at a high melting temperature and high viscosity. Therefore, it has to be noted that in-situ polymerization using monomer with a low melting temperature and low viscosity is the one of the attractive alternative method. Here, we study the in-situ polymerization of ϵ -caprolactam as a monomer in order to fabricate polyamide 6 (PA6) and its composites by using reactive molding. The thermal property and the higher order-structure of polymerized PA6 and its composites were analyzed by differential scanning calorimeter (DSC). The engineering mechanical properties, mechanical behavior were evaluated by bending test. The PA6 crystal was melted begins at the temperature of 200 °C was observed. We obtained the flexural modulus and flexural strength of 1-3.5 GPa and 50-90 MPa respectively. It found that increasing crystallinity of PA6 has resulted in enhance the flexural modulus and flexural strength in a linear relation. In the case of FRTP using PA6, the flexural modulus and flexural strength of Carbon FRTP showed 10-15 GPa and 200-250 MPa, respectively.

Keywords: in situ polymerization, polyamide 6, mechanical property, fiber reinforced composite

TOWARDS HIGH-PERFORMANCE POLY(L-LACTIDE) MELT SPUN FIBERS BY TAILORING CRYSTALLIZATION WITH THE AID OF NUCLEATING AGENT

Poster presentation

H.W. Bai, H.X. Zhang, and Q. Fu*

College of Polymer Science and Engineering, State Key Laboratory of Polymer Materials Engineering, Sichuan University, Chengdu 610065, P. R. China

Corresponding author email address: qiangfu@scu.edu.cn

Abstract - As a biodegradable polymer completely derived from renewable resources, poly(L-lactide) (PLLA) shows a tremendous potential to replace some of the traditional petroleum-based and nonbiodegradable polymers in various applications such as textile fibers. However, the current use of PLLA fiber in large-scale commercial applications still faces some barriers mainly associated with its poor heat resistance because the low crystallization rate makes it hard to crystallize during melt spinning. In this work, we propose a facile strategy to address this obstacle via simultaneously tailoring crystal morphology and lamellae orientation with the aid of the nucleating agent (tetramethylene-dicarboxylic dibenzoyl-hydrazide, TMC-306) that can be dissolved in PLA melt and re-crystallizing into fibrils capable of serving as nucleation templates to induce the crystallization of PLLA lamellae perpendicular to their long axis upon cooling. Taking advantage of elongation flow experienced in melt spinning, TMC-306 fibrils tend to align in PLLA melt along the flow direction and then induce the formation of highly orientated PLLA lamellae in melt spun fibers. In this way, a significantly improved heat resistance and tensile strength are easily achieved.

Keywords: poly(L-lactide), fiber, nucleating agent, crystallization, high performance

Creation of Polar Solvent Type TR Fluid and its Function

Poster presentation

K.Hirakawa¹ Y.Kanazawa¹ H.Sekiguchi² R.Nakano² S.Yao^{1,2*}
¹ Chemical Engineering, Fukuoka University Graduate school, Japan
² Chemical Engineering, Fukuoka University, Japan
Corresponding author email address: shyao@fukuoka-u.ac.jp

Abstract

In this time, we made a new Side Chain Crystalline Block Co-polymer (SCCBC) with using Di(ethylene glycol) ethyl ether acrylate (DEEA) as a functional monomer units. By using this monomer, we could disperse polyethylene particle to polar solvent and this dispersion system showed polar solvent type Thermal Rheological (TR) Fluid properties. We also investigated the artery embolization function of this TR fluid and found this fluid has an ability to become a good an arterial embolization material.

Keywords: Thermal Rheological Fluid / Living Polymerizations / Side Chain Crystalline Block Co-polymer

Introduction

Recently, we polymerized a block copolymer that was constructed of two monomers: a monomer with a long alkane side-chain (more than 10 carbon atoms) and another monomer with solvent affinity. This block copolymer has a melting point and shows side-chain crystallization. Thus, this block copolymer can crystallize due to its long alkane side-chain (Side-Chain Crystalline Block Copolymer: SCCBC). Polymers having long alkyl side chains have been well known to exhibit various specific properties. In this time, we found that this SCCBC is adsorbed on PE crystal through supramolecular interaction. In addition, through the use of this supramolecular interaction, the SCCBC can act as a dispersant for a concentrated PE particle dispersion, which then shows unique thermal rheological properties. In this time, we made a new SCCBC with using a functional monomer units. By using this monomer, we could disperse PE particle to polar solvent and this dispersion system showed polar solvent type TR Fluid properties. One kind of the polar solvent type TR Fluid have an ability to be an arterial embolization material.

Experimental

For the side-chain crystalline monomer, we used stearyl acrylate (STA), and for the solvent-affinity monomer, we used Di(ethylene glycol) ethyl ether acrylate (DEEA). The block copolymer was polymerized by sequential monomer addition. The weight average molecular weight (Mw) of the SCCBC was about 12,000. The Mw of the STA sequence was about 5,000 and that of DEEA was about 7,000. For a PE particle, we used Ceridust@3620 (Clariant International Ltd), which has a number average diameter of 7.4 μ m. Ethanol and Iomeron was used as the dispersion solvent. Iomeron is a non-ionic iodinated contrast agent. The concentration of particle was 35mass% and the concentration of solvent was Iomeron:40mass%, Ethanol:25mass%. SCCBC was

added at a concentration of 2mass% of the particle weight. The viscosity and viscoelastic properties were measured by a Rheosol-G2000 at 25 °C, 35 °C, 45 °C, 55 °C.

Results and Discussion

Fig.1 shows the temperature dependence of shear viscosity. From this figure, viscosity increase significantly with increasing the temperature. This effects is reversible and can be called as Thermal Rheology (TR). Also, Transition temperature of around 40 °C. This result is thought to be desirable for the application of hepatic artery embolization because the TR effect may be expressed in the vicinity of the body temperature. Fig.2 shows the images before and just after the injection of this TR fluid into rabbit renal artery. From the figures, it is obviously shown that this TR fluid was able to embolization of renal artery. Also, the embolization kept one week. From these investigations, we had found that this TR fluid can be used as a good arterial embolization material.

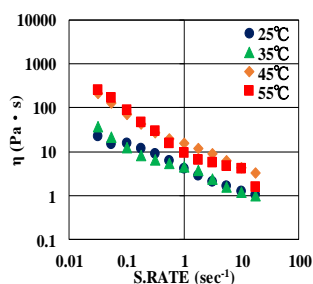


Fig.1 Temperature and shear rate dependence of viscosity.

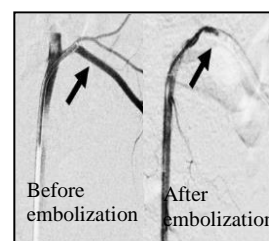


Fig.2 The application results for Transcatheter Arterial Embolization.

Acknowledgment

This research is supported by the [Practical Research for Innovative Cancer Control (15ck 0106038h002)] from Japan Agency for Medical Research and development, AMED.

INTERPHASE TRANSFER OF PLASTICIZER BETWEEN IMMISSIBLE RUBBERS

Poster presentation

Kento Yoshida, Nawaphorn Kuhakongkiat, Shogo Nobukawa
and Masayuki Yamaguchi*

School of Materials Science, Japan Advanced Institute of Science and Technology, Japan
Corresponding author email address: m_yama@jaist.ac.jp

Abstract

The transfer phenomenon of a plasticizer between immiscible rubbers was studied at various annealing temperatures. Natural rubber (NR) and poly(isobutylene) (PIB) were used as an immiscible pair with a liquid paraffin that acts as a plasticizer.

The laminated rubber sheets containing 10 phr of liquid paraffin obtained by the solution casting were piled together and annealed at various temperatures for 5 days. After the annealing procedure, the sheets were separated and characterized by the dynamic mechanical measurements.

Figure 1 shows the glass transition temperature T_g , i.e., the peak temperature of loss modulus E'' , of pure rubbers and rubbers with 10 phr of the plasticizer. It is found that T_g 's of both NR and PIB were shifted to low temperature by the plasticizer addition.

Figure 2 shows T_g 's of the separated rubber sheets after annealing at various temperatures. T_g of NR shifts to low temperature while that of PIB shifts to high temperature after annealing at 40°C. This is attributed to the interphase transfer of the plasticizer from PIB to NR during annealing. After annealing at -20°C, in contrast, T_g of NR shifts to high temperature while that of PIB shifts to low temperature. This is also owing to the interphase transfer of the plasticizer from NR to PIB during annealing.

Keywords: Polymer blend, Interphase transfer, Plasticizer, Glass transition temperature

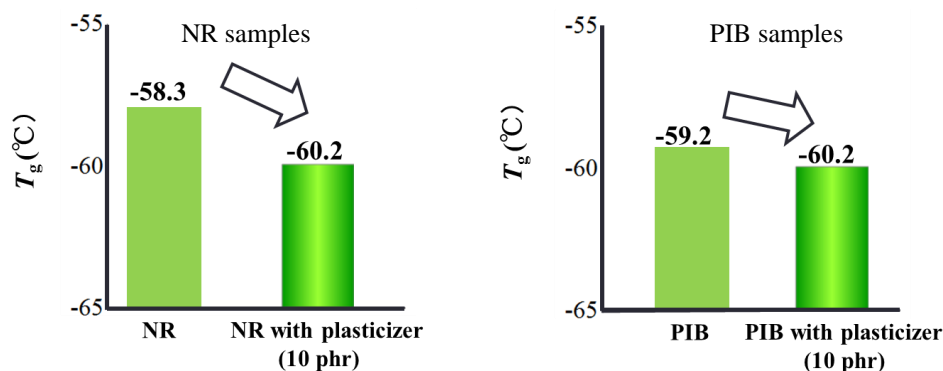


Figure 1 : T_g 's of pure rubbers and rubbers with 10 phr of the plasticizer

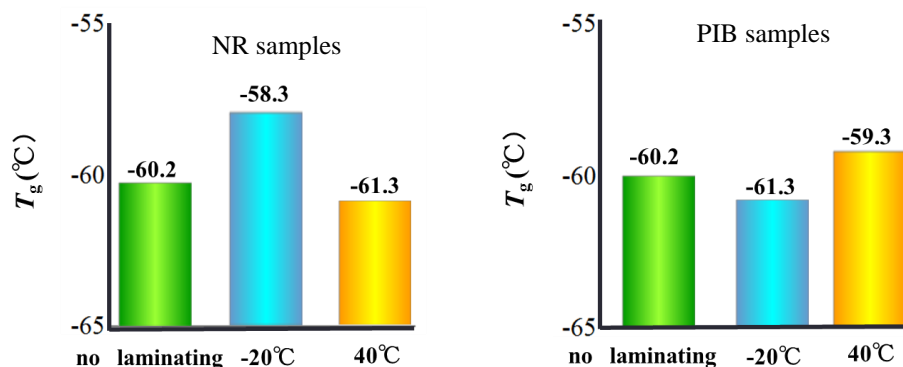


Figure 2 : T_g 's of the separated rubber sheets after annealing at various temperatures

IMPROVED ELONGATIONAL VISCOSITY OF POLYCARBONATE MELTS

Poster presentation

M. Sugimoto*, T. Isogai, S.K. Sukumaran

Graduate School of Science and Engineering, Yamagata University, Japan

Corresponding author email address: sugimoto@yz.yamagata-u.ac.jp

Abstract – We studied an improvement of elongational viscosity of polycarbonate melts. Polycarbonate as an engineering thermoplastic polymer has favorable mechanical properties such as high elastic modulus and pronounced toughness and some grades have good transparency depending on the production methods. Generally, polycarbonate is one of the linear polymers and shows low melt strength and very weak strain hardening under elongational flow. Thus polycarbonate is known to be difficult to apply in some polymer processings. Recently, there has been an increasing demand for an improvement of the elongational flow behavior of polycarbonate. In this study we studied melt rheology of some polycarbonates produced by interfacial polycondensation of bisphenol A with phosgene and melt polymerization of bisphenol-A and diphenyl carbonate. Polycarbonate by interfacial polymerization showed typical rheological properties: the terminal flow behavior in a low frequency region under dynamic shear flow and smooth increase of elongational viscosity according to the Trouton rule independent of the strain rates under elongational flow. Polycarbonate interfacial-polymerized with a functional monomer indicated extended relaxation time: gradual transition of G' and G'' from rubbery plateau region to the terminal flow region. This behavior is similar to that of polycarbonate by interfacial polymerization. Furthermore, we modified polycarbonate by melt polymerization by using a chain extender in a post-reactor stage. The modification enhanced the storage modulus G' as increasing the content of the reactive agent, though the loss modulus did show a small change in low frequency. The modified polycarbonate did not exhibit time-temperature superposition, while neat polycarbonate showed thermorheological simplicity. Furthermore, we should note that the modified polycarbonate showed a noticeable increase of the stress under elongational flow, which is never expected for standard polycarbonate. We can say that the modified polycarbonate has high potential to apply the new applications which was known to be difficult to process.

Keywords: Polycarbonate, Elongational viscosity, Viscoelasticity, Relaxation time

EFFECT OF CLAMPING FORCE SET VALUE ON INJECTION MOLDING QUALITIES

Poster presentation

M.S. Huang^{1*} and C.Y. Lin¹

¹ Department of Mechanical and Automation Engineering, National Kaohsiung First University of Science and Technology, Taiwan

Corresponding author email address: mshuang@nkfust.edu.tw

Abstract - Level of clamping force setting in an injection molding machine is important to the quality of plastic parts as well as the life duration of processed machines, in which a low clamping force may introduce defects of flashes while a high value may engage short shot caused by a poor venting effect. Traditionally, clamping force that is unnecessarily set at the highest value of machine specification may cause extra energy consumption and a heavy loading of tie bars that furtherly risks a short life time of employed machines. This work investigates the effect of clamping force set value on injection molding quality and further proposes an innovative approach to calculate proper clamping force set value that facilitates the yield rate of injection-molded parts as well as energy saving.

Keywords: Clamping force, injection molding machines, tie bar elongation, toggle-type clamping mechanism.

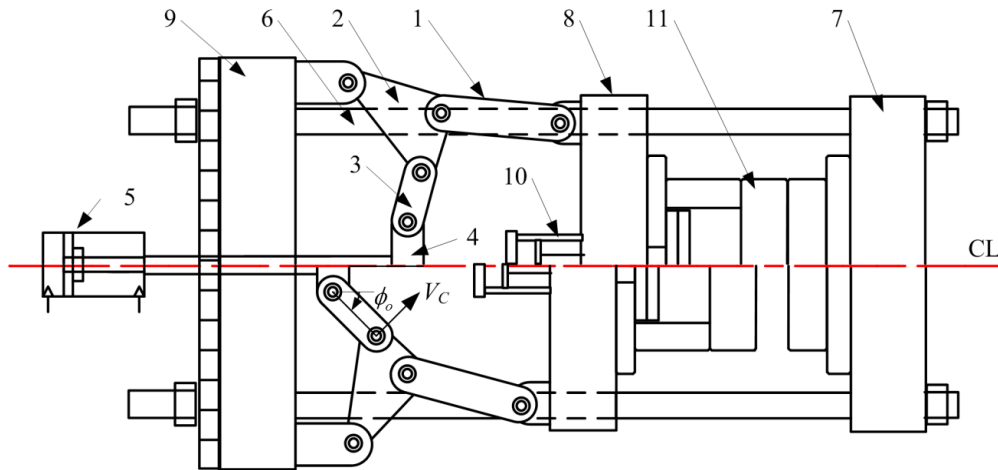


Fig. 1. Structure of a five-point double-toggle clamping mechanism.

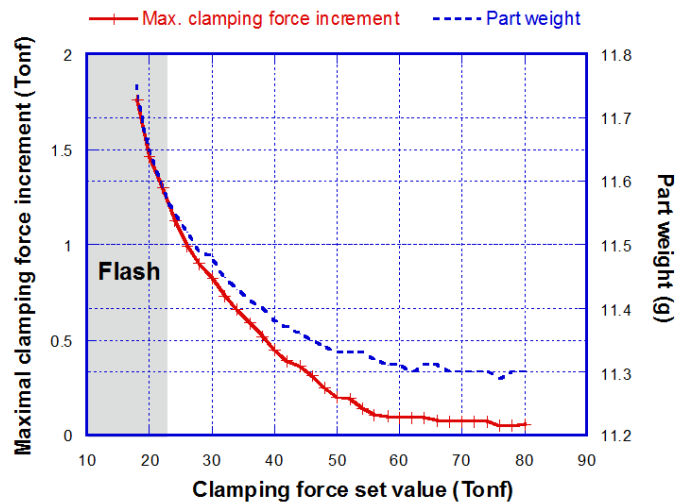


Fig. 2. Maximal clamping force increment versus part weight corresponding to various clamping force set value.

Long time structure constitution of amorphous polymer

Poster presentation

N.Oda¹ A.Tominaga¹ H.Sekiguchi² R.Nakano² S.Yao^{1,2*}
¹ Chemical Engineering, Fukuoka University Graduate school, Japan
² Chemical Engineering, Fukuoka University, Japan
Corresponding author email address: shyao@fukuoka-u.ac.jp

Abstract

Recently we had investigated mechanical properties of virgin and recycled amorphous polymers of by-products from spool site and runner site of injection molding. And we had founded that the mechanical properties depend on not only the difference of virgin or recycle, but also the molding condition. This results suggest that even amorphous polymer, the recycled polymer remain its history of molding.

In this time, we investigated long time structure constitution of these samples. And we found that the mechanical properties of amorphous polymers depend on the molding conditions and are changing with time gradually.

Keywords: Amorphous polymer, Internal structure, Molding condition, Fracture property, Inner structure

Introduction

It is well known that the crystalline polymer causes the flow induced crystallization and construct specific crystal structure. Recently, we have investigated about the recycling of crystalline polymer. In these investigation, we pointed the degradation of the mechanical properties of recycle plastics were caused by the memory of flow deformation.

On the other hand, the flow deformation memory dependence of amorphous polymer has not been well studied. In this time, we used the mechanical properties of amorphous virgin and recycled plastics of by-products from spool site and runner site of injection molding and investigated the mechanical properties of this films molded from them. From the investigation, we had founded that the mechanical properties of recycled polymer depended on not only the difference of virgin or recycle, but also the molding condition. This results suggest that even amorphous polymer, the recycled polymer remain its history of molding. And also we have found that mechanical properties of these samples can be changed greatly by changing the holding process.

Experimental

In this experiments, we used polystyrene virgin pellets (Fig.1 (a)), crushed waste polystyrene (Fig.1 (b)), and re-pelletized pellets (Fig.1 (c)). Test samples for tensile tests were press-molded at press temperature 230 °C, 210°C and pressure was 40MPa. The thickness of the films were about 50µm. Test peace were punched out in JIS K71132 (1/3) specimen from these thin films.

We also analyzed the internal structure by small-angle X-ray scattering measurements.

Melt viscoelasticity were measured by rheometer.

Results and Discussion

Figure 2 shows a small-angle X-ray scattering measurements of thin films molded from virgin pellets.

The results of 2min-press time sample, there is no scattering at the wide angle. However, increasing the pressing time, the two peaks in wide angle region begin to appear in the 6 min-press time sample. When press time increased to 10-minutes, the scattering in the wide-angle region appeared clearly. This results suggests that with increasing press time, over the longest relaxation time of the sample, the construction of inner structure are processing. The results also effect on the mechanical properties.

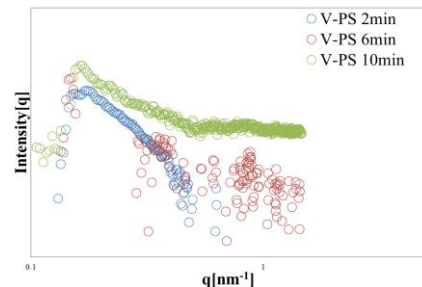


Fig.2 Small angle X-ray scattering profiles of virgin polystyrene samples.

Acknowledgment

This research was supported by the Environment Research and Technology Development Fund (3K143013) of the Ministry of the Environment, Japan. This time, in Shinei Chemical Co., Ltd. and Toyo Styrene Co., Ltd. who have provided polystyrene, I would like to thank deeply and wrote here.

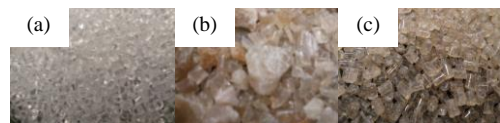


Fig.1 (a) Virgin pellets (b) Crushed sample (c) recycle sample

VALORIZATION OF PALM RESOURCE FOR GREASE LUBRICANT

Poster presentation

Z.M. Png¹, Q. Ye¹, H. Yan¹, H. Zhou¹, J.W. Xu^{1,2*}

¹*Institute of Materials Research and Engineering, Agency for Science, Technology and Research (A*Star), 2 Fusionopolis Way, #08-03, Innovis, Singapore 138634*

²*Department of Chemistry, National University of Singapore, 3 Science Drive 3, Singapore 117543, Singapore*
Correspondence to: Jianwei Xu (Email: jw-xu@imre.a-star.edu.sg)

Abstract:

Biomass based valorisation and conversion technology development had become a hot issue in the recent decade¹ as the large availability of biomass (~10¹⁴ kg annually) would provide an important replacement strategy for the industrial reliance on fossil based feedstock.

Out of all types of biomass, palm oil in particular is an important business in Southeast Asia. Global annual production of palm oil is about 60 million tonnes, with Malaysia and Indonesia contributing to 87% of the global output. Palm oil comprises fatty acids, such as saturated palmitic acid. One major application of palm oil is to prepare biodiesel². As of yet, palm oil's potential in being a feedstock for specialty chemicals is still relatively unexplored. Palmitic acid is fully saturated and its corresponding esters should possess high stability towards oxidation.

A method to prepare thickeners for grease lubricants from palm oil derived fatty acids is demonstrated (figure 1). Upon addition of about 1.5% the thickener to a base oil, the viscosity was found to increase until it becomes a greasy texture. This thickener is able to function at up to 50°C with good thermo-reversibility(figure 2). The prepared grease could be used for a wide variety of applications including food grade lubricant grease, railroad grease and sewing machine grease.

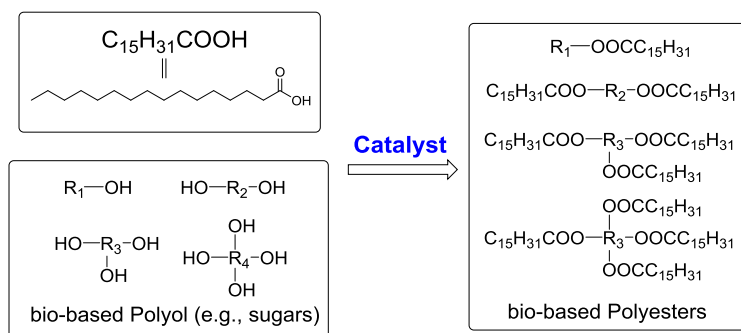


Figure 1: Reaction route between palmitic acid and selected polyols to generate ester based thickeners

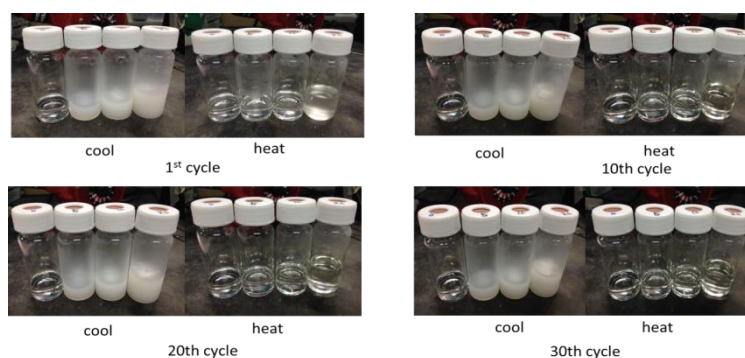


Figure 2: Thermo-reversibility test of the formed grease lubricants.

1 Tuck, C. O.; Pérez, E.; Horváth, I. T.; Sheldon, R. A.; Poliakoff, M., Valorization of Biomass: Deriving More Value from Waste. *Science* **2012**, 337 (6095), 695-699.

2. Mekhilef, S.; Siga, S.; Saidur, R., A review on palm oil biodiesel as a source of renewable fuel. *Renewable and Sustainable Energy Reviews* **2011**, 15 (4), 1937-1949

Keywords: Grease, lubricant, thickener, oil additive, palm oil

SYNTHESIS AND ANTIMICROBIAL ACTIVITIES OF QUATERNIZED PEI-G-CHITOSAN POLYCATIONS

Poster presentation

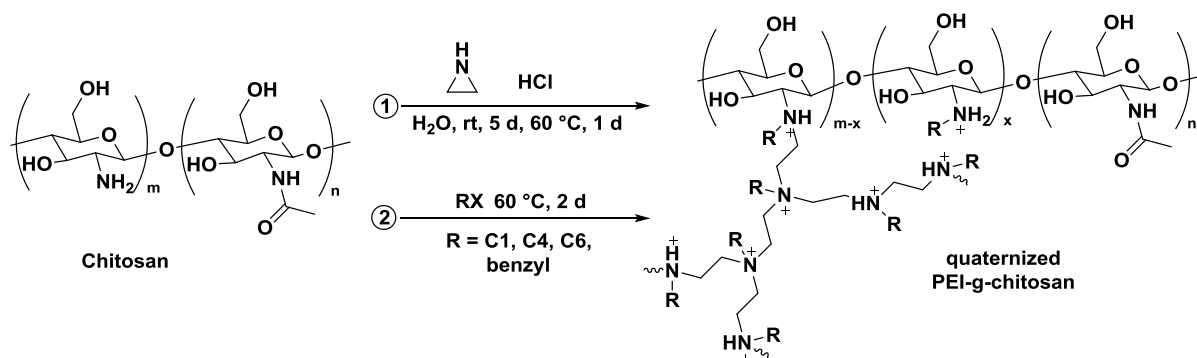
Wei Ren, and Ye Liu*

*Institute of Materials Research & Engineering, A*Star, Singapore*

Corresponding author email address: ye-liu@imre.a-star.edu.sg

Abstract

In order to reduce the threat of antimicrobial-resistant microorganisms as well as to reduce the consumption of limited fossil fuel resources, it is necessary to develop efficient antimicrobial agents based on natural polymers. In this study, the biomass-based antimicrobial polymers, quaternized polyethylenimine-graft-chitosan (Q-PEI-g-chitosan) were synthesized via a two-step reaction (Scheme 1). Firstly, PEI-g-chitosan were synthesized via cationic polymerization of aziridine with low molecular weight chitosan. Then the PEI-g-chitosan were further quaternized with different quaternary reagents (methyl iodide, n-butyl bromide, 1-Bromohexane and benzyl bromide) to afford the Q-PEI-g-chitosan, and the reaction procedure can be simplified into a one-pot manner. The structure and molecular weight of the PEI-g-chitosan and the Q-PEI-g-chitosan was characterized by ^1H NMR, ^{13}C NMR and GPC. The results show that the amines on the chitosan were successfully grafted with PEI chains, and the length of the PEI chains can be controlled by varying the molar ratio between aziridine and the amines of the chitosan. Minimum inhibitory concentration (MIC) antimicrobial activity studies of the obtained Q-PEI-g-chitosan were carried out against *Escherichia coli* (Gram-negative) and *Staphylococcus aureus* (Gram-positive). The MIC results reflect that Q-PEI-g-chitosan exhibit good antimicrobial activities. The Q-PEI-g-chitosan can be used as promising biomass-based antimicrobial agents to reduce dependence on synthetic antimicrobial polymers based on the limited fossil fuel resource, to reduce the possibilities of antimicrobial resistance and to reduce usage of small molecular chemical biocides which may cause pollution to the environment.



Scheme 1. Synthetic route for quaternized PEI-g-chitosan

Keywords: Chitosan, antimicrobial agents, antimicrobial activity, polyethyleneimine, biomass-based

SELF-HEALING BEHAVIOR OF STYRENE-BUTADIENE-STYRENE TRIBLOCK COPOLYMER

Poster presentation

Ritsuko Watanabe¹, Shogo Nobukawa¹ and Masayuki Yamaguchi¹

¹ School of Materials Science, Japan Advanced Institute of Science and Technology, Japan
Email address: m_yama@jaist.ac.jp

Abstract - Self-healing materials are known to repair their damage automatically and thus show prolonged life time. Therefore, they have been focused to be used in the wide range of applications. Since most self-healing polymeric materials that have been developed up to now have network structure, i.e, thermosetting resin, the demand for thermoplastic resins is increasing intensively. In this study, the self-healing behavior of styrene-butadiene-styrene triblock copolymer (SBS), known as a thermoplastic elastomer (TPE), was investigated. TPE behaves like a cross-linked rubber at room temperature and can be processed as a thermoplastic at high temperature. It consists of hard segments which play a role as cross-linking points to prevent flow and soft segments showing rubber elasticity. In general, both ends of soft segments are trapped in the dispersed domains of the hard segment. However, one end of some soft segments can move freely without constraints of the domain. They act as dangling chains, which show the self-healing behavior beyond the glass transition temperature.¹⁾

In this study, a commercially available SBS having 24 wt % of styrene was employed as a polymer. Two types of specimens were prepared by compression-molding at different temperatures; (1) 200 °C at heating and 5 °C at cooling and (2) 160 °C at heating and 25 °C at cooling.

The temperature dependence of loss tangent $\tan \delta$ is shown in Figure 1. The glass transition temperature of polybutadiene(PB) segment is found to be located at -90 °C, while that of polystyrene(PS) segment is at around 90 °C. The figure indicates that PS phase is formed clearly at high cooling temperature. In contrast, rapid cooling, i.e, low cooling temperature, prohibits the well-developed phase-separation.

The effect of annealing time on self-healing behaviors is investigated. After cutting into two pieces of the sample specimen, they were attached together at 25 °C for 10 min. or 72 hours. Then, the samples were stretched by a tensile machine. The result is shown in Figure 2. It is found that the stress and strain at break increases with increasing the annealing time with contact. Furthermore, the sample obtained by quench shows better healing behavior.

Reference: 1) M. Yamaguchi, R. Maeda, R. Kobayashi, T. Wada, S. Ono, S. Nobukawa, *Polym. Intern.*, 61, 9 (2012)

Keywords: Self-healing, thermoplastic elastomer, styrene-butadiene-styrene triblock copolymer

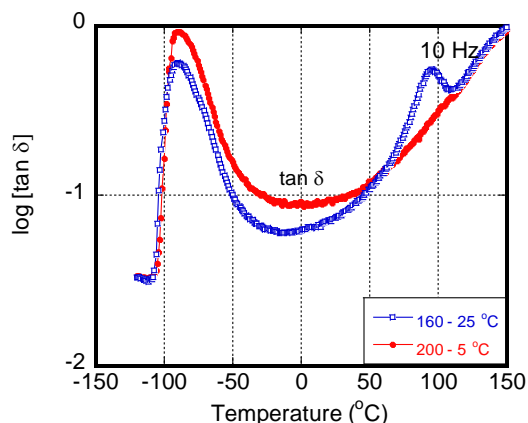


Figure 1. Temperature dependence of loss tangent $\tan \delta$ of SBS.

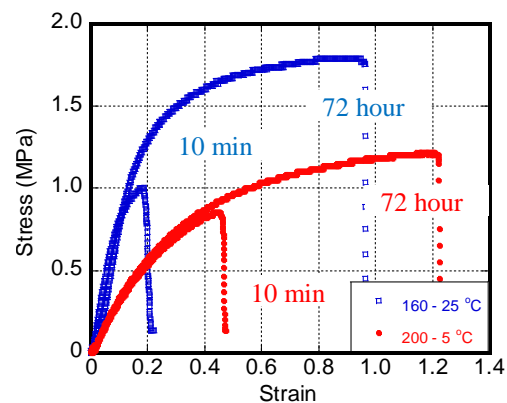


Figure 2. Stress-strain curves of SBS.

SYNTHESIS AND CHARACTERIZATION OF A SIDE-CHAIN CRYSTALLINE SILICONE PSA

Poster presentation

R. Hasuo¹, S. Yamaguchi^{2,3}, S. Kawahara² and H. Murakami^{4*}

¹ *Department of Advanced Engineering, Graduate School of Engineering, Nagasaki University, Nagasaki, Japan*

² *Nitta Corporation, Nara, Japan*

³ *Department of Science and Technology, Graduate School of Engineering, Nagasaki University, Nagasaki, Japan*

⁴ *Division of Materials Science, Graduate School of Engineering, Nagasaki University, Nagasaki, Japan*

Corresponding author email address: hiroto@nagasaki-u.ac.jp

Abstract - A side-chain crystalline acrylic pressure-sensitive adhesive (PSA) is one that its adhesion can be controlled by reversible order-disorder transition of the side-chain crystalline unit with a change in temperature. The adhesion of acrylic PSAs, however, decreases with a rise in temperature. In contrast, a silicone PSA possesses the highest heat resistance property among commercially available PSAs. In this study, therefore, we aimed development of a side-chain crystalline silicone PSA whose adhesion can be controlled with the change in temperature. Siloxane polymers with and without octadecyl group as the long alkyl side-chain were prepared; introduction of the octadecyl group to the siloxane polymer was carried out by hydrosilylation reaction. The DSC thermogram of the side-chain crystalline siloxane polymer showed an endothermic peak at 35 °C attributable to melting of the crystalline unit in a heating process and an exothermic peak at 27 °C for recrystallization of the melted side-chain unit in a cooling process. To obtain the thermosensitive silicone PSA the side-chain crystalline siloxane and a MQ resin were mixed and then crosslinked by the hydrosilylation reaction with α,ω -divinyl siloxane. The TGA results of the silicon PSA tape and acrylic PSA tape revealed that the silicon PSA tape possesses higher heat resistance compared to that of the acrylic PSA. Adhesion switching behavior of the silicon PSAs was evaluated by 180° peel test. The silicon PAS without the crystalline unit kept its adhesion in the range from 20 to 80 °C whereas the silicone PSA with the crystalline unit lost its adhesion below 30 °C. Dynamic viscoelastic measurements also revealed that the silicon PSA with the crystalline unit become hard below the transition temperature. These results suggest that the thermosensitive silicone PSA has been successfully prepared.

Keywords: Silicone PSA, Siloxane, Side-chain Crystalline polymer

"WARM-OFF" TYPE ACRYLIC PSA CONTAINING A SIDE-CHAIN CRYSTALLINE GRAFT COPOLYMER

Poster presentation

S. Tabuchi¹, S. Yamaguchi^{2,3}, S. Kawahara² and H. Murakami^{4*},

¹ Department of advanced Engineering, Graduate School of Engineering, Nagasaki University, Nagasaki, Japan

² Nitta Corporation, Nara, Japan

³ Department of Science and Technology, Graduate School of Engineering, Nagasaki University, Nagasaki, Japan

⁴ Division of Materials Science, Graduate School of Engineering, Nagasaki University, Nagasaki, Japan

Corresponding author email address: hiroto@nagasaki-u.ac.jp

Abstract – An acrylic pressure sensitive adhesive (PSA) bearing a long alkyl side group as its crystalline unit can control its adhesion, because the crystalline unit undergoes reversible order-disorder transition with a change in temperature. Among the PSAs, an acrylic PSA in which a side-chain crystalline polymer with a low molecular weight is dispersed as particles shows its adhesion below the transition temperature and loses it above the transition temperature. This behavior is known as a "warm-off" (WO) function; the low molecular weight side chain crystalline polymer is called a "warm-off" component (WOC). Adhesion-switching behavior of a WO-PSA containing a random copolymer as a WOC, however, occurs in a broad temperature range due to the presence of the crystalline units with different sizes. To solve this problem we used a copolymer grafted with a side-chain crystalline macromonomer consisting of only monomers with long alkyl side chain groups as a WOC (graft-WOC). In the DSC thermograms the random-WOC gave an endothermic peak with a shoulder. The existence of the shoulder is the evidence for the presence of the different crystalline states. In contrast, a sharp endothermic peak for the graft-WOC was observed without any shoulders, suggesting that the side chain crystalline unit is unity. The large half-width of the peak is due to the use of the two long alkyl acrylates. From the peel test results, the peel strength of the PSA containing the random-WOC decreased to less than 1 N/inch with an increase in temperature. However, the difference of the peel strengths before and after the melting point was very small. In contrast, the PSA containing the graft-WOC kept its adhesion until the melting point. In addition, rising in temperature until above the melting point caused drastic decrease of the peel strength to less than 1 N/inch. This result indicates that the WO function is improved by the use of the graft-WOC.

Keywords: Side-chain Crystalline Polymer/ Pressure Sensitive Adhesive / Graft Copolymer

Development of evaluation method capable of judging the appropriate product lifetime of the rubber material used in residential-use cogeneration systems

Poster presentation (Please select one)

Shintaro Iwasaki¹, Yuji Higuti¹

¹ *Energy Technology Laboratories, OSAKS GAS CO. LTD., Osaka, Japan*
sh-iwasaki@osakagas.co.jp

Abstract -

Gas equipment is composed of various materials, including polymeric material and metal. It is well-known that polymeric material is more prone to degradation than other materials. For this reason, evaluation of the reliability of individual cases of polymeric material used in gas equipment is important for the safety of equipment utilization.

In Japan, recent years have seen the spread of residential-use cogeneration systems (residential CGS). Residential CGS contain systems for circulation of hot water because of exhaust heat recovery. As compared to conventional water heaters, they are operated for a longer duration and used at higher temperature. Coupled with this harsh environment, there have lately been reports of the occurrence of trouble in the form of degradation of rubber parts owing to residual chlorine added to tap water. In fact, for residential CGS as well, the change of specification of solenoid valve diaphragm, from EPDM (ethylene-propylene-diene materials) to FKM (fluoro-rubber), has been made. Therefore, selection of the type of material for rubber parts used in residential CGS must continue to take account of the effect of degradation caused by residual chlorine.

The objective of this research is developing the evaluation method of the long-term durability of rubber material against residual chlorine in the field, based on laboratory reproduction of degradation caused by the combination of residual chlorine and temperature. And this paper provides the evaluation results with a focus on the solenoid valve diaphragm as exemplifying a type of rubber part used in residential CGS. The chlorine-water immersion test as the accelerated aging test was carried out to conduct a comparative evaluation on the durability of EPDM and FKM against the residual chlorine and determine whether it is possible to use each rubber for 10 years in the field.

Keywords: EPDM, fluoro-rubber, residual- chlorine, accelerated aging test

ANOMALOUS MOLECULAR ORIENTATION OF EXTRUDED SHEET FOR POLYPROPYLENE/POLYBUTENE-1 BLENDS

Poster presentation

Sato Shunma¹, Shogo Nobukawa¹, Takayuki Maeda² and Masayuki Yamaguchi^{1*}

¹School of Materials Science, Japan Advanced Institute of Science and Technology, Japan

²New Japan Chemical Co., Ltd., Japan

Email address: m_yama@jaist.ac.jp

Abstract

Various processing operations are applicable for isotactic polypropylene (PP), including extrusion. In general, chain-axis of PP orients to the molecular, i.e., flow direction in extruded films and sheets. In contrast, recent researches revealed that extruded sheets in which PP molecules orient perpendicular to the flow direction are prepared by using epitaxial crystallization on the surface of needle crystals of *N,N'*-dicyclohexyl-2,6-naphthalenedicarboxamide.^{1,2)} Although this phenomenon is interesting from the scientific point of view, it has poor impact on the industrial application expect for the manipulated morphology control.^{3,4)} In this study, an extruded sheet in which polymer chains orient both parallel and perpendicular to the flow direction is prepared by using a miscible blend composed of PP and isotactic poly(butene-1) PB.

Commercially available PP and PB were melt-blended with *N,N'*-dicyclohexyl-2,6-naphthalenedicarboxamide (New Japan Chemical, NJ Star^{TR} NU-100) as the nucleating agent. The blend ratio of PP/PB was 50/50. The content of the nucleating agent was 500ppm. The sample was fed into a twin-screw extruder with a ribbon-shaped die. The temperature of the die and barrel was controlled at 200°C and the chill-roll was at 100°C. Besides the blend, pure PB was also extruded at the same condition.

Fig. 1 shows the 2D-XRD pattern of the PB sheet. The figure demonstrates that PB shows I-form crystals which orient to the flow direction. Fig. 2 shows the edge-view pattern of the extruded blend. As seen in the figure, the (110) plane of trigonal β -form crystals of PP shows strong six spots. The result demonstrates that PP chains orient perpendicular to the flow directions in the film plane (transversal orientation). Therefore, the sheet has strong orientation in both MD and TD.

Reference: 1) Uchiyama et al., *J. Polym. Sci. Polym. Phys.* 47, 424 (2009)

2) Yamaguchi et al., *Polymer* 50, 1497 (2009)

3) Phulkerd et al., *J. Polym. Sci. Polym. Phys.* 51, 897 (2013)

4) Phulkerd et al., *Polym. J.* 46, 226 (2014)

Keywords: polypropylene, polybutene-1, nucleating agent, molecular orientation, extrusion

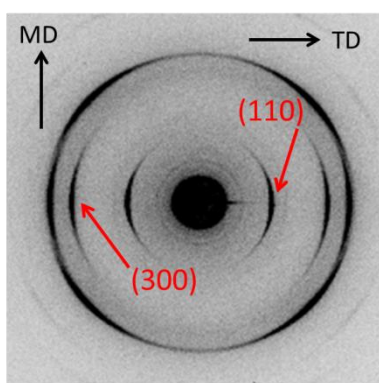


Fig. 1 2D-XRD pattern of the extruded PB sheet.

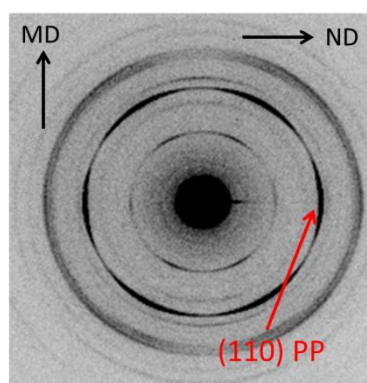


Fig. 2 2D-XRD pattern at edge-view of the extruded PP/PB blend sheet.

NUMERICAL SIMULATION OF INJECTION/COMPRESSION MOLDING FOR MULTISCALE STRUCTURE

Poster presentation

S.K. Hong¹, J.J. Kang¹ and K.H. Yoon^{2*}

¹Molds and Dies Technology Group, Korea Institute of Industrial Technology (KITECH), Republic of Korea

²Department of Mechanical Engineering, Dankook University, Republic of Korea

*Corresponding author email address: khyoon@dankook.ac.kr

Abstract – Studies of the micro- or nano-patterned functional surfaces have been actively conducted in various fields. Because these surface functionalities are highly useful, there are ongoing attempts to develop imitations of these surfaces for use in the industry and technology. However, the mass production of such surfaces is difficult because efficient methods for manufacturing the micro-scale or nano-scale patterns are unavailable at present. Injection/compression molding (ICM) is advantageous for achieving thickness uniformity and dimensional accuracy. On the other hand, only a few papers have studied the effects on micro-pattern molding. In the present paper the relationships between the micro-pattern molding properties and ICM (Fig. 1) conditions using numerical analysis were investigated. The molding subject (Fig. 2) has the sheet shape with the width, length, and nominal thickness of 160 mm, 90 mm, and 1.12 mm, respectively. The micro-pattern is cylindrically shaped with a diameter and height of 30 μm and 14 μm , respectively and a 100- μm gap between the patterns. PMMA TF8 (MFR of 10.0 g/10 min at 230 $^{\circ}\text{C}$, 37.3 N) of Mitsubishi Rayon was used for the polymer resin. An injection molding machine used in this study consists of an in-line screw-type injection unit and a toggle-type clamping unit. Simulation was performed for the behavior of the micro-pattern filled during ICM using a DDM (dual-domain method)-based technique. As a first step the filling simulation of a macro-scale model was performed, the simulation for the assumed part without the micro-scale patterns, using the commercial Moldflow software. Next, the filling simulation of a micro-scale model, which is the filling simulation for one pattern, was performed. The COMSOL Multiphysics software was used for this micro-scale filling simulation. The following results were obtained in the present study: (i) Solidification of the polymer proceeded faster farther away from the gate. This is the main cause for the lower transcription ratios of micro-pattern far from the gate. (ii) The temperature history of the polymer is almost the same in CIM (Conventional Injection Molding) and ICM. (iii) The polymer temperature reached the no flow temperature within the packing stage in CIM and within the compression stage in ICM. That is, the micro-pattern filling flow stopped even for non-zero cavity pressure. (iv) The improvement in micro-pattern filling in ICM is only due to the difference in cavity pressures history. Finally, the experimental results and simulation results for filling behavior of micro-pattern over time were compared as shown in Fig. 3.

Keywords: Injection/Compression Molding, Micro-feature, Finite Element Method, Multiscale structure

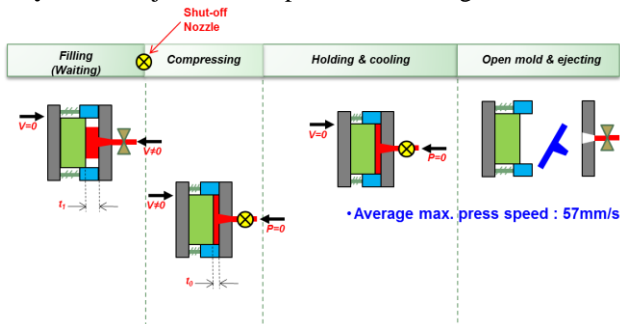


Fig. 1 Schematic drawing of injection/compression molding.

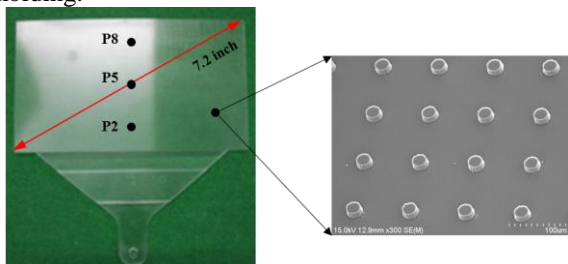
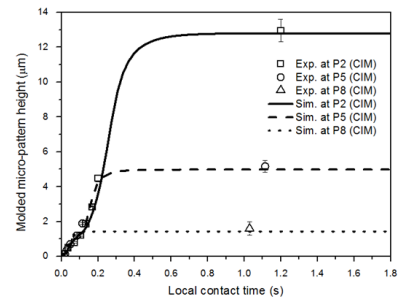
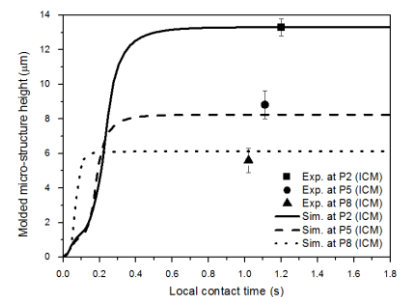


Fig. 2 Photograph of injection molded macroscale part and microscale structures.



(a)



(b)

Fig. 3 Comparison of molded micro-feature height between numerical and experimental results at various distances from gate: (a) CIM and (b) ICM.

ATOMISTIC SIMULATION OF GAS DIFFUSION IN GLASSY POLY(VINYL PYRROLIDONE) MATRIX

Poster presentation

Supanont Jamornsuriya, Visit Vao-soongnern*

Laboratory of Computational and Applied Polymer Science (LCAPS), School of Chemistry, Institute of Science, Suranaree University of Technology, Nakhon Ratchasima, Thailand. E-mail: visit@sut.ac.th

Abstract - Poly(vinyl pyrrolidone), PVP, is one of biocompatible polymers widely used in pharmaceutical application especially in tablet coating. The performance of the final coat is strongly affected by the polymer properties and the formulation parameters. Thin film of water soluble polymer like PVP is often applied to improve the stability of moisture sensitive products. Understanding the role of specific interaction between penetrant molecules and PVP matrix at atomistic level is important to elucidate the underlying diffusion mechanism in polymer matrix. In this work, we investigate the diffusion characteristics of H₂O and O₂ gasses in glassy PVP matrix at 298 K by molecular dynamic simulation. First, rotational isomeric state (RIS) model for a PVP chain was used for generation of a fully atomistic model for the amorphous material at its bulk density of 1.2 g cm³. The initial structure was relaxed by a combination of molecular mechanics and molecular dynamics. The predicted Hildebrand solubility parameter is $10.12 \pm 0.14 \text{ cal}^{1/2} \text{ cm}^{-3/2}$ and in reasonable agreement with the experimental value ($10.8 \text{ cal}^{1/2} \text{ cm}^{-3/2}$). X-Ray scattering pattern of PVP model shows two distinct peaks below $Q \approx 2 \text{ \AA}^{-1}$. One peak appears around 1.2 \AA^{-1} in the region where usually amorphous "simple" polymers. At lower Q around 0.7 \AA^{-1} , a pre-peak is present in consistent with experimental report (J. Chem. Phys. **134**, 054904 (2011)). Then, 10 H₂O or 10 O₂ were added to these polymer models. After structural equilibration, a 1 ns NVT-MD simulation was carried out to generate the trajectories for analysis. The diffusion of H₂O and 10 O₂ molecules in the PVP matrix was studied at room temperature (298 K) below the glass transition temperature. The predicted diffusion coefficients for the two penetrants are remarkably different, as water forms hydrogen bonds with PVP but oxygen gas does not. The hydrogen bonding of water and the carbonyl groups in PVP is evident in the radial distribution function (peak at 1.85 Å). Although O₂ has larger molecular mass, its diffusion rate is higher. Hence, the hydrogen bond does remarkably influence the slower diffusion of H₂O in the PVP matrix. The calculated diffusion coefficient of H₂O ($0.22 \times 10^{-6} \text{ cm}^2/\text{s}$) is about 7 times lower than that of O₂ ($1.54 \times 10^{-6} \text{ cm}^2/\text{s}$) in PVP matrix

Keywords: Poly(vinyl pyrrolidone), gas diffusion, molecular dynamics

Acknowledgement: The financial support from Advanced Organic Materials Research group and the Development and Promotion of Science and Technology Talents Project (DPST) is highly appreciated.

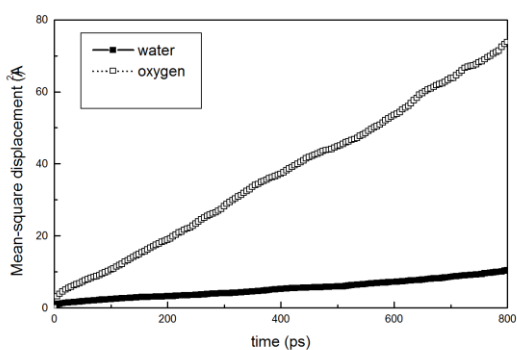


Figure 1 Averaged mean square displacement of the H₂O and O₂ molecules as a function of time interval in PVP at 298 and 473 K.

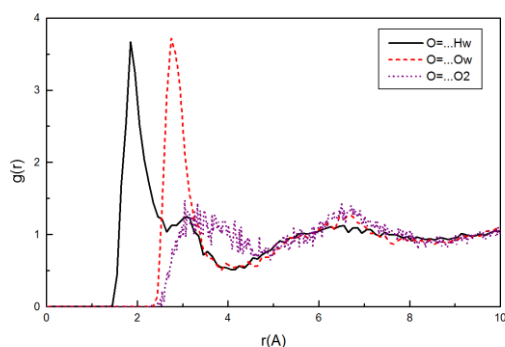


Figure 2 Radial distribution function of (1) the hydrogen (Hw) and oxygen (Ow) atom of water and (2) the oxygen (O2) atom of oxygen gas with the oxygen carbonyl (O=) group in PVP matrix at 298 K.

INFLUENCE OF SUSPENDING MEDIUM ON RHEOLOGICAL BEHAVIOR OF SHEAR THICKENING FLUIDS

Poster Presentation

Swarna¹, S. K. Pattanayek² and A.K.Ghosh^{1*}

¹ *Center of Polymer Science and Engineering, Indian Institute of Technology Delhi, New Delhi, India*

² *Department of Chemical Engineering, Indian Institute of Technology Delhi, New Delhi, India*

Corresponding Email: anupkghosh@gmail.com

Shear thickening a type of non-Newtonian phenomenon, manifesting a rise in viscosity with the increase in shear rate or shear stress after a particular value known as critical shear rate or stress, is observed in a wide range of suspensions and is referred as shear thickening fluids (STF). Several properties of both suspended particles and suspending liquid independently stimulates the uniqueness of liquid-solid transition. In this work, we present the effect of suspending medium's characteristics on the viscosity rise owing to solid-like behavior of particle suspensions. Cornstarch-water based and silica-PEG based systems were evaluated by amending their respective suspending matrix by addition of polyols. Polyols viz., glycerine, ethylene glycol and polyethylene glycol (PEG) were mixed with the matrix in 1:1 ratio which was further utilized in the preparation of different concentrations of STF by incorporating various quantities of suspending particles (cornstarch and silica). The rheological characterization of pure STFs was correlated with polyols based STFs and a unique behavior was observed for each of the additives attributing to OH interactions. Water/Ethylene glycol as suspending medium transits the so called discontinuous shear thickening activated by jamming of particles to continuous shear thickening at all the concentrations unlike glycerine and PEG. By addition of glycerine, a strong shear thickening with much less particle concentration was observed whereas PEG contributed to shear thinning with increase in particle concentration. FTIR spectra indicate the increased intermolecular hydrogen bonding associations with polyols accrediting to exclusive rheological performance of the STFs. In addition, the behavior of non-colloidal and colloidal Brownian particle suspensions in the suspending medium with respect to the flow properties of STFs was also explored. Present work provides an understanding and conceptualization of suspending medium's traits to that of rheological behavior of different material based STFs.

Keywords: Shear thickening fluids, suspending liquids, polyols, viscosity

SURFACE LOCALIZATION OF POLY(METHYL METHACRYLATE) IN A BLEND WITH POLYCARBONATE

Poster presentation

Takumi Sako, Shogo Nobukawa and Masayuki Yamaguchi*

School of Materials Science, Japan Advanced Institute of Science and Technology, Japan
Corresponding author email address: m_yama@jaist.ac.jp

Abstract

Polycarbonate (PC) is widely employed in industrial applications because of its excellent transparency and mechanical toughness. However, its ability to resist scratches is poor. Therefore, the improvement of an anti-scratch property is required to widen applications. In this research, we propose a new method to produce a transparent sheet in which PMMA is localized at the surface using PC containing a small amount of PMMA to provide the anti-scratch property.

A commercially available PC ($M_n=28,000$, $M_w=46,000$) and PMMA with low molecular weight ($M_n=8,900$, $M_w=15,000$) were used in this study. The samples were melt-mixed and compressed into a film shape. The concentration of PMMA was 20 wt%. The blend was compressed into flat sheets with a thickness of 3 mm by a compression-molding machine. Furthermore, the samples were annealed in the temperature gradient using a compression-molding machine in which temperatures of the top and bottom plates were controlled separately. The composition of both surfaces was evaluated by attenuated total reflectance Fourier-transform infrared spectroscopy (ATR-FTIR) and size exclusion chromatography.

Figure 1 shows ATR-FTIR spectra for both surfaces of PC/PMMA annealed in the temperature gradient, in which the top and bottom plates were controlled at 250 °C and 200 °C, respectively. The peaks at 1770 cm^{-1} and 1730 cm^{-1} are ascribed to PC and PMMA, respectively. The surface at the high temperature side has a stronger peak at 1730 cm^{-1} and a weaker one at 1770 cm^{-1} , whereas the peak intensities are opposite at the low temperature side. The results demonstrate that the PMMA concentration is high at the high temperature side and vice versa. Figure 2 shows the size exclusion chromatographs of samples collected from the surface of the annealed PC/PMMA sheet. The data for pure PC and PMMA are also shown. This result demonstrates that low molecular weight fraction, i.e., low molecular weight PMMA is localized at the high temperature side, which is consistent with the ATR-FTIR results.

Since this technique can be applicable to polymer processing, it becomes an important technique for the production of an ideal plastic glass.

Keywords: Polycarbonate, Poly(methyl methacrylate), Segregation, Annealing

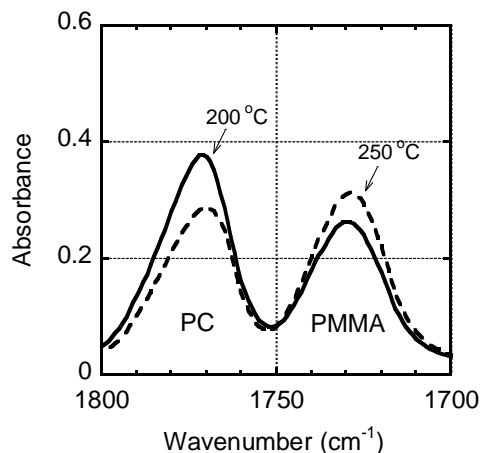


Figure 1 ATR-FTIR spectra for both surfaces of PC/PMMA (80/20) annealed under the temperature gradient for 60 min; temperatures of the top and bottom plates are 250 °C and 200 °C, respectively.

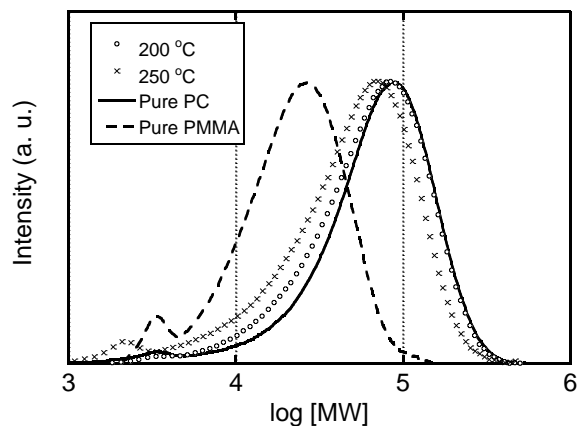


Figure 2 Size exclusion chromatograph charts as a polystyrene standard for pure PC, pure PMMA and both surfaces of PC/PMMA annealed under the temperature gradient for 60 min.

STRUCTURE AND ENGINEERING PROPERTIES OF PMMA NANO-ALLOY OBTAINED BY HIGH SPEED SHEARING PROCESS

Poster presentation

Takuya Konno, Yuki Kodama, Akira Ishigami and Hiroshi Ito*

*Department of Polymer Science and Engineering, Yamagata University, Japan
Corresponding author email address: ihiroshi@yz.yamagata-u.ac.jp*

Abstract - Recently, the reduction of the vehicle weight has been promoted in order to improve fuel efficiency in the automotive industry. Polymethyl methacrylate (PMMA) has excellent transparency, weather resistance, and rigidity is expected to substitute material for automotive glass. However, PMMA has a weakness in toughness and impact resistance. Therefore, we attend to improve the toughness and impact resistance by blending polycarbonate (PC) and PMMA utilized by a high speed shearing process. The high-speed shearing process has been attracting attention with a high resolution is a capable technique to blend the incompatible polymers. PMMA/PC blend is formed to sheet and dumbbell sample by compression molding and injection molding machine respectively. The evaluation of mechanical properties are performed to a tensile test, impact test, the surface hardness measurement. The fracture surface morphology is observed by scanning electron microscope (SEM). In this study, we expect to the toughness and impact resistance of PMMA are developed by blending method using the high-speed shearing process, the mechanical behavior is clarified by the effect of the various process parameters. Furthermore, the alternative of automotive materials is enlarged.

Keywords: PMMA/PC blend, Nano-alloy, High-speed shearing, Mechanical properties, Impact properties

NOVEL BIOMEDICAL MATERIALS BASED ON CARBON DOTS

Oral presentation/Poster presentation

G. Wang* and Y. Liu

*Institute of Materials Research and Engineering, A*STAR, Singapore*

Corresponding author email address: wangg@imre.a-star.edu.sg

Abstract – Carbon dots as novel fluorescent materials have attracted much attention in past decade. Carbon dots in free state are studied intensively including various ways of preparation and applications based on their tailored properties. However, the reports on carbon dots clusters are very limited. In this presentation, we introduce the synthesis of two carbon dots clusters using inorganic silica scaffold and polymer scaffold, respectively. The bioimaging applications using these materials will also be demonstrated.

Keywords: Biomedical, Carbon Dots, Clusters.

TR fluid function for differences in the chemical structure of the side chain crystallizable block copolymer

Poster presentation

Y.Hasebe¹ Y.Kanazawa¹ H.Sekiguchi² R.Nakano² S.Yao^{1,2*}

¹ Chemical Engineering, Fukuoka University Graduate school, Japan

² Chemical Engineering, Fukuoka University, Japan

Corresponding author email address: shyao@fukuoka-u.ac.jp

Abstract

Recently, we polymerized a block copolymer that was constructed of side-chain crystalline monomer and a solvent-compatible monomer, which we referred to as a side-chain crystalline block copolymer (SCCBC). This SCCBC has a specific melting point. We found that this SCCBC was adsorbed onto polyethylene (PE) crystal by via supramolecular interaction. In addition, through this supramolecular interaction, the SCCBC acts as a dispersant for a concentrated PE particle dispersion, and this dispersion can be considered a Thermal Rheological Fluid.

In this time, we investigated the TR fluid functions of the cases of two different side-chain monomers, one was behenyl acrylate and other was stearyl acrylate.

Keywords: bolck polymer / micelle / polyethylene / crystalline supramolecular interaction /thermal rheological fluid

Introduction

Recently, we polymerized a block copolymer that was constructed of two monomers: a monomer with a long alkane side-chain (more than 10 carbon atoms) and another monomer with solvent affinity. This block shows side-chain crystallization. Thus, this block copolymer can crystallize due to its long alkane side-chain (Side-Chain Crystalline Block Copolymer : SCCBC). We found that the side chain block of the SCCBC is adsorbed on PE crystal. At this time, PE crystal and the side chain block of SCCBC are considered to form a quasi-crystalline structure. According to this, the solvent affinity block unit covers the particle and changes the particle surface easy to wet solvent. This is because of the SCCBC can act as a dispersant for a concentrated PE particle dispersion. Additionally, we had found that increasing the temperature of the concentrated PE particle dispersion system, the viscosity increased to the non-addition dispersion system. We found this phenomenon was reversible, when cooling the dispersion the viscosity decrease to very low value. We call this Fluid as a "Thermal Rheological (TR) Fluid".

In this time, we investigated the difference dependence of the length of side chain.

Experimental

This time, the side chain crystalline sites we used were stearyl acrylate (STA) and behenyl acrylate (BHA). Synthesis of SCCBC were living radical polymerization as previously reported. The PE fine particle was Ceridust@3620. Diethyl phthalate (DEP) was used as solvent. The concentration of particle was 40wt%. SCCBC was added 1wt% to PE particle concentration.

Temperature and shear rate dependence of viscosities were measured by using a rheometer (Rheosol-G2000).

Results and Discussion

Fig.1 shows the temperature and shear rate dependence of the shear viscosity. From this figure, the shear rate dependence at low temperature were much depends on the length of the side-chain. And the transition temperature also depends on the length of the side-chain. On the other hand, at high temperature, the shear rate dependence were almost same to the original dispersion.

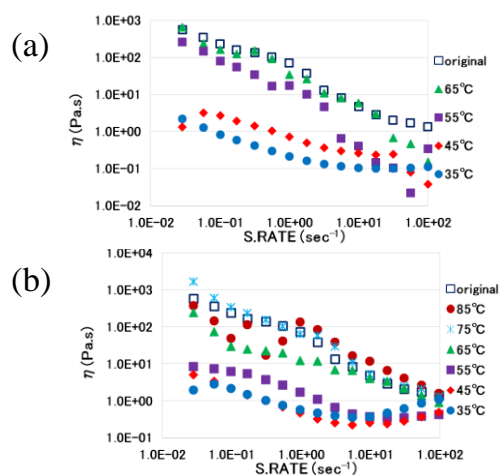


Fig.1 Temperature and shear rate dependence of viscosity of 1wt% SCCBC PE particle dispersion. (a) behenyl acrylate (BHA), (b) stearyl acrylate (STA).

Acknowledgment

This research is supported by the [Practical Research for Innovative Cancer Control (15ck 0106038h002)] from Japan Agency for Medical Research and development, AMED.

STRUCTURAL ENGINEERING OF POLYURETHANE FOR MULTIPLE FUNCTIONAL COATINGS

Poster presentation

Hong Yan,¹ Hui Zhou,¹ Xiaobai Wang,¹ Jianwei Xu^{1,2*}

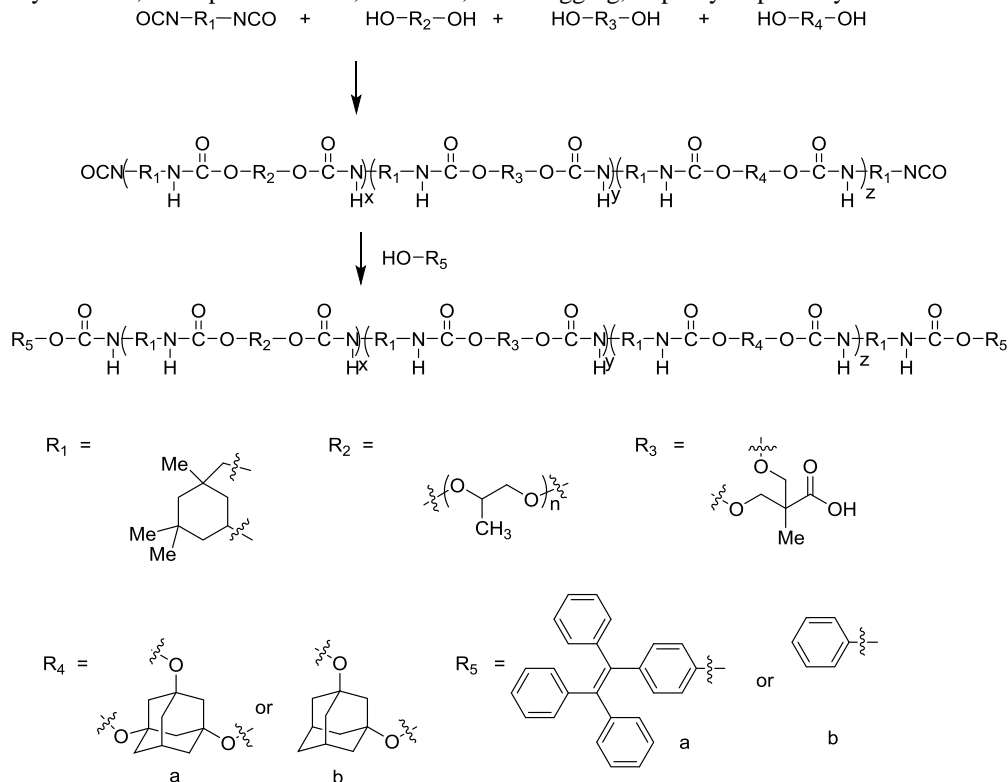
¹ Institute of Materials Research and Engineering, A*STAR (Agency for Science, Technology and Research), 2 Fusionopolis Way, Innovis, Singapore 138634

² Department of Chemistry, National University of Singapore, 3 Science Drive 3, Singapore 117543. E-mail: jw-xu@imre.a-star.edu.sg

Abstract - Versatile polyurethane with predominant properties, e.g. chemical, temperature and abrasion resistant, bondable to various substrates, and highly flexible, have shown great promise in wide applications. For instance, it is widely used to insulate surfaces such as wood, metal and paint to protect them from rot, corrosion or fading. Nevertheless, the ability to deliver additional functions on the target surface and comply with the requirements of multiple functions usually involves another coating layer or materials. As a result, applications of polymeric materials and hybrid composites for surface coating still suffer from simplex function and insufficient performance. Nonetheless, the lack of abilities in the preparation of a multi-functional coating material on a substrate and improvement of surface properties with simple processing constitutes an obstacle to achieving multi-functional coating. With these problems, utilization of such multi-functional coating materials is inevitably seen as a viable alternative to improve the surface properties with minimal processing, light weight and low cost. Therefore, the development of truly durable multiple functional coating based on sole polyurethane is therefore highly desirable for advanced applications.

Herein, we present a method for producing multipurpose polyurethane that contains functional molecular entities in the polymeric backbone that are addressable or controllable. The tunable functions and applicability of polyurethane by selection of monomeric components from different combinations of macrodiols, diisocyanates and chain extender are a viable method for organization of molecular components into polymeric framework. As a result of grafting functional moieties, the prepared polyurethanes were deserved additional functions compared with conventional polyurethane films, such as anti-UV, anti-fogging, and superhydrophilicity as well as fluorescence capability for multi-functional surface coating.

Keywords: Polyurethane, Multiple Functions, Anti-UV, Anti-Fogging, Superhydrophilicity



Scheme. A schematic illustration for the synthesis of P1~P5. (P1: R1, R2, R3, R5a; P2: R1, R2, R3, R4a, R5a; P3: R1, R2, R3, R4b, R5a; P4: R1, R2, R3, R5b; P5: R1, R2, R3, R4a, R5b.)

HYDROTHERMAL SYNTHESIS OF CARBON SPHERES FROM GLUCOSE

Poster presentation

R.C.C. Yap, J.T. He, S.Y. Wong and X. Li*

Institute of Materials Research and Engineering (IMRE), 2 Fusionopolis Way, Innovis, #08-03, Singapore 138634

**Corresponding author email address: x-li@imre.a-star.edu.sg*

Abstract:

The uses of sustainable materials as precursors to produce nano-materials are very important to the economy, environment and health issues. Glucose, a form of carbohydrates and simplest form of sugar is widely found in nature. Carbon sphere from hydrothermal carbonization have display many superior and promising properties which can be used in many important applications. For example, carbon spheres can encapsulate metal nanoparticles which can be used in drug delivery or water filtration technologies. They can also be decorated with different nano-materials to exhibits different properties to be use in sensing applications. Mesoporous carbon spheres with high BET surface area can also be used for super capacitors gas absorption.

The starting materials are glucose mixed with water to form glucose solution. Using a stainless-steel autoclave, carbon spheres can be synthesized from glucose solution. Carbon spheres with average diameter of 150 nm have been synthesized at 800 °C for 3 hours. By using different biomass precursors, the physical size and surface properties of carbon sphere can be tuned. A symmetrically study on the different conditions such as concentration, time and temperature were varied. The particle morphology was compared using SEM and TEM, and the chemical composition was studied using FTIR and EDX. Large scale production of carbon spheres using hydrothermal reactor was also demonstrated. The carbon spheres can then be mixed with polymer solution for application in polymer coating technologies for UV shielding. The UV shielding can be measured using UV-VIS.

Keywords: carbon spheres, glucose, hydrothermal, polymer

EVALUATION OF HIGHER-ORDER STRUCTURE AND THERMAL PROPERTIES OF HIGH THERMAL CONDUCTIVITY PC COMPOSITES OBTAINED BY STRUCTURAL PHASE SEPARATION METHOD

Poster presentation

Yumi Yamada¹, Hiroshi Ito^{1*}, Yuu Takahashi², Fumio Keitoku², Hironari Sano²,
and Yuji Fujita²

¹*Graduate School of Science and Engineering, Yamagata University, Japan*

²*Mitubishi Chemical Co., Japan*

Corresponding author email address : ihiroshi@yz.yamagata-u.ac.jp

Abstract - This study demonstrates the effects of ceramic filler with high thermal conductivity on the thermal conductivity of PC/PP blends by structural phase separation method. PC/PP polymer blends in the difference of viscosities were used as polymer matrix. The PC/PP blends were well known in the phase separation behavior of the blending structure. In this investigation, Boron Nitride (BN) as a high thermal conductive filler with high proper dispersion into the lower viscosity phase of PC was used. BN disperse in PC/PP blends with the phase separation structure was observed. PC-based composites with BN-rich phase were successfully fabricated by structural phase separation structure method. The results show that thermal conductivity was improved by the creation of high filler content in the phase.

Keywords: polymer composites, thermal conductivity, polymer blend, phase separation structure

EFFECT OF MODIFIED STARCH AND NANOCLAY ON BIODEGRADABILITY AND MECHANICAL PROPERTIES OF POLYLACTIC ACID TERNARY BLENDS

Poster presentation

X.K. Zhang, S.X. Wang, S.Y. Wong and X. Li*

¹ *Institute of Materials Research and Engineering, A*STAR, Singapore*
Corresponding author email address: x-li@imre.a-star.edu.sg

Abstract: Starch-based biopolymer composites reinforced by nanoclay are reported in this paper. The starch was modified by glycerol and Poly (butylene succinate), which showed good interfacial adhesion to polylactic acid (PLA). Nanoclay was successfully incorporated into Starch/PLA blends via a twin screw extruder to produce Starch/PLA/Clay nanocomposites. It was found that the nanoclay loading affected the mechanical properties and morphology of starch/PLA composites. The incorporation of nanoclay particles accelerated the crystallization process of the PLA matrix; meanwhile, the nanoclay improved the compatibility between starch and PLA. The starch-based composites incorporating nanoclay presented considerable improvements to the thermal and mechanical properties of PLA, and accelerated the degradation of PLA and PLA/thermoplastic starch (TPS). This study also suggested that there is potential for such materials to be used for film applications.

Keywords: Starch, Nanoclay, Polylactic acid, Biodegradability